Topical nanomedicine for the combination delivery of immuno-modulatory peptides for

accelerated chronic wound healing and anti-bacterial activity

by

Miral Fumakia

A Thesis submitted to the Faculty of Graduate Studies of

The University of Manitoba

in partial fulfillment of the requirements of the degree of

MASTER OF SCIENCE

College of Pharmacy, Faculty of Health Sciences

University of Manitoba

Winnipeg, Manitoba

TABLE OF CONTENTS

LIST OF TABLES

LIST OF FIGURES

ACKNOWLEDGEMENTS

I am grateful to many people who have supported me throughout my Master of Science degree at the University of Manitoba, please note the following acknowledgements (in no particular order):

I would like to first acknowledge and express my gratitude to my supervisor and mentor Dr. Emmanuel A. Ho for giving me this incredible opportunity to work in his lab and contribute to research. Dr. Ho has been an outstanding mentor, and as a student, I have gained a deeper understanding and appreciation for research from him. He has always encouraged me to think critically and challenge myself. He has the ability to crack even the most complicated situations, tangible and has provided monumental advice in all aspects of career development from lab work, to publishing, to networking, but most importantly, he has always given me the freedom to follow my interests. He possesses outstanding qualities as a person, these qualities which then filter down to his students. His sense of understanding, his support, motivation and most notably his patience makes him a great supervisor. It has been my pleasure to learn under such a talented, ambitious and dedicated scientist. I appreciate all the time taken by him to sit and pass along his understanding of this field to me and I truly feel that because of his great efforts I am a better and much more informed scientist. If opportunity arose in the future it would be a pleasure to work with Dr. Ho again.

Secondly, I would like to thank my committee members, Dr. Xiaochen Gu and Dr. Song Liu, for their valuable insight and critiques throughout my studies. It has been a privilege to work with such brilliant and accomplished scientists.

I am also grateful to all the members of the Ho lab for their support and friendship throughout my project and for making the lab a great place to work every day. I feel there aren't enough words to significantly express my thanks for all their support, encouragement and the scientific knowledge I have gained has truly benefited me in this field, but beyond this they have helped me understand how

to deal with troubleshooting not only in the lab, but also in my everyday life. A heartfelt thank you to the lovely Sidi Yang, who trudged through the nanoparticle and cell culture studies with me, and for providing me with a constant source of friendship and for answering my many questions in the lab. I would also like to thank Andy Chen for always lending me a helping hand and for providing me with his insightful advice and mentorship throughout my studies. Thank you to Yannick Traore for all his help by sharing his expertise in bacterial studies and for always answering my pesky questions regarding the project. I would also like to thank our summer students Jessica, Tarun, Kelsie, Fernanda, Celine, Jimmy and Vincent for their support.

I would like to thank everyone at the College of Pharmacy for making Winnipeg a home away from home. Lastly, I would like to thank my family and friends for their unconditional love and support.

DEDICATION

I dedicate this thesis to my parents who have always been patient, supportive, motivational and inspirational to me through this incredible journey. Both of you have sacrificed many things in life for your children, and have instilled in us the importance of education. You both are the most selfless human beings who have always put their children's needs first and foremost before their own. Thank you for being my parents and I love you both dearly. I would also like to thank Jayesh uncle and Bhavana aunty for their unyielding trust, support, love and encouragement.

Over the past years, I have found many difficulties with research and it is only through the mistakes I have done, that my appreciation for research and researchers has immensely increased. I have gained valuable knowledge for what research truly is, and the amount of dedication it takes to conduct it.

ABSTRACT

Wound treatment remains one of the most prevalent and economically burdensome healthcare concerns, often complicated by prolonged inflammation and bacterial infection, contributing to morbidity and mortality. Agents commonly used to treat chronic wound infections are limited due to their toxicity, multifactorial etiology of chronic wounds, deep skin infections, lack of sustained controlled delivery of drugs, and development of drug resistance. LL37 is an endogenous host defense peptide that has been shown to exhibit antimicrobial activity and is involved in the modulation of wound healing. Serpin A1 (A1) is a neutrophil elastase inhibitor and has been shown to demonstrate wound-healing property. Hence, our goal was to develop a topical combination nanomedicine for the controlled sustained delivery of LL37 and A1 that at precise combination ratios will significantly promote wound closure, reduce bacterial contamination, and enhance anti-inflammatory activity. We have successfully developed a solid lipid nanoparticle (SLN) formulation that can simultaneously deliver LL37 and A1 at specific ratios resulting in accelerated wound healing by promoting wound closure in BJ fibroblast cells and keratinocytes as well as synergistic enhancement of antibacterial activity against *S. aureus* and *E. coli* in comparison to LL37 or A1 alone.

CHAPTER 1: INTRODUCTION

From simple to complex organisms an 'intact outer sheath' is considered to be the most important survival feature. Healing of the wound displays an extra ordinary mechanism of cellular events that are unique in nature. It is essential to maintain the skin's integrity as without proper treatment options, insults from surgical incision, burns or injuries can lead to severe life-threatening injuries. Wound healing is a complex physiological and cellular process that works to restore the tissue integrity after injury.

1.1. FACTS ABOUT WOUND HEALING PROCESS

1.1.1. Anatomy and physiology of skin

Skin is often referred to as the largest and most visible organ of the body, comprising up to 15-20% of the total body weight [1]. Skin serves several complex functions such as protection, sensation, thermoregulation, communication and metabolism. Skin is constantly exposed to factors such as aging, soaps, hydration status, medications, exposure to UV, medications, and nutritional status which influence the skin's ability to retain its functionality, jeopardizing its integrity [2-5]. Normal skin comprises of 2 main layers: outermost epidermis and the underlying dermis. Beneath the dermis is the hypodermis [6].

1.1.1.1. Epidermis

The epidermis is a thin stratified, avascular, outermost layer of the skin consisting mostly of tissues called stratified epithelium [6]. Epidermis is composed of a total of 5 layers of epithelial

(squamous) cells, each gradually differentiating into the next layer where these cells are pushed towards its upper surface as rapid and ongoing cell division produces new cells beneath them [6]. These 5 layers are stratum corneum, stratum lucidum, stratum granulosum, stratum spinosum, and stratum basale.

The outermost stratum corneum is composed of thin layer of anucleate cells, which are mainly filled with keratin. The thickness of this layer varies depending on the age, gender, and comorbid diseased state. This is the least permeable layer [7].

After stratum corneum is the stratum lucidum. This layer is found in areas such as the palms of the hands, and sole of the foot where the epidermis is thicker. This layer is generally transparent and the cell boundaries are difficult to identify [8].

The stratum granulosum is beneath the stratum lucidum. This layer is composed of granules between the keratinocyte cells. The protein stored in these granules help maintain the structure of the keratin filaments in the intracellular space [9].

After stratum lucidum is the stratum spinosum. The cells in this layer have cytoplasmic structure like morphology. Desmosome a type of cell-cell junction is found in this layer that provides adhesion between cells and protects the layer against mechanical forces [7].

Stratum basale also called as stratum germinativum is the innermost epidermal layer. It is composed of a single layer of basal keratinocytes (basal cells). This layer responds to several factors, such as growth factors, hormones, extracellular matrix, and vitamins.

Epidermal cells during the wound healing process migrate to resurface the wound. Primary cells of the epidermis are the keratinocytes (water-insoluble, tough, keratin producing cells) [6,10,11]. Protection and

regulation are the primary functions of this layer. However, the epidermis has limited capacity to regenerate itself and can only withstand limited mechanical and chemical assaults.

1.1.1.2.   Basement membrane zone (BMZ)/ dermal-epidermal junction

BMZ (sometimes called dermal-epidermal junction) is the area that anchors the epidermis to the dermis [12]. The BMZ is divided into 2 distinct zones: the lamina lucida and the lamina densa [12]. The major proteins found in the BMZ are fibronectin (aids in the adhesion of the healing elements and water retention), type IV collagen, and non-fiber forming collagen (that adds thickness to the skin). During the wound healing process, BMZ gets disrupted and needs to be re-formed [13].

1.1.1.3.   Dermis (corium)

This is the thickest tissue layer of the skin. Dermis comprises of blood vessels, lymphocytes, nerve fibers, sweat glands, sebaceous glands, and hair follicles [10]. It is sparsely populated (primarily by the fibroblast cells). Major proteins found in the dermis are collagen and elastin. Collagen is responsible for providing tensile strength whereas elastin is responsible for the skin's elastic recoil function [10]. Dermis primarily consists of the cells responsible for wound healing like the fibroblasts (secrete collagen), mast cells (inflammatory mediators), macrophages, and lymphocytes. These cells are also involved with the immune surveillance of the skin, thus are often referred to as the 'skin's immune system' [11].
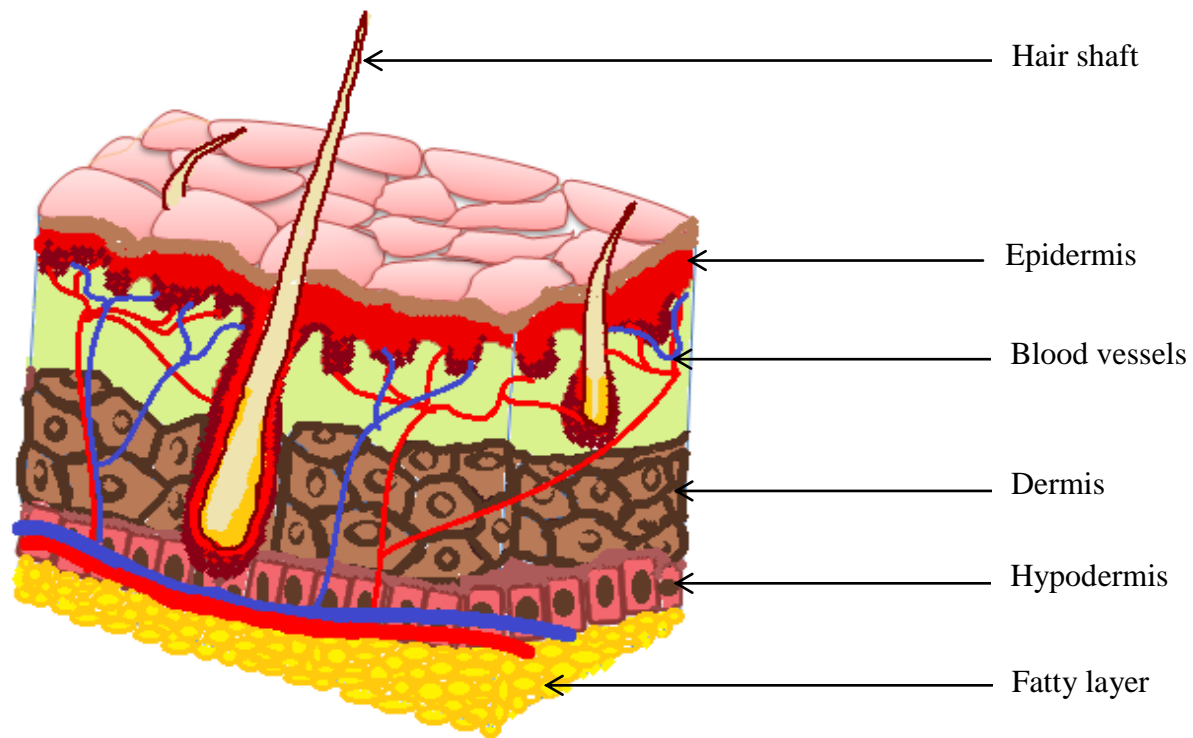
Figure 1. Layers of the skin. The skin is composed of two main layers: the outermost epidermis which is made of closely packed epithelial cells and underlying it is the dermis, made up of dense connective tissue that houses hair follicles, sweet glands, and blood vessels. Beneath dermis is the hypodermis, which is primarily composed of loose connective and fatty tissues.

1.1.1.4.   Hypodermis (superficial fascia)

Hypodermis forms a subcutaneous layer below the dermis that supports and anchors the epidermis and dermis to the underlying body structures. This layer is composed largely of adipose tissues, connective tissues, blood vessels, fatty tissue and collagen cells. Insulating the body, reserving energy within, providing mobility of the skin over underlying structures, providing protection and additional cushioning are the main functions of this layer. It also stores fat as an energy reserve for the body. The lymph vessels, blood vessels and hair follicles divide into the rest of the body through this layer [7].

1.1.2.   Physiology of wound healing

From simple bacteria to complex multicellular organisms, an 'intact outer sheath' is considered to be one of the most important feature for survival [14]. The ability to heal occurs differently in the various species from simple tissue repair to complete organ regeneration. For centuries, wound healing has been regarded as a complex and dynamic process involved in restoring the tissue integrity after injury. The wound healing process involves numerous cell types (epithelial cells, endothelial cells, fibroblasts, and lymphocytes) and an array of soluble factors such as growth factors, cytokines, etc.) [14]. Researchers over the past 3 decades have contributed much information in understanding this intricately regulated, tightly orchestrated sequence of events that is affected by a number of systemic and local factors including the wound environment/ extra cellular matrix [15,16].

Wound healing is best understood as a cascade of physiological responses, which under normal circumstances, results in repair [16]. The ability of the body to repair tissue damage is an important survival tool for living organisms. Repair is an extremely complex process where hundreds of overlapping and "linked" processes are involved [13]. They are commonly conceptualized as four major sets of events, beginning with the activation of the coagulation cascade immediately after injury followed by inflammation, proliferation and remodeling [7,16].

1.1.2.1.   Mechanisms of wound healing

Irrespective of the wound injury or severity, repair generally occurs only by 2 mechanisms [17],

   a.   Regeneration of new tissue or replacement of the damaged tissue

b. Scar formation by replacing the damaged or lost tissue by connective tissue which is lacking some of the functions and integrity of the original tissue [18].

Epidermal and superficial dermal layer wounds generally heal by regeneration as epithelial, endothelial, and connective tissue can be regenerated. Whereas wounds confined to deep dermal layers, subcutaneous tissues, tendons, ligaments, bone, and muscle heal by scar formation as they lack the capacity to regenerate and they lose their structures permanently [19,20]. Regeneration is the preferred mechanism of repair as it maintains the normal function and appearance of the injured tissue. In contrast, scar formation is a less satisfactory alternative as tissues are incapable of complete regeneration and are prone to lose their function. The mechanism of wound healing is dependent upon factors such as the type of wound closure (primary, secondary or tertiary intention), onset of the wound, wound type (acute or chronic), duration of wounding, and tissues involved (partial-thickness or full-thickness) [18-20].

1) Hemostasis and coagulation

Hemostasis and the formation of a provisional wound matrix occur immediately upon wounding. Injuries that are beyond the epidermis and lead to blood loss activate the hemostasis event. Disruption of blood vessels upon injury triggers platelet activation and aggregation. Simultaneously, clotting factors that activate both extrinsic and intrinsic factors are released to the wound site by the injured cells. A more durable fibrin clot composed of fibrin, aggregated platelets and blood cells later replaces this temporary plug. Hemostasis is accomplished further by vasoconstriction of blood vessels, mediated by thromboxane A2 and prostaglandin 2α [21-25].

Clot formation is followed by fibrinolysis (clot breakdown), which is a critical event [26,27]. Platelet activation and degranulation cause the α granules and dense bodies of the platelets to rupture,

releasing cytokines and growth factors that activate the inflammatory phase (IL-1 α,IL-1β, IL-6 and TNF- α) [28]. Platelet activation also stimulates collagen synthesis, transforms fibroblasts to myofibroblasts, helps the re-epithelialization process, and initiates angiogenesis. These substances are known to attract the cells which play a prime role in beginning the repair process [25].

2) Inflammatory phase

The second stage of wound healing is dedicated to inflammatory phase, which is the body's natural response to injury. After hemostasis, controlling the infection and establishing a clean wound bed are the primary focus of this phase. Thus, it is often referred to as the wound "clean-up period" involving breakdown of any devitalized tissue and eliminating excess bacterial bioburden [15,16,29,30]. Inflammatory phase can be roughly divided into an initial early neutrophil recruitment phase and appearance/transformation of monocytes as a late phase. Damaged cells and platelets from the injured vessel produce cytokines and growth factors that attract neutrophils, which dominate the wound scene for 2-5 days unless the wound is chronic [31,32]. Neutrophils are associated with the phagocytosis of bacteria and foreign debris.

By day three-four post-injury, the neutrophils as a result of apoptosis begin to disappear and are replaced by macrophages that support the ongoing process by performing the breakdown of devitalized tissues and phagocytosis of pathogens [33,34]. In addition, macrophages release a large amount of growth factors, chemokines and cytokines that stimulate angiogenesis, fibroblast migration, connective tissue synthesis, removal of apoptotic cells, and tissue restoration following injury [35,36]. By day five-seven post-injury, T-lymphocytes are present at the site that secrete additional cytokines, eliminate viral organisms and foreign cells. Elimination of these cells can lead to delayed or compromised repair process [37].

1.1.2.2.   Cascade of Events in wound healing process

	INJURY
	HEMOSTASIS
Phase I	- Activation of coagulation pathway
	- Vascular constriction, thrombin formation
	- Degranulation of platelets, release of growth factors
	INFLAMMATION
Phase II	- Recruitment of neutrophils and macrophage at the wound site
	- 'Wound-clean up' phase
	- Debridement of devitalized tissues, phagocytosis of bacteria
	PROLIFERATION/REPAIR
Phase III	- Recruitment of growth factors, differentiation
	- Neoangiogenesis, granulation tissue formation
	- Contraction of wound, resurfacing
	REMODELING/MATURATION
Phase IV	- Collagen synthesis
	- Cross-linking and alignment of collagen
	- Well-healed scar formation

Table 1. Cascade of events in wound repair process [15,17]. **Wound healing phases are commonly conceptualized as four major sets of events; beginning with the activation of the coagulation cascade immediately after injury followed by inflammation, proliferation and the last phase is the remodeling/maturation phase.**

The end result of inflammation phase is a 'clean wound bed', allowing the wound to transit to the rebuilding phase [38,39]. However, if the wound fails to resolve due to necrosis and/or infection, the inflammation phase is protracted for a longer duration and healing is delayed [35,40].

3) Proliferation and repair

The third phase of wound healing is the proliferation phase, which begins approximately 3-10 days after wounding. The main focus of this phase is the covering-up of the wound surface with new epithelium, formation of granulation tissue, vascular network restoration, and bacterial barrier due to biofilm formation [14]. Epithelialization, neoangiogenesis and collagen synthesis/ matrix deposition are the key processes of this phase.

Neoangiogenesis

The restoration of the skin's vascular system is a complex cascade of humoral, cellular, and molecular events. This "neoepithelium" is composed of only a few cells but is sufficient to provide a bacterial barrier and to close the wound surface. The process of lateral, vertical, and differential migration continues throughout the proliferative phase and will gradually reestablish the epidermal layer and its functions [40,41]. This new epidermis is slightly thinner than the original epidermis that is the rete pegs (regular protrusions of the epithelial layer that extends into the upper layers of the underlying dermis) that normally exists is lacking as neoepidermis is covering the scar tissue in comparison to normal dermis [37]. The first step is the binding of growth factors produced by the cells present at the wound site for example vascular endothelial growth factor (VEGF), platelet-derived growth factor (PDGF), basic fibroblast growth factor (bFGF) to their receptors on the endothelial cells that activate intracellular signaling cascade to secrete proteolytic enzymes which can dissolve the basal lamina [42]. Provisional matrix is also known to affect the migration of endothelial cells [22]. Thereafter, new vessels

differentiate into arteries and venules. Blood flow through the new blood vessels finally completes the angiogenic process.

Granulation tissue formation

Three to four days post injury, the granulation tissue formation begins as the inflammatory phase subsides [40]. Granular tissue is primarily composed of granulocytes, newly synthesized connective tissue protein (extracellular matrix), macrophages, high-density fibroblasts, and loosely arranged collagen bundle. They replace the fibronectin-based provisional wound matrix to form a new matrix which will fill the wound defect [43]. Fibroblasts in this phase are responsible for the production of ECM substances (proteoglycans, aminoglycans, hyaluronic acid, fibronectin) and collagen. ECM provides a scaffold for the adhesion of cells, which helps organize the movement, growth and differentiation of cells within it [44,45].

Thus, neoangiogenesis is responsible for the formation of new capillaries and restoration of nutrient and oxygen delivery to the wound bed. Simultaneously, connective tissue proteins synthesize the 'new-provisional extracellular matrix' [43].

4) Remodeling/Maturation

The last phase of wound healing is the remodeling or maturation. This phase occurs around day 21 post-injury and continues beyond 1 year. Granulation tissue formation is ceased by consecutive apoptosis and maturation begins [46]. During maturation, the early collagen is characterized by weak tensile strength fibers, which are poorly organized. Three weeks post-injury, the fibers exhibit only 20% tensile strength in comparison to the intact matrix. During mature scar formation, collagen III in

the provisional matrix is converted to collagen I which is different from the basket-weave collagen pattern found in a healthy dermis [47]. Next, myofibroblasts form multiple attachments with collagen, causing a reduction in the surface of the developing wound by contraction [33,34,47]. Imbalance between matrix synthesis and matrix breakdown can lead to serious wound complications [48,49].

1.1.2.3.   Mediators involved in wound healing

In order for the wound healing phases to proceed under normal circumstances, a number of critical cells need to be recruited at the wound site (at an appropriate time) to be able to carry out their functions like re-epithelialization, neoangiogenesis, granulation formation and connective tissue synthesis. Complex array of bioactive molecules, extracellular matrix, regulatory factors, and matrix proteins, control and coordinate the recruitment process of cells [23,50]. The recruitment process is further influenced by environmental factors, co-morbid conditions, nutrient and oxygen availability, as well as co-factors like phagocytosis and collagen synthesis, senescence of cells, and cell-receptor activation [22].

Matrix proteins like matrix metalloproteinases (MMPs), tissue inhibitors of metalloproteinases (TIMPs) and a disintegrin metalloproteinases (ADAMs) are the "controllers" for the activation of growth factors and cytokines at the wound site. These growth factors and cytokines play key roles in recruiting critical cells at the wound site [22]. Matrix proteins are responsible for the "up-regulation" of these critical cells by activating growth factors and cytokines. Simultaneously, they can also "down-regulate" these critical cells by either degrading them or inhibiting their release [22].

Growth factors and cytokines are the bioactive molecules produced at the wound site by critical cells such as neutrophils, fibroblasts, macrophages and platelets. They are responsible for attracting the cells during the healing process by stimulating their proliferation and directing them to complete their

22

functions. For example, VEGF is responsible for the migration and proliferation of endothelial cells, which are essential during neoangiogenesis [23,50].

Regulatory substances such as growth factors, MMPs and cytokines regulate the process of epithelial proliferation and migration by stimulating the cells to respond to them. However, only the cells that have specific binding receptors for these regulatory substances, respond [19,51,52]. Senescence cells also lack the ability to respond to the regulatory substances. Failure to respond results in impaired healing [53].

Extracellular matrix (ECM)

ECM is responsible for providing scaffold to the migrating cells and influencing the response of cells to growth factors. Matrix proteins and integrins found in ECM are responsible for cell migration during the repair process. ECM supports the movement of nutrients, cells, and growth factors to the wound bed and also promotes cell-to-cell communication [21]. Current treatments also incorporate the use of ECM for promoting migration of cells, granulation formation, and re-epithelialization [54,55].

1.2.   ACUTE VS CHRONIC WOUNDS

1.2.1. What makes non-healing wound chronic

1.2.1.1.   Epidemic of chronic wounds

Chronic wounds are a serious health care concern imposing profound clinical, economic, and personal implications [38]. The number of patients with chronic wounds either due to compromised

immune system, or systemic comorbidities like diabetes, malnutrition is increasing, leading to a staggering increase in the economic and financial "burden" in treating these wounds. For too long, the health care management has tried to apply acute care wound healing model (i.e. hemostasis, inflammation, proliferation, remodeling) into chronic wound management but with limited success [56].
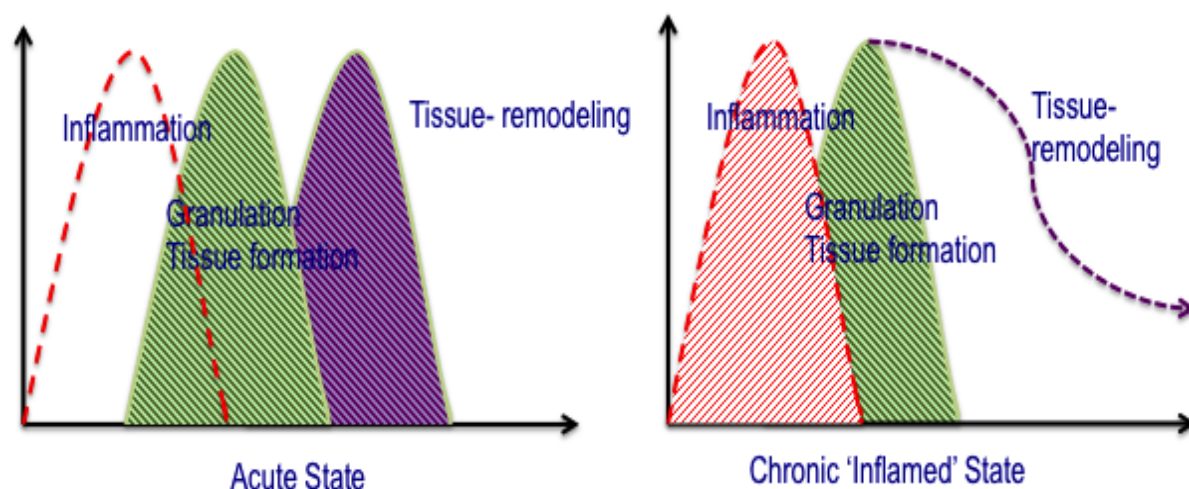
Figure 2. The order and overlap of the acute wound healing phases vs. protracted inflamed phase during chronic wound healing phases. Adapted from [18].

1.2.1.2.   Underlying pathology of acute and chronic wounds

Acute wounds are typically traumatic or surgical in origin characterized by early and late inflammatory responses that occur suddenly, move rapidly and predictably through the repair process

and resolve as healing progresses. In contrast, chronic wounds fail to resolve normally through the repair process and are characterized by an apparent conversion from a "resolving" to a "non-resolving" chronic inflammatory response (Figure 2) [57]. In order to induce resolution, these chronic wounds must be converted to a response that is characteristic of the normal healing wound. In order to understand chronic wounds, attempts have been made to better understand the biochemical components involved in the healing process that are responsible for altering the wound environment [58]. Based on the analysis of the components of chronic and acute wound fluids, the growing consensus is that chronic wounds remain in the inflamed state for a protracted period of time [59]. Tensile strength of acute wound tissue is enhanced primarily by the reorganization of type I collagen, the dominant fibrillar collagen by increased covalent cross-linking of collagen during granulation process which results in restoration of the tensile strength to a maximum of about 80% in comparison to normal unwounded tissue. In contrast, prolonged inflammatory state during chronic wounds prevents the tissue from building its tensile strength by damaging the collagen deposition resulting in an increased risk for wound dehiscence [18].

Chronic wounds are frequently caused by repetitive insults to the tissue, vascular damage, and inflammation that are chronic resulting in the failure of these wounds to proceed through an orderly and timely process to produce an anatomic and functional integrity [60,61]. Hypoxia, local infection, trauma, systemic diseases like diabetes mellitus, malnutrition, immuno-compromised state or medications are most frequently responsible for this non-healing wounds [18]. There has been growing interest in understanding the immune cells suspected to be involved in the healing process because of the predictable sequence of neutrophils, macrophages and lymphocytes migration into the wounds, controlled by a myriad of signaling molecules like cytokines, growth factors and systemic factors such

as steroid levels, nutritional status and perfusion in order to find a proper treatment modality for chronic wounds [38,62].

1.2.2. Acute vs. chronic inflammation- extremes of inflammatory mediators

There is a marked difference between the inflammation of acute and chronic wounds. Under normal acute wound conditions, the inflammatory phase is involved in 'clean-wound bed' preparation by removing the debris, bacterial contaminants, dead tissues as well as activating and recruiting fibroblasts.[18] The inflammation phase should last 3-4 days post injury [63]. In contrast, chronic inflammation serves only to worsen the injury by protracting the inflammatory phase. Tissue trauma due to surgery, bacterial overgrowth, pressure or ischemic condition leads to the activation and recruitment of neutrophils that accelerate inflammation [64-67]. These activated neutrophils are virtually non-existent in acute wounds after the first 72 hours post injury.

Activated neutrophils produce neutrophil elastase as well as matrix metalloproteinases (MMPs) especially MMP-8 [68-71]. In a non-healing chronic wound, abnormal ratio ensues between MMPs and tissue inhibitors of MMPs [20,72]. The inflammatory cells further affect the cytokine profile as the TNFα predominates [70,73] as well as there is reduction in PDGF and TGFβ [28]. The end result is the continuous up-regulation of the inflammatory phase in non-healing wounds. Studies have demonstrated that some fibroblasts also undergo premature senescence that disrupts the wound healing process [74].

Normal healing: Acute wounds

Non-healing: Chronic wounds

Bacterial growth

MMPs

Neutrophil elastase
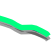
-Fibroblast	-Neutrophil	-Mast cells	-Laminin	-Bacterial biofilm
-Epidermal cells	-Lymphocytes	-Decorin	-Fibronectin	- Neutrophil elastase

Figure 3. Acute vs. chronic wound. Increase in bacterial bioburden and inflammatory mediators in chronic wounds.

1.2.3. Impact of bioburden on wound healing

When the body's greatest defense against infection gets breached, the body fluids and normal skin flora quickly arrive at the wound site. These microorganisms produce exotoxins and endotoxins that alter the normal wound healing activity like collagen deposition. They compete for nutrients and oxygen at the wound site. Extremes of these activities lead to fluid leakage from vasculature, coagulation, increased capillary permeability, and shock [18]. Persistent inflammation ultimately deteriorates into infection. Infections concomitantly lead to pain and suffering of the patients, high hospitalization costs and cause serious complications like multi-organ failure and death. Every wound has some level of bacterial burden called as 'bioburden'. The range of this bioburden determines the severity of the wound infection [75].

Colonies of microorganism adhere to the moist/wet surface of the wound and form a persistent barrier layer of microorganisms called the 'Biofilm' which is resistant to antimicrobials, immunological and chemical attacks [76]. Biofilms generally persist in chronic persistent infections. Multiple species of bacteria have been identified to be residing in chronic wounds [76-80]. In contrast to acute wounds, which have only 6% of documented biofilm, chronic wounds have up to 70% presence of bioburden comprising of various types of microorganisms living in a symbiotic relationship [56]. It is difficult to identity one effective therapy in eradicating this bioburden due to the vast number and variety of microorganisms at the wound site.

1.2.4. Chronic wounds in immune-compromised patients

Chronic wounds are a serious health care concern presenting unique healing challenges specifically to those whose immune system has been compromised. In immuno-compromised patients the common chronic wounds include skin and soft tissue wounds, diabetic foot ulcers, venous stasis ulcer and pressure ulcers [81]. Contaminated wound site can successfully resist invasive infection. In contrast, immuno-compromised patients face unique healing challenges where the infection frequently ensues leading to excruciating pain and debilitation that can undermine the morbidity associated with the severely impaired healing process. Healing wounds in immuno-compromised patients demographically can be quite challenging. When assessing a wound, many factors need to be taken into consideration like comorbidities, nutritional and compliance status of the patient. Increase in any of these factors, directs to know that the wound is chronic as the patient is immuno-compromised [56].

1.3. CURRENT TREATMENT MODALITIES

Wound care needs may change frequently throughout the various phases of healing. Therefore a variety of treatment options are currently available. The selection of an appropriate treatment agent is based on the correct identification of the chronic wound etiology as well as the local and systemic factors that may contribute to the impaired healing. Traditional strategies for the treatment of chronic wounds have shown limited success. The difficulties to treat chronic wounds have been underscored by the limited success of growth factors and the failure of many agents, during clinical trials [82]. Ischemic preconditioning, anti-inflammatory agents, anti-oxidants complement therapy have shown promising potential but still lack in proper clinical trial evaluation [40,83]. Research on the combination role of growth factors has shown modest increase in wound healing if not synergistically [83].

Currently, the potential for developing an effective, and long-term therapeutic that will act for a prolonged period of time, still remains to be proposed. Chronic wounds being multifactorial in etiology mean that a single agent may prove to be ineffective. Although wound infection will heal with antimicrobial therapy, many particularly in immuno-compromised or anatomically compromised hosts will process to deep wound exudate [18]. Wound healing agents such as the cytokines/chemokines, hyaluronic acid/collagen, growth factors have drawbacks such as the induction of adverse events, as they are not constrained to one specific cellular type [18]. The most deceptively simple of all therapeutic procedures is the use of topical antibiotic therapy but this therapy cannot be used for a longer duration due to the likelihood of these agents losing their effectiveness due to the emergence of resistant organisms [84-86]. Furthermore, recent studies have demonstrated that in many chronic wounds bacteria may persist in adhesive, polymeric matrix film.

Newer treatment options such as cadexomer-iodine [87-90] and silver compounds [91,92] have been gaining attention as topical antiseptics in various types of wound dressing as they have proven efficacies against methicillin-resistant staphylococcus aureus (MRSA). Silver nanoparticles containing dressing has been widely tested in vitro for its wound healing potential. However, recent studies showing the possible toxic effects of silver on human fibroblasts and keratinocytes have rendered it to be unsafe in wound healing [34,35]. Carter et.al, reported that there is some wound healing effects of silver-impregnated dressings when used short term but the long term effects still remain unclear [93].

1.4. POTENTIAL OF TOPICAL COMBINATION NANOMEDICINE

1.4.1. Neutrophil elastase inhibitor- serpin A1 as a potential wound healing agent

Patients suffering from chronic wounds remain in the inflamed state for protracted period of time and are unable to undergo normal healing process. Elastase is one of the major components released from neutrophils under inflammatory conditions, which is responsible for the degradation of fibronectin and cartilage matrix proteoglycans [54,94]. Elastase plays a role in the degradation of foreign microorganisms that are phagocytosed by neutrophils and are also involved in the modulation of cytokine expression at the epithelial and endothelial surfaces, influencing the initiation of the adaptive immune response [95]. However, upon upregulation of cellular activation, elastase is one of the major pathological factors involved in the development of severe chronic inflammatory conditions [95]. Persistent expression of high levels of unregulated proteinases at the wound site contributes significantly to the chronic condition of wounds [96]. It has been reported that chronic non-healing wound fluid under inflamed phase has ten to forty fold higher levels of elastase (3 to 8 mU/mg protein) released from neutrophils in comparison to AW fluids (0.1 to 0.3 mU/mg of protein) [56,57]. Thus, it can be postulated that lowering the level of elastase in chronic wounds to a level normally found in acute wounds may accelerate the healing process. This can be accomplished by either controlling the release of the elastase inhibitor or by the elastase sequestration from the wound fluids to achieve neutralization of high levels of elastase. Interestingly, serpin A1 (A1) also known as α1 anti-trypsin/anti-proteinase is a major physiological elastase inhibitor and immuno-modulator that is found to be degraded and non-functional in CW fluids but is active and functional in AW fluids [97]. Because of the strong elastase inhibition, due to its ability to effectively inhibit elastase, serpin A1 seems to be a powerful anti-inflammatory agent in CW healing.
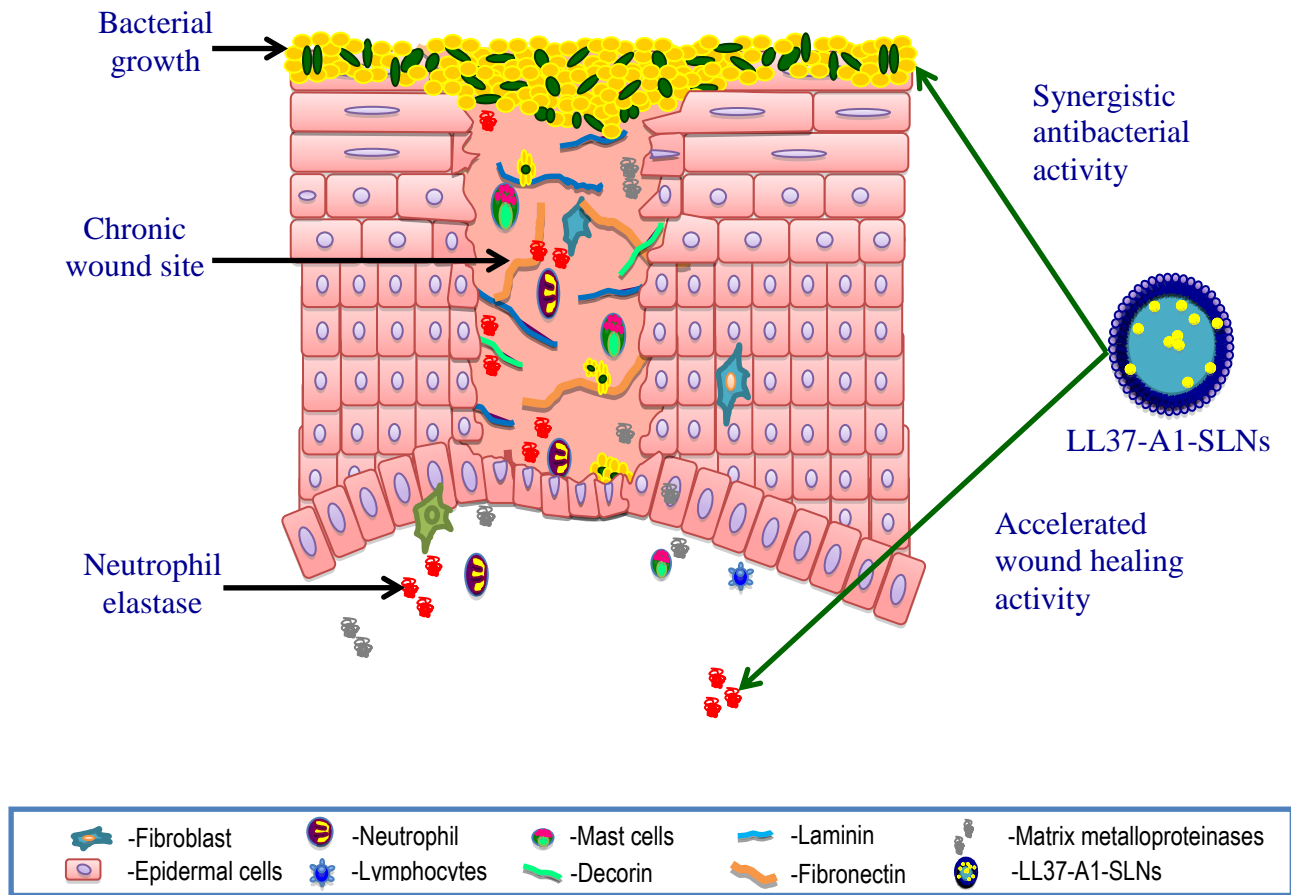
Figure 4. Schematic representation of the potential LL37-A1-SLNs in promoting accelerated chronic wound healing and enhancing antibacterial activity. The figure represents a chronic wound site producing high levels of provisional matrix components (fibronectin, laminin and decorin) preventing the migration and proliferation of fibroblast cells and keratinocytes. Over production of inflammatory cytokines and chemokines stimulate the production of more matrix metalloproteinases (MMPs) and neutrophil elastase which prolongs the inflamed state and prevents timely healing. LL37-A1-SLNs can potentially accelerate timely healing by reducing the over-inflamed state as well as demonstrating antibacterial activity against bacterial growth.

1.4.2. Host defense peptide LL37 as an anti-microbial agent

LL37 belonging to the cathelicidin family is a host defense peptide/antimicrobial peptide that has been described to be an important mediator of the body's innate immune system by demonstrating first line defense against invading pathogens [98]. From the cathelicidin family, LL37 is the only antimicrobial peptide that is identified to be present in humans and is overly expressed in keratinocytes and neutrophils of the inflamed skin [69,99-101]. LL37 is an immunomodulator with broad physiological activities including: antiviral, antifungal, antimicrobial, endotoxin-binding properties, modulator of the inflammatory response, and is a promoter of wound healing by influencing cell proliferation and differentiation [102]. It has also been suggested that LL37 plays a role in the process of re-epithelialization [103]. LL37 has previously been shown to induce the healing of epithelial wounds in the airways by chemotaxis and by stimulating the proliferation of epithelial cells [104]. Wound healing activity of LL37 has been attributed to its ability to induce the migration of keratinocytes via EGFR transactivation [105]. LL37 and LL37-derived peptides have demonstrated potent inhibitory activity in preventing multidrug-resistant bacterial infections and biofilm formation, thereby contributing to the resolution of infections and maintenance of epithelial barrier function [106-108]. Multiplicity of their diverse mechanisms of action is a major reason in restricting the development of resistant strains.

1.4.3. Nanoparticles for topical delivery of peptides

Despite certain advantages proteins/peptides may have over conventional small molecule drugs [109], they are prone to lose their conformation and native structure due to disruption/non-covalent

interactions such as aggregation, precipitation and adsorption. Proteolysis, oxidation, deamidation and β-elimination lead to the cleavage of peptide bonds and destroy the amino acid residues [110]. Nanoparticles can specifically diminish these issues by offering protection to the protein/peptide mainly by reducing their toxicity levels, preventing their degradation and improving their bioavailability [110]. Drug delivery systems that can precisely control the release of drug as well as target the drug to specific sites in comparison to systemic delivery may improve therapeutic outcomes.

The therapeutic potential of proteins/peptides is gaining increasing attention recently. The American association of pharmaceutical researchers and manufacturers (PhRMA) has identified 418 protein/peptide based 'Biotechnology medicines in development' which are in human clinical trials or under United States Food and Drug Administration (FDA) review for over 100 diseases including chronic diseases [111]. However, obstacles in the delivery often hamper the therapeutic potential of protein/peptide drugs [112-115]. Due to their native structure, proteins/peptides are prone to degradation due to environmental factors like ionic strength, temperature, pressure, adsorption, agitation, non-aqueous solvents, pH, detergents and metal ions [113,116]. The stability of proteins is due to the balance between destabilizing and stabilizing forces. Disruption in any of these interactions shifts the balance between these factors [115].

At the site of injury, the physiological concentrations of serpin A1 are around 20-50 μM [97]. Thus, maintaining this concentration at the chronic wound site for a prolonged period of healing could be achieved using the controlled release from the nanoparticle formulation. The direct anti-microbial activity of LL37 is rather weak under physiologically relevant conditions and significant proportion of this peptide loses its activity since it is antagonized by monovalent and divalent cations, serums and polyanions. The nanoparticles will preserve the biological activity of these peptides during acceptable shelf lives and ideally offer effective and safe delivery to the active wound site.

1.4.3.1.   Solid lipid nanoparticles
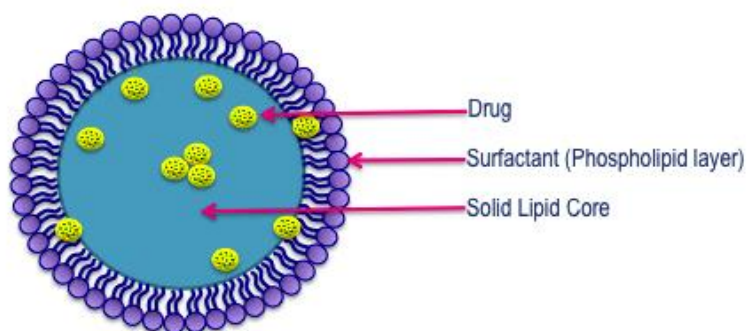
Figure 5. Structural representation of a solid lipid nanoparticle (SLN)

Solid lipid nanoparticles (SLNs) have been gaining increasing attention and interest in the scientific community as alternative carrier system to polymeric nanoparticles, liposomes, emulsions, and microparticles [117-119]. SLNs are colloidal carriers ranging from 50 to 1000 nm in size, composed primarily of a solid lipid core (high-melting lipids or waxes) dispersed in an aqueous surfactant solution at room temperature (Figure 5) [118,120]. They offer distinct advantages of large surface area, small size, improved tissue distribution, high drug loading of both hydrophilic and lipophilic drugs at optimum conditions, and the possibility to modulate drug release [121-124]. SLNs can be prepared by various techniques such as high-pressure homogenization, ultra-sonication, solvent-evaporation, solvent emulsion diffusion method, supercritical fluid method, spray drying, double emulsion, micro-emulsion, precipitation technique and film-ultrasound dispersion [117,124-127].

SLNs are ideal for protein/peptide delivery, as their formulation does not employ toxic organic solvents, which may have deleterious effects on the protein/peptide [128,129]. Researches where SLNs

have been used for the topical delivery of drugs have already reached clinical trials, while some are already in the market like Dr. Rimpler, NanoRepair Q10[®] [128-130]. Various therapeutically relevant peptides such as cyclosporine A, insulin, calcitonin, somatostatin, hepatitis B, bovine serum albumin and luteinizing hormone-releasing hormone (LHRH) have already been investigated for SLN-based delivery [127]. The versatility of SLNs suggests that they can potentially be effective carrier systems for the topical delivery of therapeutic peptides in chronic diseases including chronic wound healing.

1.5. RATIONALE

The difficulty to treat chronic wounds has been underscored by the limited success of growth factors and the failure of many agents, during clinical trials [82]. Chronic wounds being multifactorial in etiology mean that a single agent may prove to be ineffective. Although topical anti-microbials, antiseptics, antibiotics, surgical debridement, ischemic preconditioning, anti-inflammatory agents and anti-oxidant complement therapies are some of the current strategies in the management of chronic wounds, proper clinical trial evaluations are still lacking [83]. Specifically, research involving immuno-compromised hosts, where the infection has progressed to deeper wound beds is currently unclear. Common wound healing agents such as growth factors, cytokines/chemokines, hyaluronic acid/collagen, have drawbacks such as the induction of adverse events, as they are not constrained to one specific cellular type [131]. Thus, new paradigms for CWs that elucidates the cellular and biochemical events are urgently required. Combination therapy involving immuno-modulatory peptides may prove to be effective in resetting the chronic inflamed phase back to an acute healing phase. Keeping the inflamed phase low, the wound will then be able to progress forward and begin to heal [58]. Providing continuous delivery of drugs to an active wound site over a prolonged period of time is challenging, resulting in poor patient compliance due to the need for repeated applications. The use nanoparticles (nano-sized drug carriers) can overcome these obstacles and provide a platform for

controlled, sustained release and protect the peptides from degradation, resulting in complete rapid wound healing.

1.6. HYPOTHESIS

We hypothesize that the potential of combining the immunomodulatory peptides LL37 and A1 into a single nanoparticle formulation will accelerate chronic wound healing and enhance antibacterial activity, in comparison to individual drugs alone.

Combination therapy may prove to be effective in resetting the chronic inflamed phase back to an acute healing phase.

1.7. RESEARCH OBJECTIVES

Aim 1: To design, develop and characterize a novel nanoparticle formulation for the combination delivery of LL37 and A1.

Aim 2: To determine *in vitro*, the release profile of these peptide-encapsulated nanoparticles and perform *ex vivo* skin permeation studies.

Aim 3: To evaluate and confirm the *in vitro* potential of these dual peptides in accelerating wound healing and evaluate their synergistic anti-microbial properties.

Aim 4: To evaluate the wound healing property of LL37-A1-SLNs in a murine mice model.

CHAPTER 2: MATERIALS AND METHODS

Peptides

Serpin A1 (α1 antitrypsin, antiproteinase) isolated from human plasma was obtained from Athens Research and Technology (cat# 16-16-011609; GA, USA) (Table 2). LL37 (host defense peptide) (Table 2) was a purchased from (custom synthesized by CPC Scientific Inc., CA, USA)

Table 2. Sequence of peptides used in the current study

Peptide	Theoretical molecular mass	Amino-acids	Sequence
LL37	4.5 kDa	37	LLGDFFRKSKEKIGKEFKRIVQRIKDFLRNLVPRTES
Serpin A1	52 kDa	394	LYHSEAFTVNFGDTEEAKLQHLENELTHDIITKTDTS HHDQDHPTFNKLYHSEAFTVNFGDTEEAKK

2.1.   HPLC method for LL37 and A1 quantitation

Chromatographic separation was performed on a XBridge™ BEH300 C18 Column (300 Å, 5μm, 3.9 mm x 150 mm; Waters, MA, USA) at 60°C protected by a Symmetry C18 guard column (300 Å, 5 μm, 3.9 × 20 mm; Waters, MA, USA), fitted to a Waters® Alliance® HPLC system equipped with Waters® 2690 Separation module and Waters® 996 Photodiode Array detector. Detection was performed with a tunable UV-Visible detector Waters 486 working at 210 nm which is connected to the liquid chromatography (LC) systems. The concentrations of LL37 and A1 were determined using a gradient elution HPLC-method with slight modifications [132]. Mobile phase A: 90% deionized water (v/v), 10%

acetonitrile (v/v) (HPLC grade; EMD Serono, MA, USA); 0.01% trifluoroacetic acid (v/v) (EMD Serono, MA, USA); mobile phase C: 90% Acetonitrile (v/v), 10% deionized water (v/v), 0.01% trifluoroacetic acid (v/v); the linear gradient was increased from 85% Phase A to 99% within the first 8 min and then decreased to the start conditions during the last 2 min. Total run was 12 min for each 200 μL injection. The flow rate was 2 mL/min and the analysis was conducted at 60°C. LL37 and A1 solutions of known concentrations (0.065-20 μg/mL) were used to generate calibration curves. This method was checked with respect to linearity ($r^2 > 0.99$) and LL37 and A1 were quantitated using area under the curve (AUC).

2.2. Fabrication of LL37-A1 encapsulated SLNs

Preparation of SLNs is based on the emulsion solvent diffusion method in water as previously described with slight modifications whereby a water/oil/water (w/o/w) double emulsion was introduced into the method [133,134]. Briefly, glyceryl monostearate (molecular weight 358.56 g/mol, Sigma-Aldrich, ON, Canada) (10 mg) and ∝-L-phosphatidylcholine (Soy-95%) (Molecular weight 770.123 g/mol; Avanti Lipids, AL, USA) (20 mg) were dissolved completely in a mixture of equal volumes (1 mL) of acetone and ethanol (HPLC grade; EMD Serono, MA, USA) at 55°C. LL37 and A1 were dissolved in 100 μL of deionised water and added to the lipid mixture under continuous sonication for 30 sec by a microtip probe sonicator (Branson sonifier 150D; QSonica, CT, USA) to form a w/o primary emulsion. The resultant w/o emulsion was then emulsified with an aqueous phase solution containing 2% poly vinyl alcohol (PVA; molecular weight 31-50 kDa; Sigma-Aldrich, ON, Canada) (10 mL) for 50 sec under continuous sonication to form a w/o/w secondary emulsion. The resultant dispersion was then stirred overnight at 4°C to evaporate the organic solvent. LL37 and A1 encapsulated SLNs (LL37-A1-

SLNs) were collected by centrifugation (20,000g, 40 min, 4°C) (Sorvall RC6+; Thermo Fisher Scientific, ON, Canada) and washed twice with autoclaved Milli-Q water. Two SLN formulations loaded with varying concentrations of LL37 and A1 were prepared: prep 1= 100 µg of LL37 and 500 µg of A1; prep 2 = 200 µg of LL37 and 750 µg of A1.

SLNs were re-suspended in a 25% trehalose solution, stored at -80 °C for 5 h and then freeze-dried for 12 h (FreeZone 2.5-L freeze-dry system; Labconco, MO, USA). Recovery of SLNs was defined as the weight ratio of the freeze-dried SLN to the initial theoretical weight and calculated from the following equation:

$$Recovery = \frac{Actual\ weight\ of\ SLN}{Theoretical\ weight\ of\ SLN} \times 100$$

2.3. LL37-A1-SLNs characterization

2.3.1. Particle Sizing and Zeta Potential Measurements

Lyophilized SLNs were re-suspended in autoclaved Milli-Q water (25 µg/mL) and its size was measured by dynamic light scattering (ZetaPALS, Brookhaven Instruments, NY, USA). Measurements were obtained at a 90° fixed-angle and scattering intensity data was analyzed by a digital correlator and fitted by the method of inverse Laplace transformation. Measurements were made in triplicate at room temperature for three runs of 2 min each. The net surface charge of SLNs was determined by zeta

potential measurements (100 µg/mL; Smoluchowski mode) (ZetaPALS, Brookhaven Instruments, NY, USA). LL37-A1-SLNs and blank SLNs were re-suspended in autoclaved Milli-Q water (pH 7). Measurements were performed in triplicates at room temperature for three runs of 2 min each.

2.3.2. LL37 and A1 encapsulation efficiency (EE%)

To determine the EE% of LL37 and A1 in LL37-A1-SLNs, the amount of un-encapsulated LL37 and A1 in the wash solutions was quantified using HPLC. Encapsulation efficiency was determined using the following equation:

$$\text{Drug Encapsulation Efficiency (\%)} = \frac{(\text{Amount of total drug in } \mu g) - (\text{Amount of unentrapped drug in } \mu g)}{\text{Amount of total drug in } \mu g} \times 100$$

2.4. *In vitro* drug release profile

The release rates of LL37 and A1 were determined in artificial wound fluid (AWF; pH 7.4; consisting of 2% bovine serum albumin (BSA), 0.02 M calcium chloride, 0.4 M sodium chloride, and 0.08 M tris methylamine in deionized water) [135]. BSA, calcium chloride anhydrous, and tris methylamine were purchased from Amresco, OH, USA. Sodium chloride was purchased from Fisher Scientific, ON, Canada. Briefly, 10 mg post-lyophilized LL37-A1-SLNs were re-suspended in the release media and maintained at 37 °C on an orbital shaker at a speed of 100 rpm (VWR, AB, Canada). Over a period of 15 days, the samples were centrifuged at different time points and 200 µL of release medium was removed and replenished with equal volumes of fresh medium [136]. After filtering the samples through a

0.2 µm GHP filter (Pall, ON, Canada), the concentration of LL37 and A1 released was quantified using HPLC

2.5. *Ex vivo* skin permeation studies

The animal care and ethical committee of University of Manitoba approved the entire animal study. In accordance to the guidelines from the Canadian Council on Animal Care, female New Zealand white rabbits (4-4.5 kg, 6-8 months old; Charles River) were sacrificed, ears removed, and the skin from the inner side of the ear (where the pinna is located) was peeled away from the underlying cartilage. Skin samples were washed twice with saline solution (0.9% NaCl) and stored at -80 °C (for no longer than 4 weeks). Studies have shown that there were no differences in tissue integrity between fresh and frozen samples [137]. Before initiating the permeation studies, the skin samples were allowed to equilibrate with buffer solution for at least 12 h. The skin was mounted onto a modified Franz diffusion cell (model # FDC-6 at 05 amplitude and 60 Hz; Logan Instruments, NJ, USA) and clamped carefully between the receptor and donor compartment. 5 mL of AWF (pH 7.4) was filled in the receiver compartment and the diffusion cells were maintained at 37 °C by a circulating water bath. The AWF in the receiver compartment was stirred continuously at 500 rpm/min. Prep 1 (10 mg/mL) and prep 2 (10 mg/mL) suspended in 1 mL of AWF pH 7.4 were added to the donor compartment and covered with Parafilm® (VWR, AB, Canada) to prevent evaporation. At specific intervals, 500 µL of receiver solution was withdrawn from the receiver compartment and replaced with fresh AWF. The drug concentrations in the samples were analyzed by HPLC. The influence of temperature and AWF on the stability of LL37 and A1 was evaluated over 5 days. Samples were incubated in 5 mL of AWF (pH 7.4) at 37 ºC and stirred at 500 rpm/min. At specific time intervals, 500 µL of the medium containing the peptides was withdrawn and replaced with equal volume of fresh AWF (pH 7.4). The concentrations of LL37 and A1 in the samples were analyzed using HPLC.

2.6. __Antibacterial studies__

Antibacterial activity was evaluated against gram-positive *Staphylococcus aureus* subsp. *aureus* rosenbach (*S. aureus*) (ATCC 25923) and *Escherichia coli* (Migula) Castellani and Chalmers (E.coli) (ATCC 25922) cultured in tryptic soy broth number 2 (catalogue # 51228-500G-F) and stored at 4 ºC on tryptic soy agar (catalogue # 22091-500G) and mannitol salt phenol agar (catalogue # 63567-500G F) purchased from Sigma-Aldrich, respectively. The minimum inhibitory concentrations (MIC) of LL37 and A1 were determined by the broth microtiter dilution method. Briefly, 100 μL of tryptic soy broth was added to each well of a 96-well plate. Treatment groups included prep 1 (2 mg/mL), prep 2 (2 mg/mL), LL37 only (5 μg/mL), and A1 only (20 μg/mL). To each well, 10 μL of 10^7 colony forming units (CFU)/mL bacteria were added. Positive control included cells treated with 10 μg/mL of ampicillin and negative control included cells treated with 10 μL of PBS (pH 7.4). The plates were incubated at 37 °C for 20 h and the Optical density (OD) was measured at 620 nm using a spectrophotometer. Synergistic potential of the drug combination was assessed using a checkerboard method with a modified dilution scheme. [138] We first titrated LL37 and A1, and then determined the concentration at which these peptides could not exhibit significant antibacterial activity when used alone and these concentrations were further used for combination experiments. Briefly, two-fold serial dilutions of each drug (LL37 and A1) up to at least double the MIC were prepared. A total of 50 μL of tryptic soy broth was added into each well of a 96-well plate. The first drug (LL37) was serially diluted along the coordinate while the second drug (A1) was diluted along the abscissa. Each well was inoculated with 10 μL of 10^7 CFU/mL of bacterial inoculum and the plates were incubated at 37 °C for 20 h. After the addition of alamarBlue (DAL 1025; Thermo Fisher, ON, Canada) (10 μL) to each well, cells were further incubated at 37ºC for 4 h. The OD was read at 565 and 595 nm using a microplate reader. Synergy was calculated based on the degree of drug interaction in terms of synergism for a

given endpoint of the effect measurement using compusync Chou-Talalay combination index (CI) measurement by the following equations:

Eq. 1: $D = Dm\left[\dfrac{fa}{1-fa}\right]^{\frac{1}{m}}$

Dm for each drug was determined based on the median-effect equation 1, which was derived from the median-effect principle of the mass-action law. The dimensionless value as specified by Eq. 2 and Eq. 3 are termed the "Combination Index" (CI).

Thus, when D1: D2 = P: Q for $D_{1,2}$ = D1 + D2, we can obtain the two-drug combination index algorithm using the equation 2:

Eq. 2: $CI = \dfrac{D_{1,2}\left(\frac{P}{P+Q}\right)}{(Dm)_1\left[\left(\frac{fa}{fu}\right)^{\frac{1}{(m)_1}}\right]} + \dfrac{D_{1,2}\left(\frac{P}{P+Q}\right)}{(Dm)_2\left[\left(\frac{fa}{fu}\right)^{\frac{1}{(m)_2}}\right]}$

Where fa is the fraction affected; fu is the fraction unaffected $(1- fa) = fu$; D is the dose of drug; Dm is the dose required to produce a median-effect; and m is the slope of the median-effect plot signifying the shape of the dose-effect curve.

Eq. 3: $CI = \dfrac{(D)1}{(D_x)1} + \dfrac{(D)2}{(D_x)2}$

Where in the numerators, (D)1 and (D)2 are the combination doses of drug 1 and drug 2 that inhibits x%. In the denominators, $(D_x)1$ and $(D_x)2$ are the doses of individual drug 1 and drug 2 that inhibits x%. Where, CI = 1 indicates additive effect, CI < 1 indicates synergism, CI > 1 indicates antagonism.

2.7.   Cellular Assays

BJ fibroblast cells (ATCC CRL-2522) were cultured in eagle's minimum essential medium (EMEM) (ATCC-30-2003) supplemented with 10% heat-inactivated FBS along with 1% penicillin-streptomycin (Lonza). Primary human epidermal keratinocytes (ATCC PCS-200-011) were cultured in dermal basal medium (ATCC-PCS-200-030) supplemented with 1% v/v solution of antibiotics (10 units/mL of penicillin, 10 µg/mL of streptomycin, 25 ng/mL of amphotericin B) and keratinocyte growth kit (ATCC PCS-200-040).   BJ fibroblast cells and keratinocytes were cultured between 80-90% confluence at 5% CO_2 and 37°C before passaging, and the medium was changed every two days. BJ fibroblast cells and keratinocytes were used between passages four to six. Based on the synergistic combination ratios (Table 1), the concentration of prep 1 and prep 2 selected for studies will provide a 24 h release profile maintained between 2.5 – 5 µg/mL for LL37 and 10 – 20 µg/mL for A1. In order to compare prep 1 and prep 2 with the individual activities of LL37 and A1, the highest concentration of LL37 (5 µg/mL) and A1 (20 µg/mL) were selected for all cellular assays.

2.7.1. *In vitro* cellular cytotoxicity studies

Cellular cytotoxicity was determined using the CellTiter 96® Aqueous One Solution Cell Proliferation Assay (MTS; Promega, WI, USA). BJ fibroblast cells and keratinocytes were seeded in a 96-well microtiter plate at a concentration of 5 x 10^5 cells/well in 100 µL culture medium. After 24 h, varying concentrations of prep 1 (0.156 mg/mL to 20 mg/mL), prep 2 (0.156 mg/mL – 20 mg/mL), blank SLNs (5mg/mL), LL37 only (0.781 µg/mL – 100 µg/mL), and A1 only (0.781 µg/mL – 100 µg/mL), premixed with culture media were added to the cells in triplicate wells and were incubated for 24 h in

5% CO_2 at 37°C. Negative control (NC) was blank cell medium and positive control (PC) was 1% triton in cell media. At the end of the treatment periods, cells were washed with phosphate-buffered saline (PBS pH 7.4) (Lonza) and replaced with fresh cell media containing 20 μL of MTS. Following incubation for a period of 4 h, the plates were analyzed on a microplate reader (BioTek, VT, USA) at 490 nm.

2.7.2. *In vitro* wound healing assay

BJ fibroblast cells and keratinocytes were each seeded in 24-well plates and incubated for 24 h in 5% CO_2 at 37°C until they were over 90% confluent. Cells were serum-starved for 12 h and then were wounded using a sterile 200 μL pipette tip. The wells were washed twice with PBS (pH 7.4) to remove any adhering cell debris. Cells were cultured at 37°C in serum-starved medium containing the 2 combination concentration ratios of LL37-A1-SLNs (3 mg/mL of prep 1 and 3 mg/mL of prep 2), blank SLNs (5 mg/mL), LL37 only (5 μg /mL), A1 only (20 μg/mL) and untreated cells in serum-starved medium as well as untreated cells in serum-rich medium (with growth stimulating factors) as negative and positive controls, respectively. For cell membrane staining, DiO dye (3,3′-Dioctadecyloxacarbocyanine perchlorate) (catalogue # D4292, Sigma-Aldrich, ON, Canada) was used at a final concentration of 2 μM dye for 1 x 10^7/mL cells in FACS solution. The adherent cells were incubated with the dye solution for 30-45 min. The staining reaction was stopped by aspirating the dye solution and the washing the cells twice with PBS (pH 7.4). Images of the *in vitro* wounds were taken at 0 h, 12 h, and 24 h with a fluorescent microscope (Nikon TE2000) and the average extent of "healing" was evaluated by measuring the width of wound closure (the distance migrated by the cells into the denuded area). Similarly, images of the *in vitro* wounds were also taken at 0 h, 12 h, and 24 h

with a phase contrast microscope and the average extent of "healing" was evaluated by measuring the width of wound closure and was analyzed using Image J software.

2.7.3. Cellular monolayer integrity

Integrity of the BJ fibroblast cells and keratinocytes each grown as monolayers on Millicell- 24 cell culture inserts (12 mm in diameter, 0.4 μm membrane pore size; Millipore) was evaluated by measuring transepithelial electrical resistance (TEER) using a millicell ERS-2 epithelial volt-ohm meter (Millipore) attached to a STX01 electrode (Millipore). The cells were seeded onto cell culture inserts at a density of 2 x 10^5 cells/well containing 400 μL of growth medium, while the culture plates were filled with 800 μL of growth medium. The cells were allowed to grow on the inserts until they formed a confluent monolayer. The cells were then exposed for 24 h with LL37-A1-SLNs (3 mg/mL of prep1 and 3 mg/mL of prep 2), LL37 only (5 μg/mL), and A1 only (20 μg/mL). Controls include untreated naïve cells (negative control) and LPS treated cells (positive control) (10 μg/mL; pH 7.4). The electrical resistance of the insert without skin (blank resistance) was subtracted from the experimental values and TEER was calculated using the following formula:

TEER = resistance x area of the insert (Ω x cm^2)

2.7.4. Measurement of cytokine and collagen-I production in LPS-activated BJ fibroblast cells and keratinocytes

Briefly, BJ fibroblast cells and keratinocytes were each seeded at a density of 5 x 10^5 cells/well in 24-well plates and incubated for 24 h in 5% CO_2 at 37°C until over 90% confluent. The cells were then exposed for 24 h with the combination concentration ratios of LL37-A1-SLNs (prep 1 and prep 2) as well as LL37 only (5 μg/mL) and A1 only (20 μg/mL). Controls including untreated naïve cells (negative control) and LPS only treated cells (positive control) were exposed to sterile PBS (pH 7.4). LPS, which was prepared in sterile PBS (pH 7.4), was then added to each treatment group at a final concentration of 10 μg/mL, except for the negative control group (naïve cells treated with PBS alone). After incubation for 24 h, supernatants from cell cultures were collected and analyzed for IL-6, IL-1β, TNF-α, and collagen-I concentrations using ELISA (R&D Systems, MN, USA).

2.8. *In vivo* wound healing model

Five to eight week old balb/c male mice (Charles River) were randomly selected and grouped following the standardized animal experimental protocols. Mice were anesthetized with isofluorane and the dorsal area was shaved using an electric shaver. Full-thickness wounds excisional wounds were created on the back of the mice on either side of the dorsal midline approximately 5 mm distance between them using 5 mm round single skin biopsy punch (Catalog # 10192-404; VWR, AB, Canada). Two 0.5-mm-thick polymer donut-shaped splints were fixed centering the wound using krazy glue. The splints were used in order to minimize contraction of the skin and mimic human wound healing [139]. Temperature and relative humidity (RH) of the animals were maintained constant throughout the study period. The animal study was approved by the animal care and ethical committee of University of Manitoba.

Mice were randomly assigned into groups (n=3) and treated on day 0, 5 and 9 with either 1) Prep 2, 2) LL37-SLNs, 3) A1-SLNs, 4) LL37-A1-only, 5) Blank-SLNs, 6) untreated, to evaluated the % wound closure. The wounds were dosed with 50 µL of the respective treatment groups and were covered with transparent sterile semi-occlusive dressing (Tegaderm 3M, 2-3/8 inches X 2-3/4 inches), followed by adhesive bandage. On day 5, 9, and 13 the wounds were photographed and the wound thickness was measured. Wound sizes were expressed as percentage of the respective initial wound.

2.9. <u>Histology and Immunohistochemistry</u>

2.9.1. Hematoxylin and eosin (HE) and Masson's trichrome (MT) staining

On day 13, the animals were sacrificed and wounds along with the surrounding tissue were collected and bisected into three halves for further experiments. The wound halves (n=3) were immediately fixed with paraformaldehyde (4% PBS, 0.01 M, pH 7.4) and after 24 h the samples were transferred to PBS buffer at 4 ºC. Wound tissue was embedded in paraffin blocks and sequentially sectioned at 5 μm. Skin sections will be stained with HE to assess the predominant stages of healing and with MT green staining to study the extent of collagen deposition in healed tissue during the course of wound healing. Images will be taken respectively.

2.9.2. CD-31 marking

The wound halves will be embedded in Tissue-Tek O.C.T. compound and frozen. Sections will be cut at 10 μm thickness using a cryostat. An antibody directed against the murine endothelial cell surface marker (CD-31) will be used to determine the extent of endothelial cell colonization in the wound sections. After permeabilization (Triton X-100 0.1% (v/v) in PBS) and blocking (5% (w/v) BSA in PBS), the primary antibody at 1: 50 dilution (rabbit anti-CD-31; catalog # ab28364, Abcam, ON,

Canada), will be applied overnight at 4 °C. Secondary antibody (Alexa Fluor® 488 at 1: 500 dilution (goat anti-rabbit IgG H&L; catalog # ab150077, Abcam, ON, Canada), will be used to visualize the antigen. A microscope will acquire images of tissue sections. Red fluorescence of CD-31+ will be quantified using imageJ software. Results were expressed as percentage of red pixels over the analyzed surface area [140].

2.9.3. Collagen (Sirius Red/Fast Green) assay

The homogenate of wound tissue will be used to measure the total collagen content (type I–V) and non-collagenous proteins colorimetrically using a Sirius Red/Fast Green Assay kit (catalog # 9046, Chondrex; WA, USA) following the manufacturer's instructions. Briefly, frozen tissue sections will be sliced using a cryostat of approximately 30-50 nm^2, 10 μm thicknesses and will be wasked three times with PBS for 15 minutes each time at room temperature. The tissue sections will then be completely immersed in Kahle fixative (solution containing a mixture of distilled water, ethanol, formaldehyde, and acetic acid) and incubated for 10 minutes at room temperature. The sections will then be washed with PBS and immersed in dye solution for 30 minutes at room temperature. The dye solution will be completely rinsed with distilled water and the tissue sections will be observed under the microscope. The dye from the tissue sections will then be extracted using the extraction buffer and the OD of the collected elute will be read using a spectrophotometer at 540 nm and 605 nm respectively. The amount of collagen and non-collagenous proteins in tissue sections will be calculated based on the following equation. Collagen concentrations will be expressed as μg collagen per section of the tissue.

$$\text{Collagen (μg/section)} = \frac{[\text{OD 540 value} - (\text{OD 605 value} \times 0.291)]}{0.0378}$$

$$Non - collagenous\ proteins\ (\mu g/section) = \frac{[OD\ 605\ value]}{0.00204}$$

Statistical Analysis

The values are expressed as the mean ± standard deviation. One-way ANOVA followed by Bonferroni's post hoc test was performed in order to determine significant differences between the study groups (* *P<0.05* and ** *P<0.01*, and *** *P<0.001*).

CHAPTER 3: RESULTS

3.1. <u>Physicochemical characterization of SLNs</u>

3.1.1. Particle size, zeta potential and encapsulation efficiency %

Particle size, zeta potential, and encapsulation efficiency (EE%) of LL37-A1-SLNs are presented in Table 3. In our study, the average diameter for LL37-SLNs was 232.2 ± 7.8 nm and for A1-SLNs was 210 ± 5.6 nm. Formulating both LL37 and A1 as a combination nanoparticle resulted in a slight increase in the diameter of prep 1 to 214.9 ± 2.2 nm and prep 2 to 261.7 ± 4.4 nm. All of the SLN formulations were able to achieve >80% EE% and exhibited a net negative surface charge.

Table 3. Particle size, Zeta potential and EE% of LL37-A1-SLNs, LL37-SLNs, and A1-SLNs

	LL37-SLNs	A1-SLNs	LL37-A1-SLNs (Prep 1)	LL37-A1-SLNs (Prep 2)
Size (nm)	232.2 ± 7.8	210 ± 5.6	214.9 ± 2.2	261.7 ± 4.4
Zeta potential	-16.04 ± 1.1	-20 ± 1.5	-20 ± 1.8	-21 ± 2.1
EE%	85.4 ± 3.2	88.7 ± 3.5	LL37: 84.8 ± 2.7	LL37: 81.6 ± 3.2
			A1: 87 ± 3.5	A1: 83.3 ± 4.1

N=3; Data represents means ± Standard Deviation.
Abbreviations: EE%- Encapsulation Efficiency, SLNs- Solid lipid Nanoparticles.
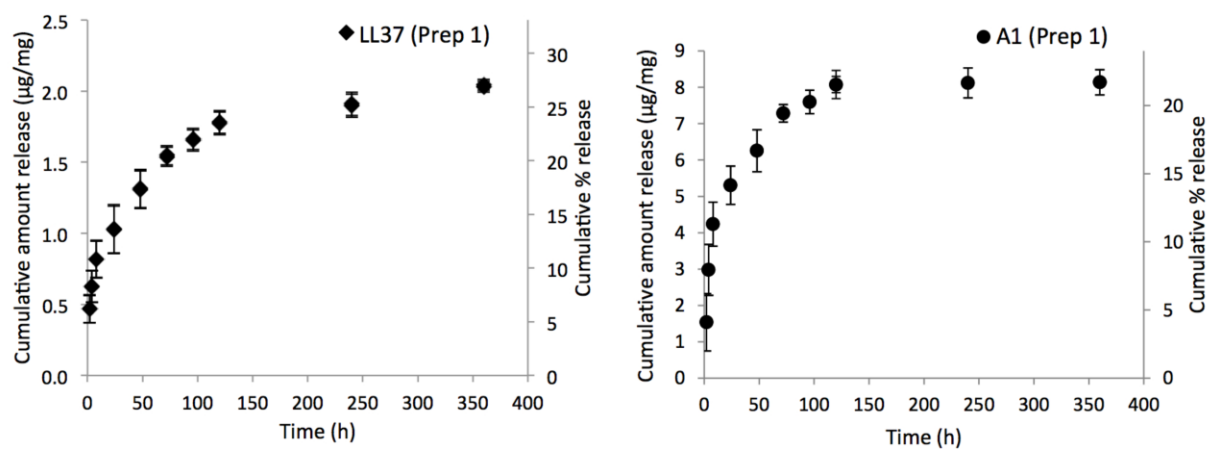
3.1.2. *In vitro* release study of LL37 and A1 from LL37-A1-SLNs

The release of LL37 and A1 from 10 mg of LL37-A1-SLNs occurred in a controlled and sustained manner throughout the study period. LL37 and A1 release profile followed a biphasic pattern with a release of $13.6 \pm 2.24\%$ (1.025 ± 1.68 µg/mg of SLNs) and $14.1 \pm 1.4\%$ (5.30 ± 5.2 µg/mg of SLNs) of LL37 and A1, respectively, for prep 1 (combination SLNs with an initial loading of 100 µg of LL37 and 500 µg of A1) (Figure 6A) in the first 24 h. Prep 2 (combination SLNs with an initial loading of 200 µg of LL37 and 750 µg of A1) released around $10.4 \pm 1.20\%$ (1.565 ± 1.81 µg/mg of SLNs) and 12 $\pm 1.22\%$ (6.80 ± 6.8 µg/mg of SLNs) of LL37 and A1, respectively (Figure 6B) in the first 24 h. This was followed by a slow and sustained release over the entire study period of 15 days.

3.1.3. *Ex vivo* skin permeation studies

The cumulative amount of LL37 and A1 that permeated across the skin (per diffusion area as a function of time) from LL37-A1-SLNs is shown in Figure 7. Approximately, $14 \pm 1.73\%$ (1.053 ± 1.29 µg/mg of SLNs) and $13.4 \pm 1.83\%$ (5.048 ± 6.86 µg/mg of SLNs) of LL37 and A1, respectively, from prep 1 permeated across the skin (Figure 7A) while $7.3 \pm 0.73\%$ (1.09 ± 1.10 µg/mg of SLNs) and $11.1 \pm 1.13\%$ (6.24 ± 6.3 µg/mg of SLNs) of LL37 and A1, respectively, from prep 2 permeated across the skin (Figure 7B) in the first 24 h.

A

B
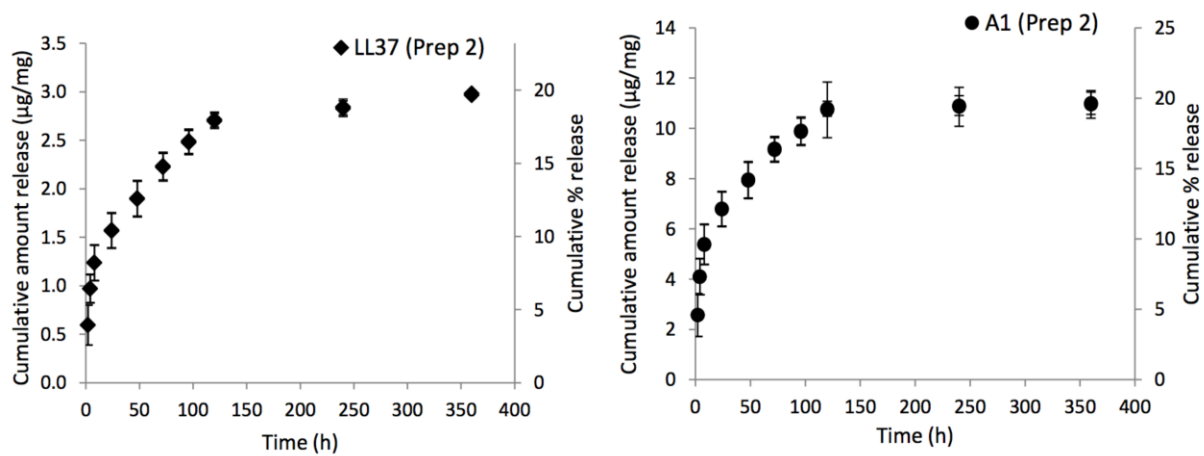
C
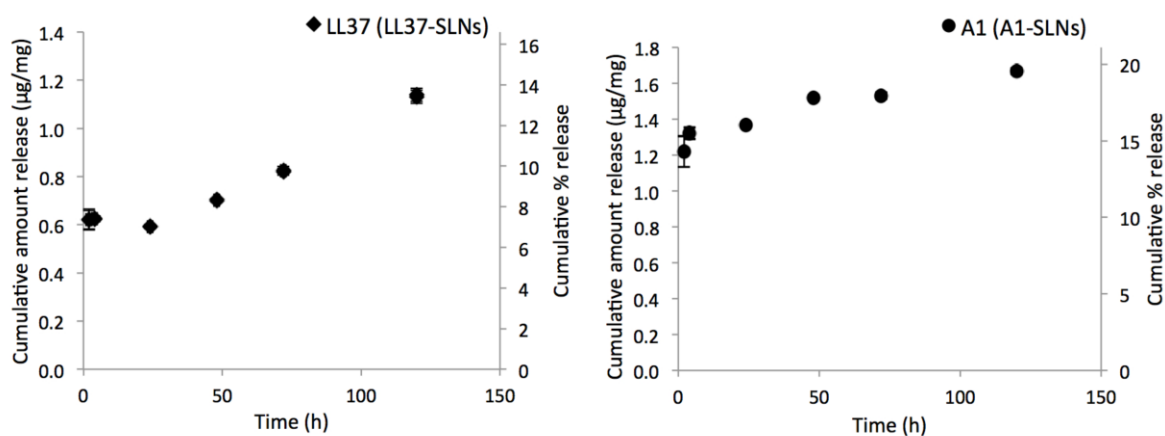
Figure 6. In vitro release profile of LL37 and A1 from LL37-A1-SLNs (A) prep 1 (loaded with 8.48 µg of LL37 and 43.5 µg of A1 per mg of SLNs) and (B) prep 2 (loaded with 16.32 µg of LL37 and 62.47 µg of A1 per mg of SLNs) (C) Release profile of LL37 loaded into LL37-SLNs at a concentration of 8.54 µg/mg of SLNs and A1 was loaded into A1-SLNs at a concentration of 44.35 µg/mg of SLNs in 1 mL of AWF (pH 7.4) at 37 °C. Values represent the mean±S.D; n=3.

A
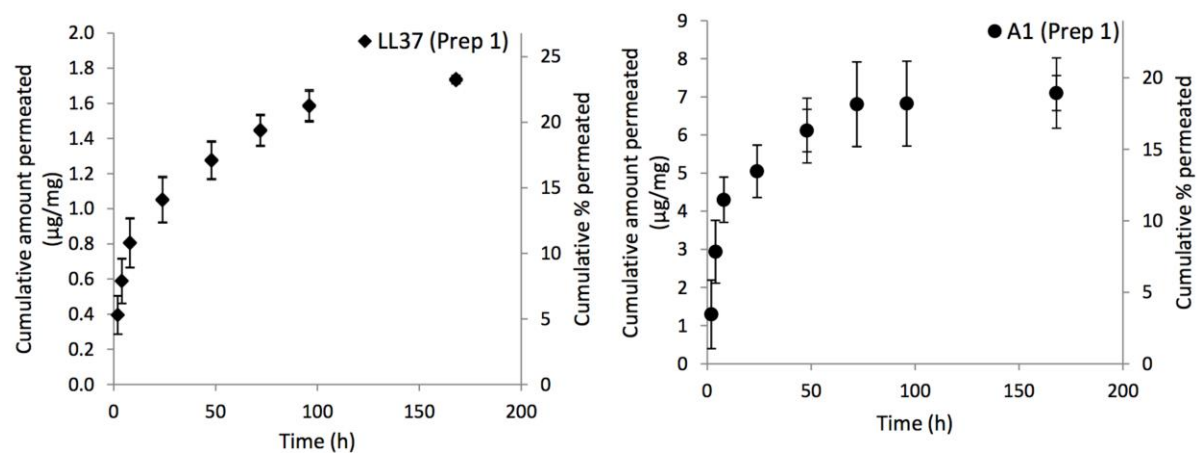
B
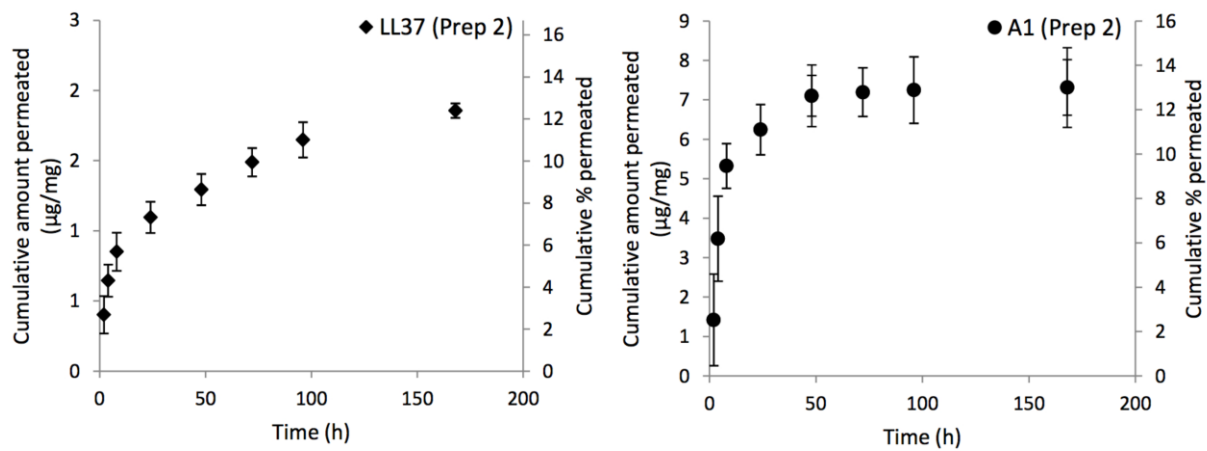
C
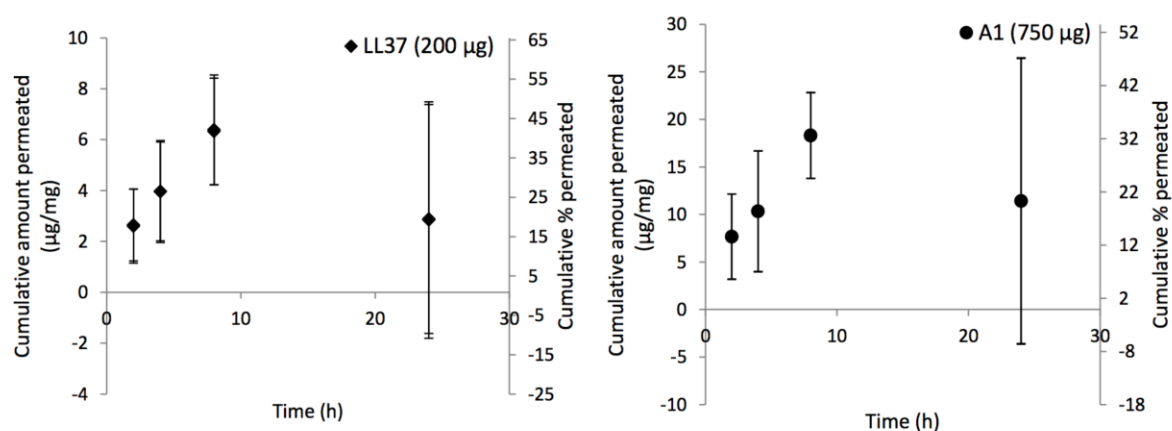
Figure 7. *Ex vivo* **rabbit inner ear skin permeation profile** of LL37 and A1 released from LL37-A1-SLNs after permeation across the (A) prep 1 (loaded with 8.48 µg of LL37 and 43.5 µg of A1 per mg of SLNs) and (B) prep 2 (loaded with 16.32 µg of LL37 and 62.47 µg of A1 per mg of SLNs) in 1 mL of AWF (pH 7.4) at 37 °C. (C) *Ex vivo* rabbit inner ear skin permeation studies of LL37 only (200 µg/mL) and A1 only (750 µg/mL) at 37 °C in 5 mL of AWF (pH 7.4).Values represent the mean±S.D; n=3.

3.2. <u>Antibacterial studies</u>

3.2.1. Synergistic antibacterial effects of LL37 and A1 on *S. aureus* and *E. coli*

We evaluated the synergistic effects of various combination concentration ratios of LL37 and A1 against gram-positive *S. aureus* and gram-negative *E. coli* in neutral pH milieu by using sub-lethal doses of LL37 and A1. When LL37 and A1 were combined, we observed that several combination ratios could result in synergistic enhancement of antibacterial activities against *S. aureus* and *E. coli* in comparison to individual concentrations (Table 4) (Figure 8A and 8B) with few combination ratios showing additive and antagonistic effects. Figure 8C is the median-effect plot using the Chou-Talalay equation of combination LL37-A1 concentrations, LL37 only and A1 only. Checkerboard method was performed each individual drug and for all the drug combinations in order to determine the total fractional inhibitory concentration ($\sum$FIC) respectively. $\sum$FIC results for the combination concentrations of LL37 and A1 against both *S. aureus* (Table 5) and *E. coli* (Table 6) yielded synergy mainly for concentration ratios of LL37 and A1 between the ranges of $2.5 - 5$ µg/mL and $10 - 20$ µg/mL, which have been used in the formulation of our combination SLNs. Some combination concentration ratios demonstrated indifference however, none of the combination concentration ratios demonstrated antagonism respectively.

A
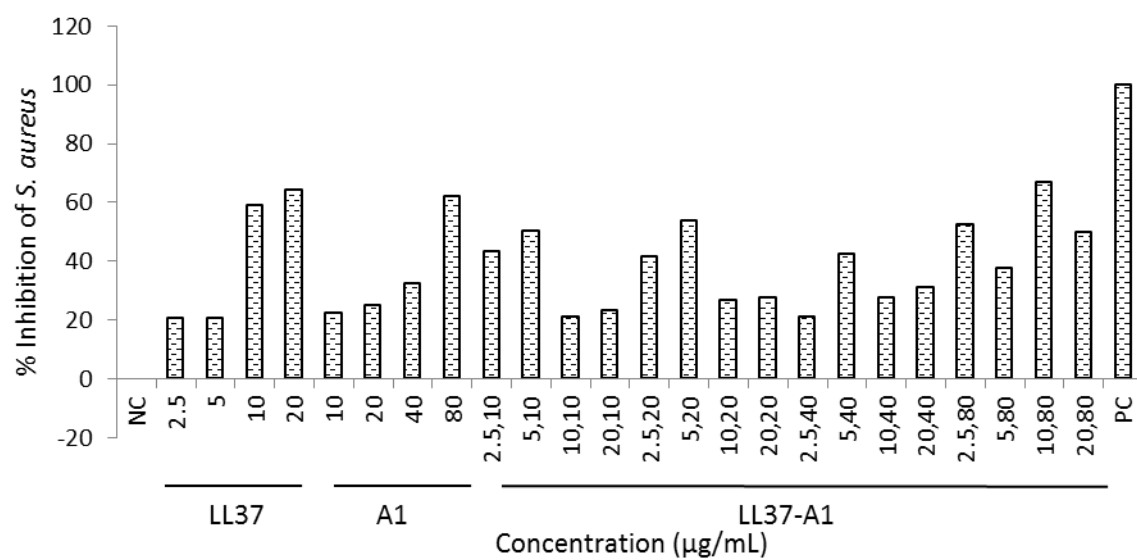
B
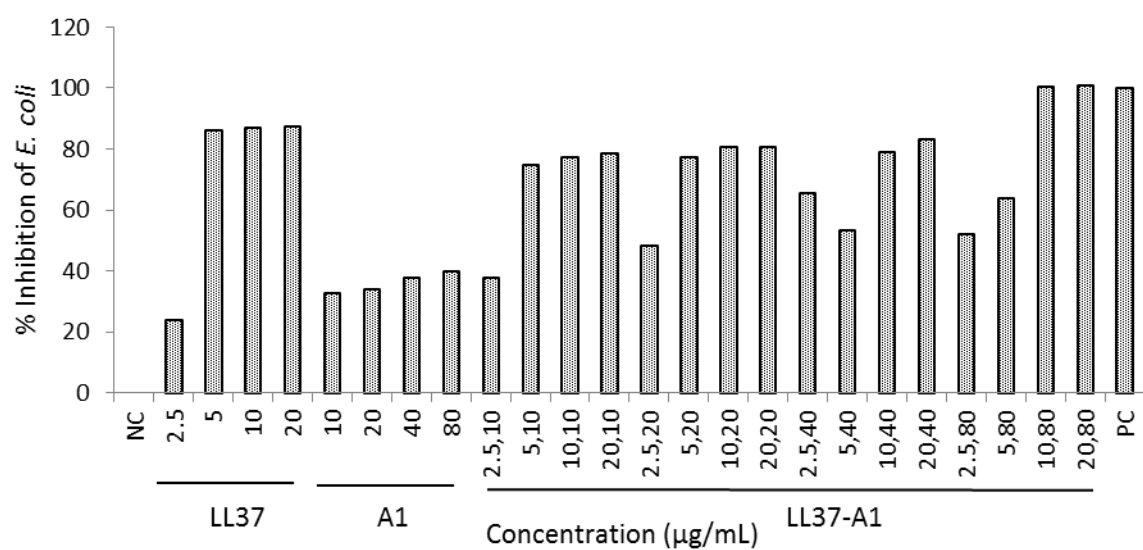
C
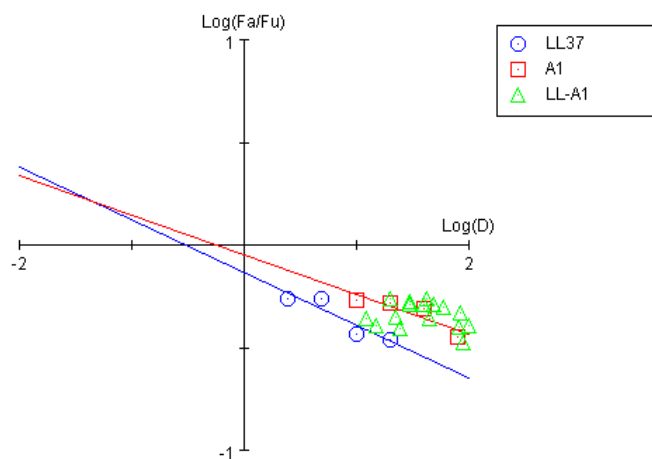
D
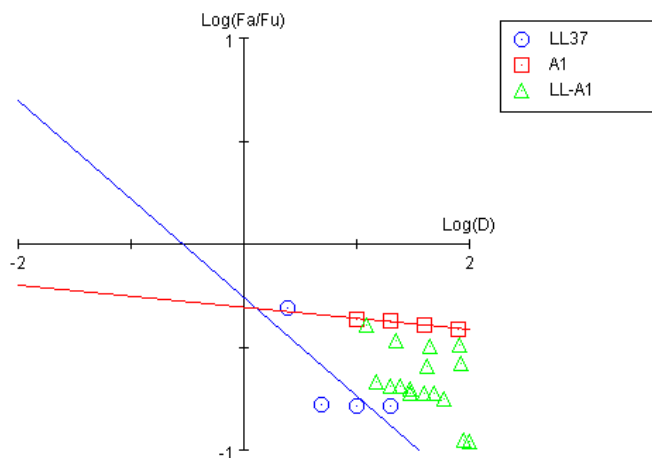
Figure 8. Combination effects of LL37 and A1 against (A) *S. aureus* **and (B)** *E. coli* as evaluated with compusync Chou-Talalay combination index (CI) measurement. Studies were performed using bacteria at a concentration of 1 x 10^7 CFU/mL incubated for 6 h at 37°C in PBS (pH 7.4). After the addition of 10% alamarBlue, cells were further incubated for 4 h at 37°C. Positive control (PC) are cells treated with 10 μg/mL of ampicillin; negative control (NC) = cells treated with 10 μL of PBS (pH 7.4). (C) The median-effect plot of combination LL37-A1, LL37 only and A1 against (C) *S. aureus* and (D) *E. coli.* n=1.

Table 4. Combination index for combination concentrations of LL37 and A1 using the Compusync Chou-Talalay method [141]. CI = 1 indicates additive effect, CI < 1 indicates synergism, CI > 1 indicates antagonism.

A

LL37 (µg/mL)	A1 (µg/mL)	Combination index (CI) for *S. aureus*
2.5	10	0.576
5	10	0.666
2.5	20	0.889
5	20	0.696
10	20	3.709
2.5	40	3.896
5	40	1.680
2.5	80	1.369
10	80	0.968
20	80	3.369

B

LL37 (µg/mL)	A1 (µg/mL)	Combination index (CI) for *E. coli*
2.5	10	1.541
5	10	0.697
2.5	20	0.950
5	20	0.631
10	20	1.073
2.5	40	0.505
5	40	1.593
2.5	80	0.855
10	80	0.357
20	80	0.695

Table 5. ΣFIC of combination concentrations of LL37 and A1 against *S. aureus* by checkerboard method. $\sum$FIC = ≤ 0.5 indicates synergism, $0.5 < \sum$FIC ≤ 4 indicates indifference. $\sum$FIC > 4 indicates antagonism.

Combination #	LL37		A1		ΣFIC= (FIC of LL37 + FIC of A1)	Interpretation
	Conc (µg/mL)	FIC of LL37	Conc (µg/mL)	FIC of A1		
1	2.5	0.142	10	0.133	0.275	SYN
2	5	0.28	10	0.133	0.413	SYN
3	10	0.571	10	0.133	0.704	IND
4	20	1.142	10	0.133	1.275	IND
5	2.5	0.142	20	0.266	0.408	SYN
6	5	0.28	20	0.266	0.546	SYN
7	10	0.571	20	0.266	0.837	IND
8	20	1.142	20	0.266	1.408	IND
9	2.5	0.142	40	0.533	0.675	IND
10	5	0.28	40	0.533	0.813	IND
11	10	0.571	40	0.533	1.104	IND
12	20	1.142	40	0.533	1.675	IND
13	2.5	0.142	80	1.066	1.208	IND
14	5	0.28	80	1.066	1.346	IND
15	10	0.571	80	1.066	1.637	IND
16	20	1.142	80	1.066	2.208	IND

Abbreviations: SYN, synergism; IND, indifference; FIC, fractional inhibitory concentration.

Table 6. ΣFIC of combination concentrations of LL37 and A1 against *E. coli* by checkerboard method. ∑FIC = ≤ 0.5 indicates synergism, 0.5 < ∑FIC ≤ 4 indicates indifference. ∑FIC > 4 indicates antagonism.

Combination #	LL37		A1		∑FIC= (FIC of LL37 + FIC of A1)	Interpretation
	Conc (µg/mL)	FIC of LL37	Conc (µg/mL)	FIC of A1		
1	2.5	0.166	10	0.147	0.313	SYN
2	5	0.333	10	0.147	0.48	SYN
3	10	0.666	10	0.147	0.813	IND
4	20	1.333	10	0.147	1.48	IND
5	2.5	0.166	20	0.294	0.46	SYN
6	5	0.333	20	0.294	0.627	IND
7	10	0.666	20	0.294	0.96	IND
8	20	1.333	20	0.294	1.627	IND
9	2.5	0.166	40	0.588	0.754	IND
10	5	0.333	40	0.588	0.921	IND
11	10	0.666	40	0.588	1.254	IND
12	20	1.333	40	0.588	1.921	IND
13	2.5	0.166	80	1.176	1.342	IND
14	5	0.333	80	1.176	1.509	IND
15	10	0.666	80	1.176	1.842	IND
16	20	1.333	80	1.176	2.509	IND

Abbreviations: SYN, synergism; IND, indifference; FIC, fractional inhibitory concentration.

3.2.2. Antibacterial activity of LL37-A1-SLNs against *S. aureus* and *E. coli*

The antibacterial activities of LL37-A1-SLNs, blank SLNs, LL37 only, and A1 only were evaluated against 10^7 CFU/mL of *S. aureus* or *E. coli*. As shown in Figure 9, LL37-A1-SLNs exhibited 42.3 ± 0.56% (prep 1) and 46.93 ± 0.52% (prep 2) inhibition against *S. aureus* and 65 ± 0.34% (prep 1) and 72.3 ± 0.27% (prep 2) inhibition against *E. coli*. LL37 only and A1 only inhibited the growth of *S. aureus* by 34 ± 0.64% and 28.3% ± 0.70%, respectively, and inhibited the growth of *E. coli* by 50 ± 0.48% and 45.8 ± 0.53%, respectively.
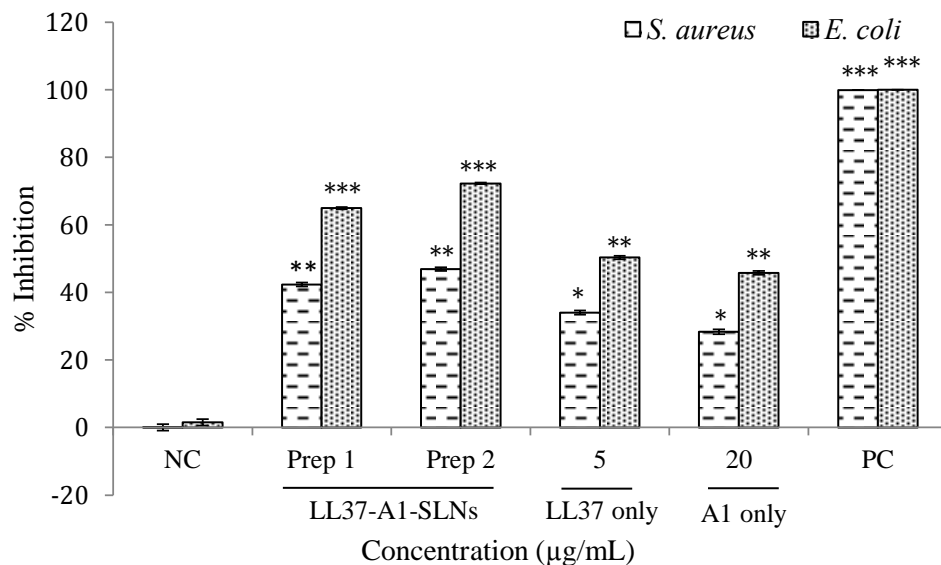
Figure 9. Antibacterial activities of LL37-A1-SLNs (prep 1 and prep 2), LL37 only, and A1 only in PBS (pH 7.4) against *S. aureus* and *E. coli* cells. Studies were performed using bacteria at a concentration of 1 x 10^7 CFU/mL incubated for 6 h at 37°C. Cells were treated with prep 1 (2 mg/mL), prep 2 (2 mg/mL), LL37 only (5 µg/mL) and A1 only (20 µg/mL). After the addition of 10% alamarBlue, cells were further incubated for 4 h at 37°C. Negative control (NC) = cells treated with 10 µL of PBS (pH 7.4); positive control (PC) = cells treated with ampicillin (10 µg/mL). Values represent mean±S.D; n=3. * *P<0.05,* ** *P<0.01*, and *** *P<0.001* vs. NC.

3.3. <u>Cellular assays</u>

3.3.1. *In vitro* cytotoxicity studies

To investigate the effects of LL37-A1-SLNs on cell oxidative metabolism, an MTS assay was performed on BJ fibroblast cells and keratinocytes. Our studies showed that prep 1, and prep 2 (up to a concentration of 5 mg/mL), and blank SLNs (5 mg/mL) had no significant impact on cell viabilities (Figure 10). While on treating the cells with LL37 only (higher than 25 µg/mL) and A1 only (higher than 50 µg/mL) the cell viabilities reduced to less than 80 % respectively.

3.3.2. *In vitro* wound healing assay

The effects of LL37-A1-SLNs, LL37 only, and A1 only on the migratory capacities of BJ fibroblast cells and keratinocytes were determined by their abilities to induce *in vitro* wound closure. Both BJ fibroblast cells and keratinocytes were successfully stained with DiO dye. The cell membrane picked up the stain and imparted green fluorescence to the cells under a fluorescent microscope (Figure 11). Cells treated with LL37-A1-SLNs (prep 1 and prep 2) showed faster migration whereas LL37 only and A1 only treated cells showed lower migratory effects. By 24 h post-wounding, LL37-A1-SLNs significantly improved closure of *in vitro* wounds by 79.38 ± 7.5% (prep 1) and 103 ± 4.04% (prep 2) for BJ fibroblast cells (Figure 11A and 11C) and by 65 ± 19.5% (prep 1) and 107 ± 4% (prep 2) for keratinocytes (Figure 11B and 11D), respectively. In comparison, LL37 only and A1 only treatment groups showed 60.31 ± 10.14% and 70.62 ± 5.85% of wound closure, respectively, in BJ fibroblast cells. In keratinocytes, LL37 only and A1 only treatment improved wound closure by 47.85 ± 6.9% and 61.26 ± 16.5%, respectively.

A
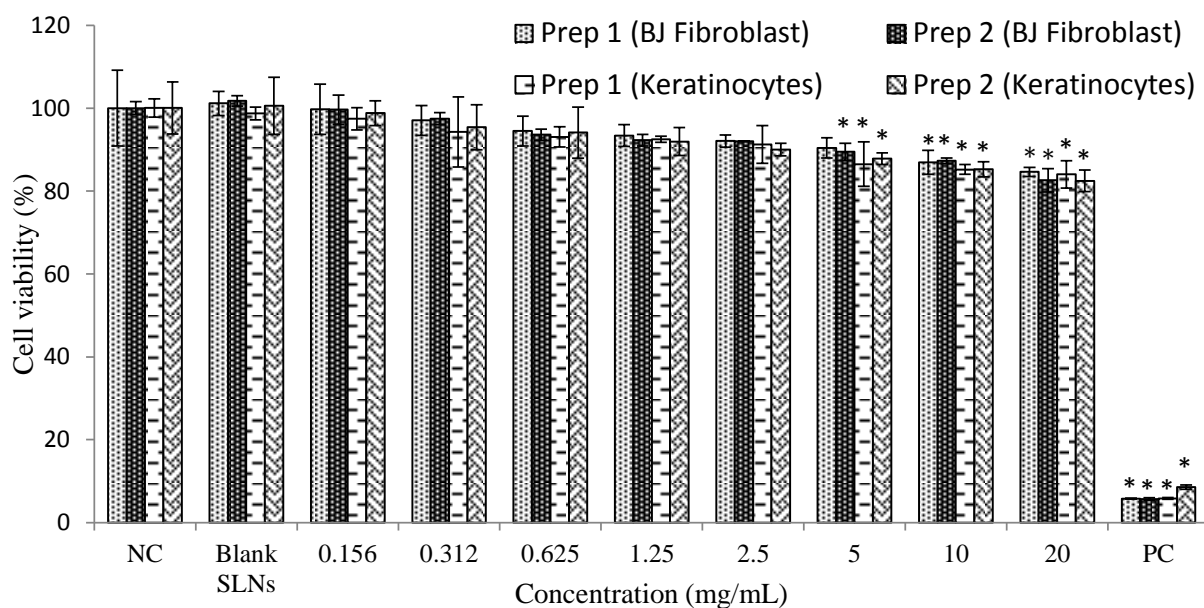
B
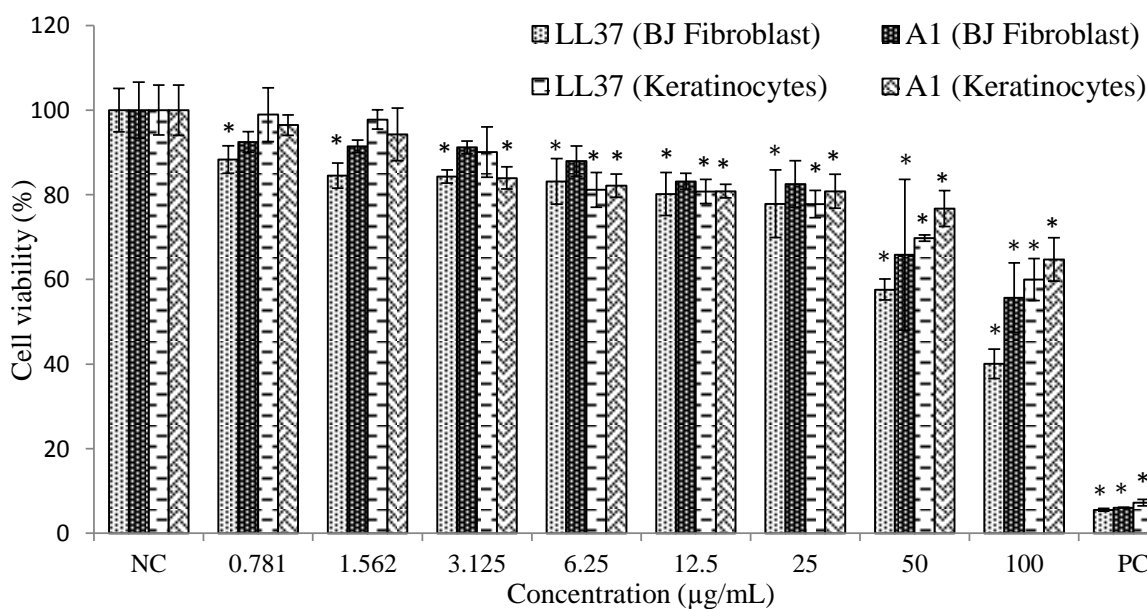
Figure 10. *In vitro* **cytotoxicity studies using BJ fibroblast cells and keratinocytes** (A) prep 1, prep 2 and blank SLNs (B) LL37 only and A1 only. Values represent mean±S.D; n=3. * *P<0.05* vs. NC. Negative control (NC) = cells treated with blank cell media; positive control (PC) = cells treated with 1% triton in cell media.

A

	0h	12h	24h

NC

LL37-A1-SLNs
(prep 1)

LL37-A1-SLNs
(prep 2)

LL37 only
(5 µg/mL)

A1 only
(20 µg/mL)

PC

B

	0h	12h	24h

NC

LL37-A1-SLNs
(prep 1)

LL37-A1-SLNs
(prep 2)

LL37 only
(5 µg/mL)

A1 only
(20 µg/mL)

PC
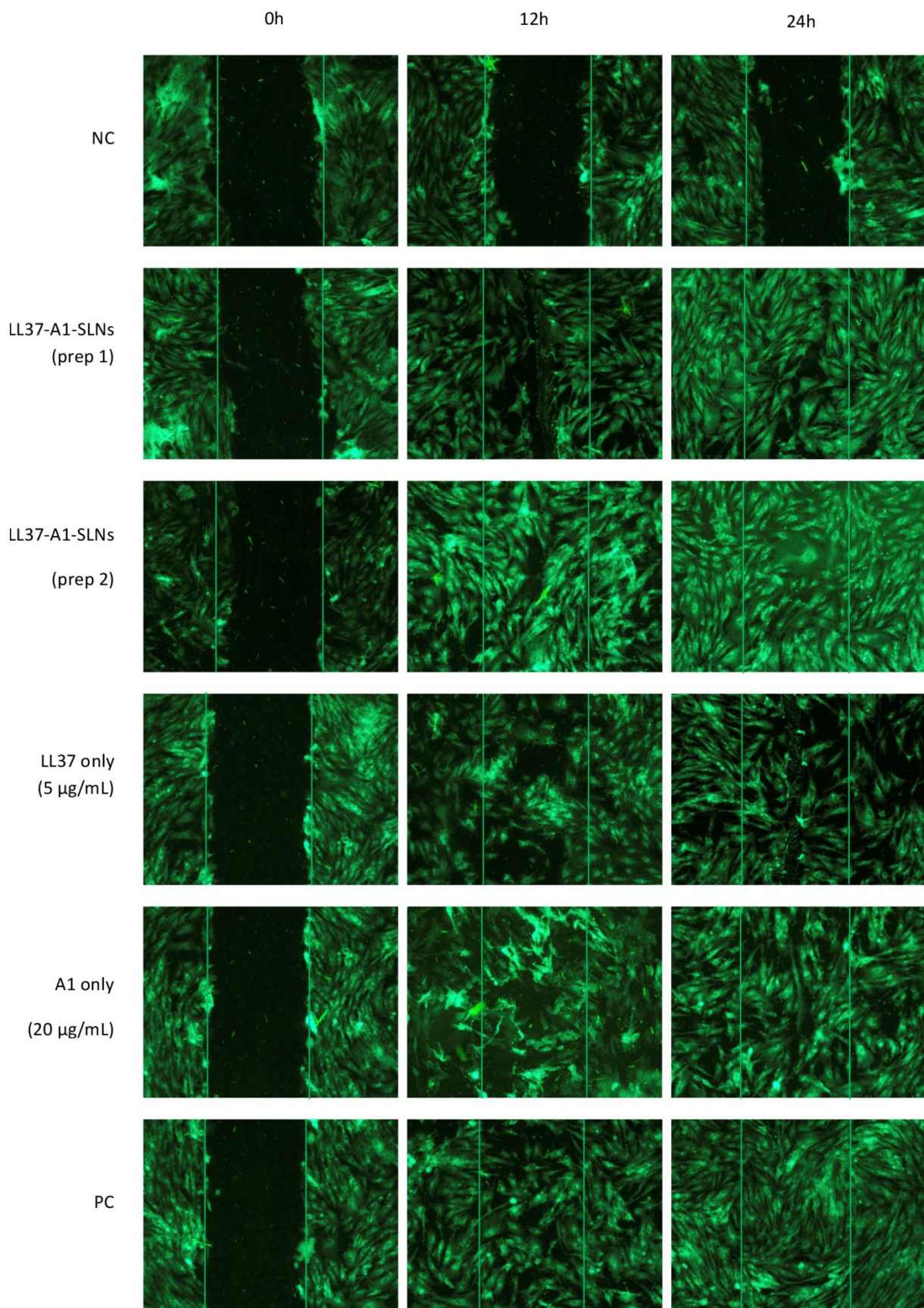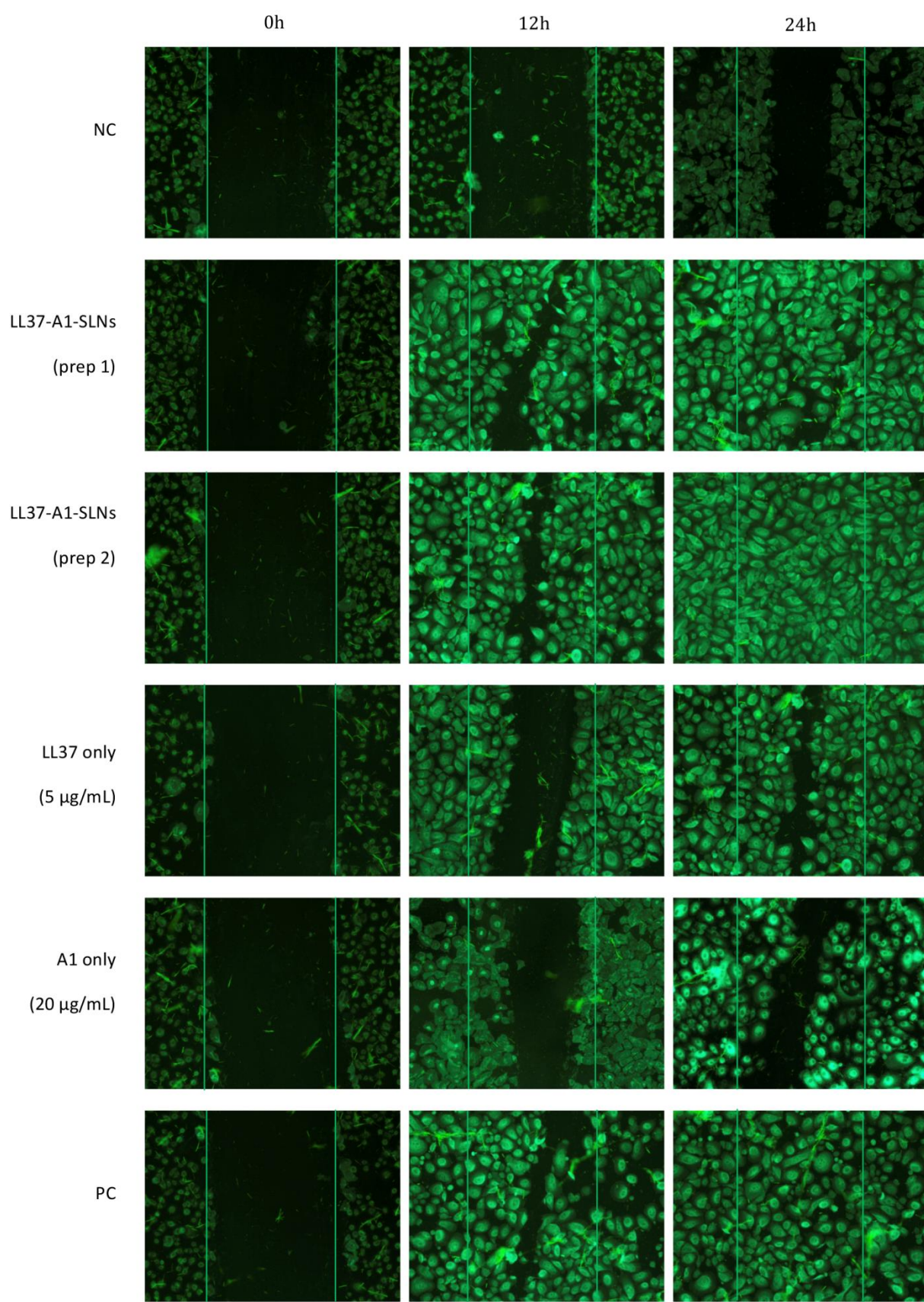
C
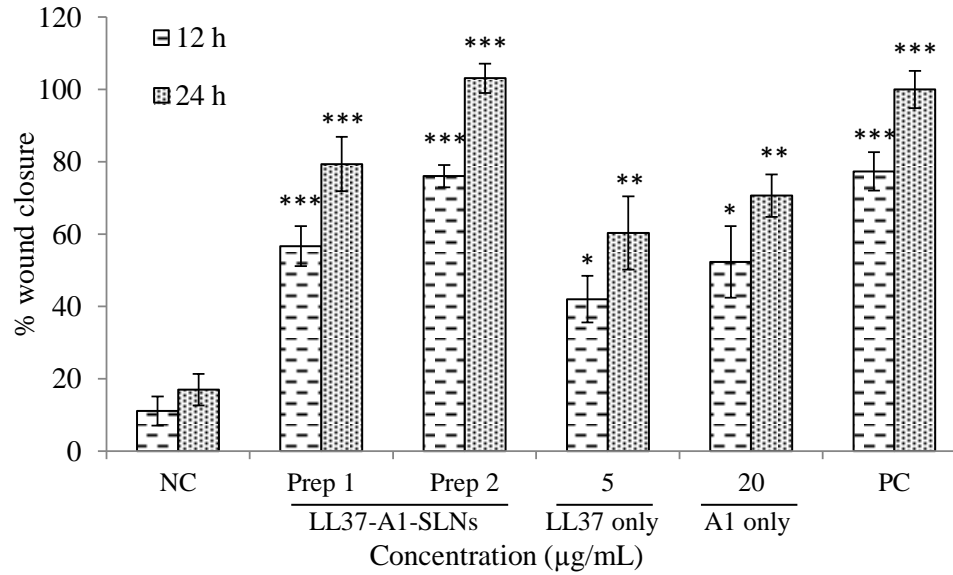
D
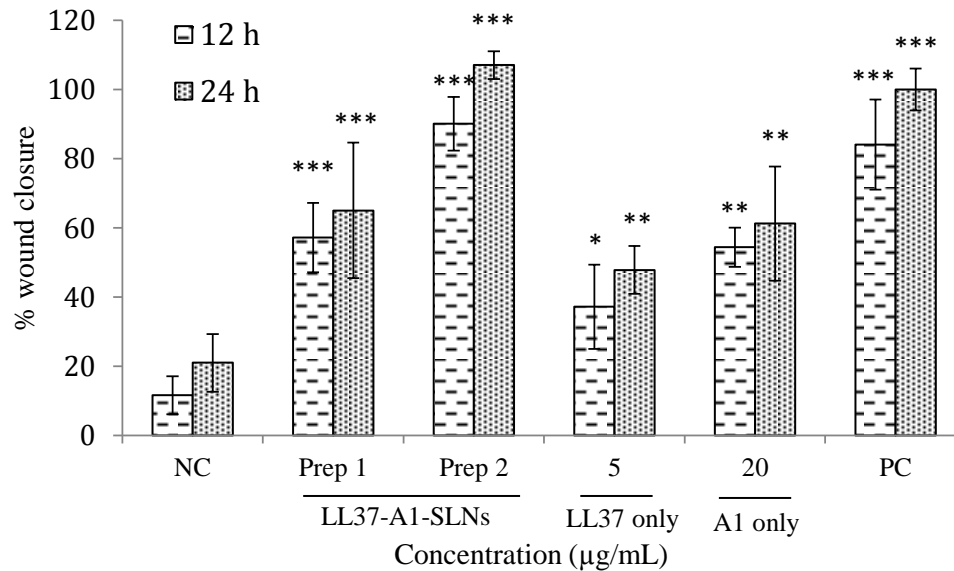
Figure 11. *In vitro* wound healing studies of LL37-A1-SLNs (A) BJ fibroblast cells and (B) keratinocytes. Cells were treated with prep 1 (3 mg/mL), prep 2 (3 mg/mL), LL37 only (5 µg/mL) and A1 only (20 µg/mL).The fluorescent marker DiO Dye was used to track the migration of cells. (C) Wound closure of BJ fibroblast cells expressed as percentage of the initial wound. (D) Wound closure of keratinocytes expressed as percentage of the initial wound. Negative control (NC) = untreated cells in serum-starved medium; positive control (PC) = cells in serum-rich medium containing growth factors. Values represent mean±S.D; n=3. * *P<0.05* and ** *P<0.01*, and *** *P<0.001* vs. NC.

3.4.   Impact of LL37-A1-SLNs on TEER of LPS-treated BJ fibroblast cells and keratinocytes

Treatment of cells with LPS resulted in a significant reduction in TEER ($P<0.05$) (Figure 12) in comparison to untreated naïve cells. TEER values were augmented in LPS-treated cells in response to co-exposure to LL37-A1-SLNs (prep 1) showing a $57.6 \pm 4.6\%$ and $66.8 \pm 7\%$ enhancement in TEER values for BJ fibroblast cells and keratinocytes, respectively. Furthermore, treatment with LL37-A1-SLNs (prep 2) enhanced TEER values by $60.6 \pm 2\%$ for BJ fibroblast cells and by $91.4 \pm 16.6\%$ for keratinocytes. In contrast, treatment with LL37 only enhanced the TEER of BJ fibroblast cells by $48 \pm 4.5\%$ and keratinocytes by $43 \pm 9.6\%$. Treatment with A1 only enhanced the TEER of BJ fibroblast cells by $50 \pm 2.6\%$ and keratinocytes by $34.8 \pm 11\%$, respectively.

3.5.   Anti-inflammatory activity of LL37-A1-SLNs: Impact on production of key inflammatory cytokines

Treatment of BJ fibroblast cells and keratinocytes with LPS resulted in a marked increase in IL-6, IL-1β, and TNF-α production (Figure 13) in comparison to untreated naïve cells. However, co-treatment of cells with LL37-A1-SLNs (prep 1 and prep 2) and LPS significantly attenuated LPS-induced production of IL-6 (Figure 13A), IL-1β (Figure 13B), and TNF-α (Figure 13C). Production of IL-6, IL-1β, and TNF-α did not vary significantly between LL37 only and A1 only treatment groups. Furthermore, treatment of BJ fibroblast cells and keratinocytes with LPS resulted in a marked decrease in collagen-I production (Figure 13D). However, co-treatment of cells with LL37-A1-SLNs (prep 1 and prep 2) and LPS significantly increased LPS-induced deposition of collagen-I. Production of collagen-I did not vary significantly among keratinocytes treated with LL37 only or A1 only
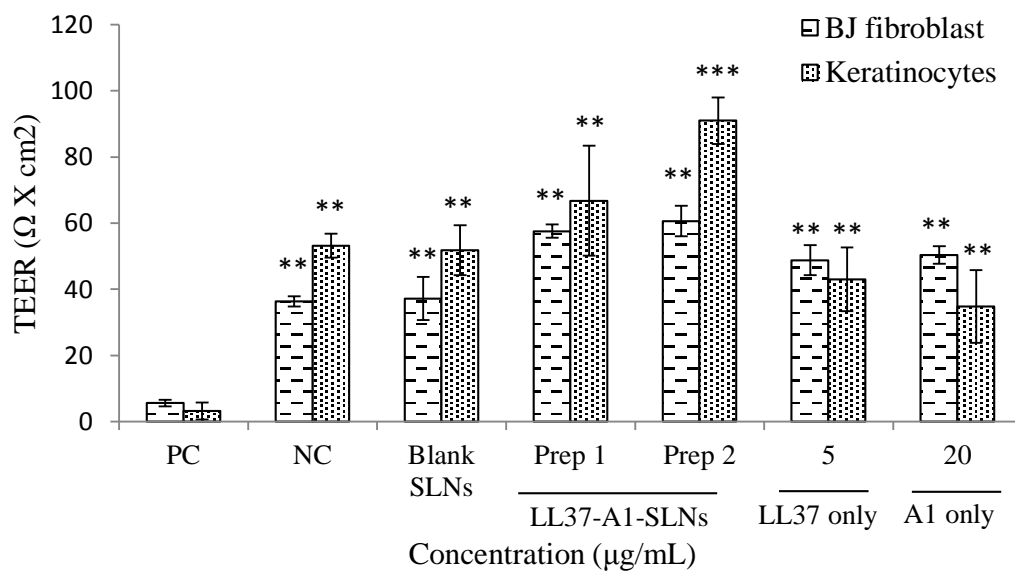
Figure 12. The impact of treatment on the transepithelial electrical resistance (TEER) of BJ fibroblast cells and keratinocytes exposed to LPS treatment (10 µg/mL) after 24 h. Cells were treated with prep 1 (3 mg/mL), prep 2 (3 mg/mL), Blank SLNs (5 mg/mL), LL37 only (5 µg/mL) and A1 only (20 µg/mL). Negative control (NC) = naïve cells; positive control (PC) = cells treated with LPS. Values represent mean±S.D; n=3. ** *P<0.01*, and *** *P<0.001* vs. PC.

A
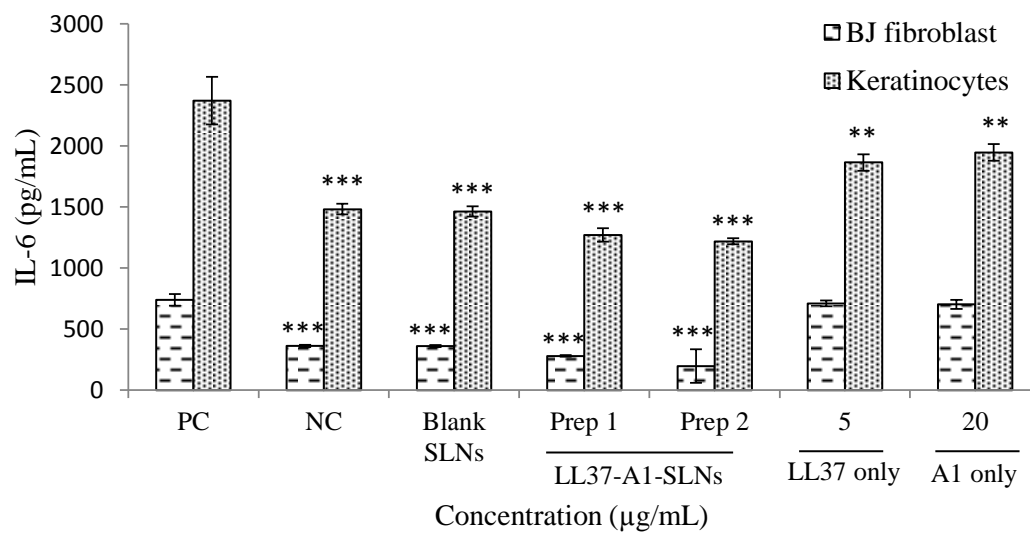
B
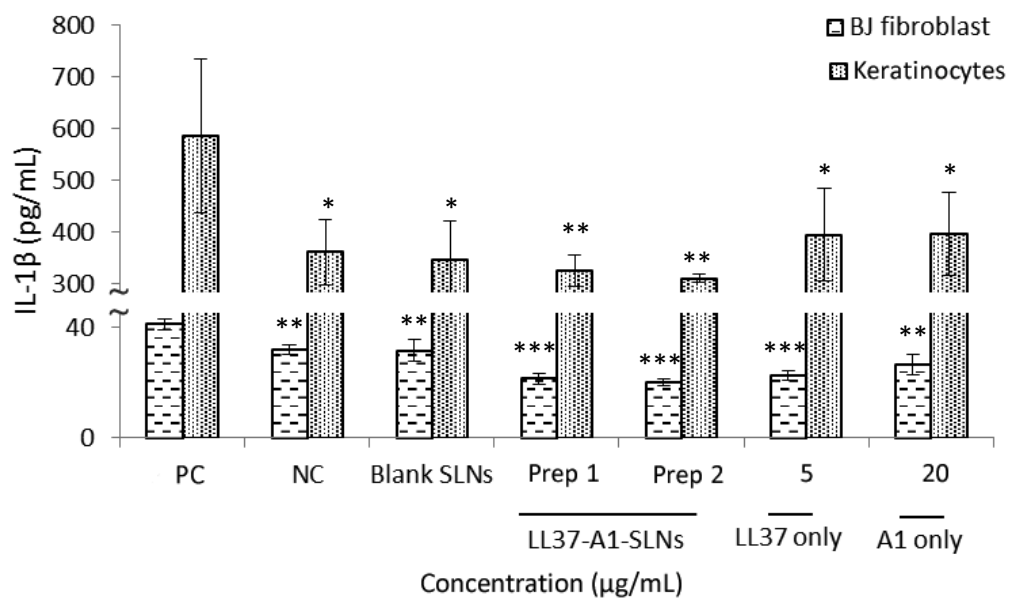
C
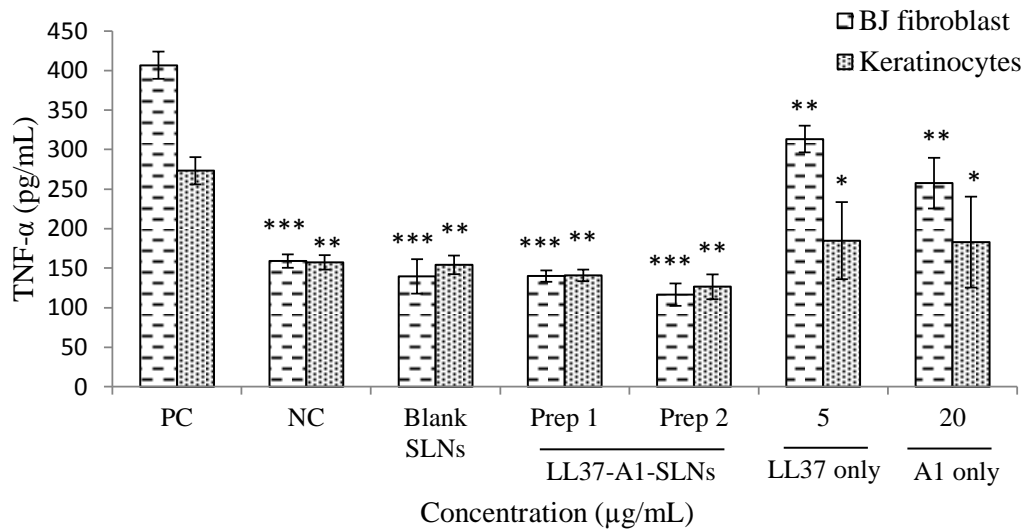
D
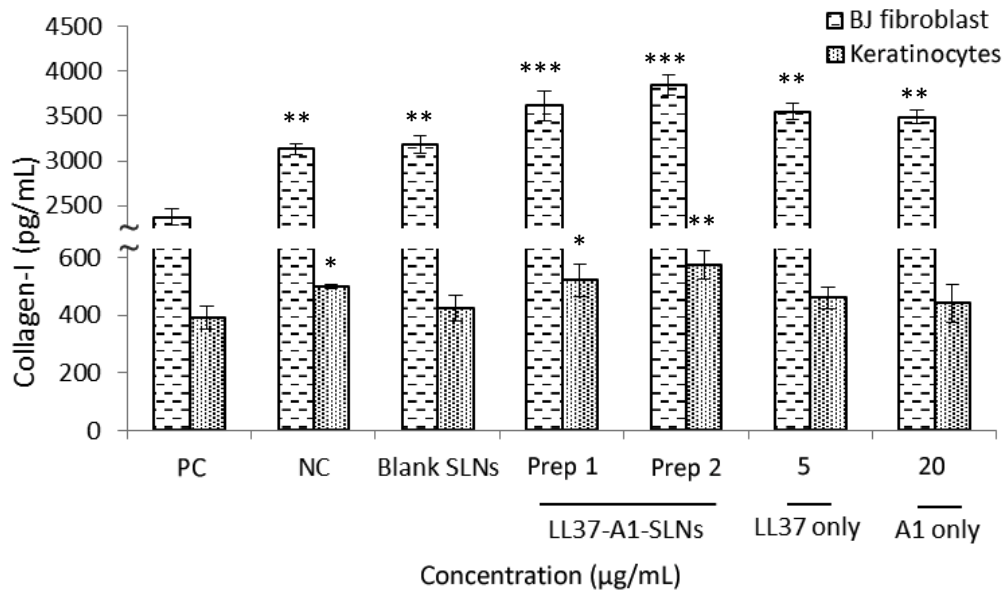
Figure 13. The effects of treatment with LPS in combination with different concentrations of LL37-A1-SLNs, LL37 only, and A1 only on the production of (A) IL-6 (B) IL-1β (C) TNF-α and (D) collagen-I by BJ fibroblast cells and keratinocytes after 24 h. Cells were treated with prep 1 (3 mg/mL), prep 2 (3 mg/mL), LL37 only (5 µg/mL) and A1 only (20 µg/mL). Negative control (NC) = cells treated with PBS (pH 7.4); positive control (PC) = cells treated with LPS only (10 µg/mL). Values represent mean±S.D; n=3. * *P<0.05*, ** *P<0.01*, and *** *P<0.001* vs. PC.

3.6.   Combination effects of SLNs on dermal wound healing *in vivo*

From day 9 of post wounding, both LL37-A1-SLNs and LL37-A1-only groups showed faster healing effect than untreated and individual treated groups (Figure 14A). Topical administration of LL37-A1-SLNs significantly accelerated wound healing in mice compared to untreated control group with 70.86 ± 6.7 % versus 51 ± 3.27 % for untreated at day 13 (Figure 14B). While, LL37-SLNs and A1-SLNs showed an average healing of 56.5 ± 1.55 % and 55.06 ± 2.08 % respectively. Similar to LL37-A1-SLNs treated group, by day 13 of post wounding the LL37-A1-only combination group showed nearly complete wound closure in comparison to untreated control with a 64.2 ± 4.3% recovery (Figure 14B).

3.7.   Combination effects of SLNs on re-epithelialization and granulation tissue formation *in vivo*

Histological examination of wound sections with HE staining presented insights into the predominant stages of dermal wound healing along with the morphology of the skin layers during the healing process. While, the extent of collagen deposition was determined using the MT staining of the wound sections. By day 13 post wounding, compared to all other groups, LL37-A1-SLNs showed a significant healing response similar to that of LL37-A1-only group. In untreated, blank-SLNs and individual drug treatment groups, the granulation tissues formed were hypocellular and covered by a thin immature epithelium. It is clearly visible that the epidermal and subepidermal layers were well organized in the case of both LL37-A1-SLNs and LL37-A1-only groups (Figure 15). Both MT staining (Figure 16) and Sirius Red/Fast Green assay (Figure 17) revealed that the extent of collagen deposition was significantly higher in LL37-A1-SLNs and LL37-A1-only groups in comparison to untreated or individual treated groups. It is clearly evident that the deposited collagen showed a compact and denser alignment in case of both LL37-A1-SLNs and LL37-A1-only groups in comparison to untreated or individual treated groups respectively (Figure 16 and 17).

A
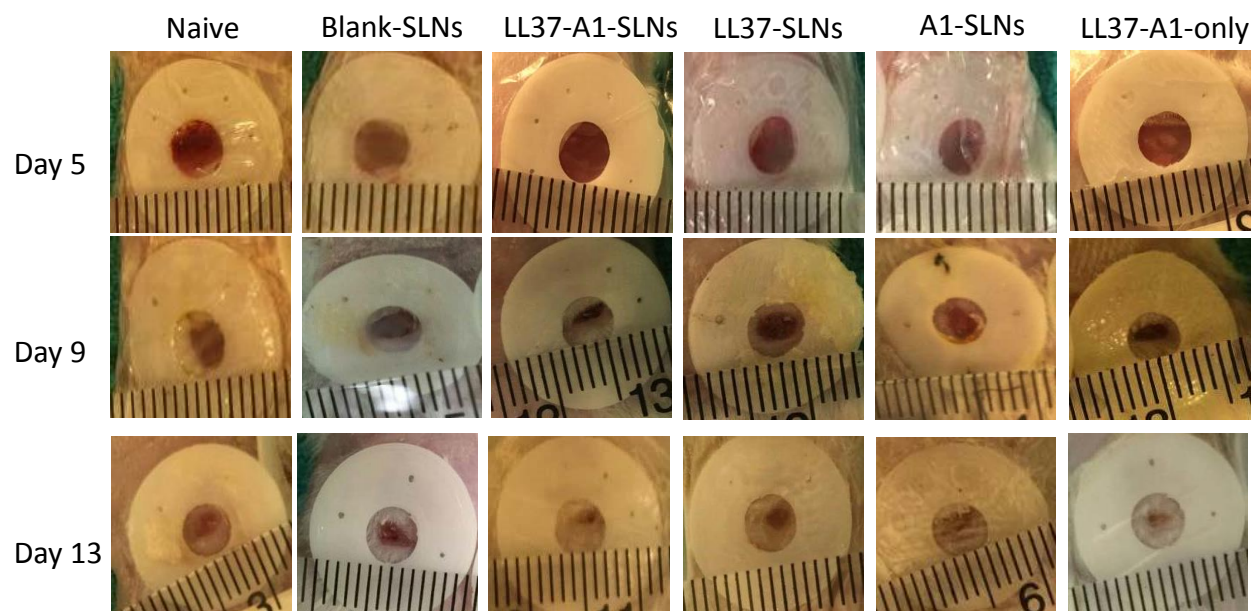
B
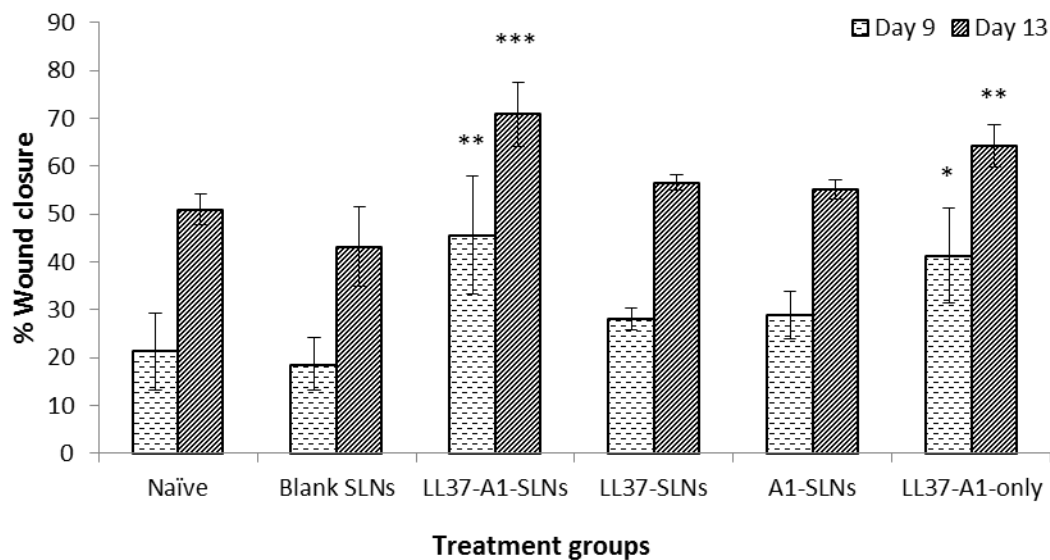
Figure 14. Combination SLNs accelerates wound healing. (A) Wound images of untreated naïve, Blank-SLNs, LL37-A1-SLNs, LL37-SLNs, A1-SLNs and LL37-A1-only treatment groups at day 5, 9 and 13 respectively. (B) % Wound closure at day 9 and 13. Values represent mean±S.D; n=2 (LL37-SLNs group); n=3 (all other treatment groups). * *P<0.05*, ** *P<0.01*, and *** *P<0.001* vs. Naive.
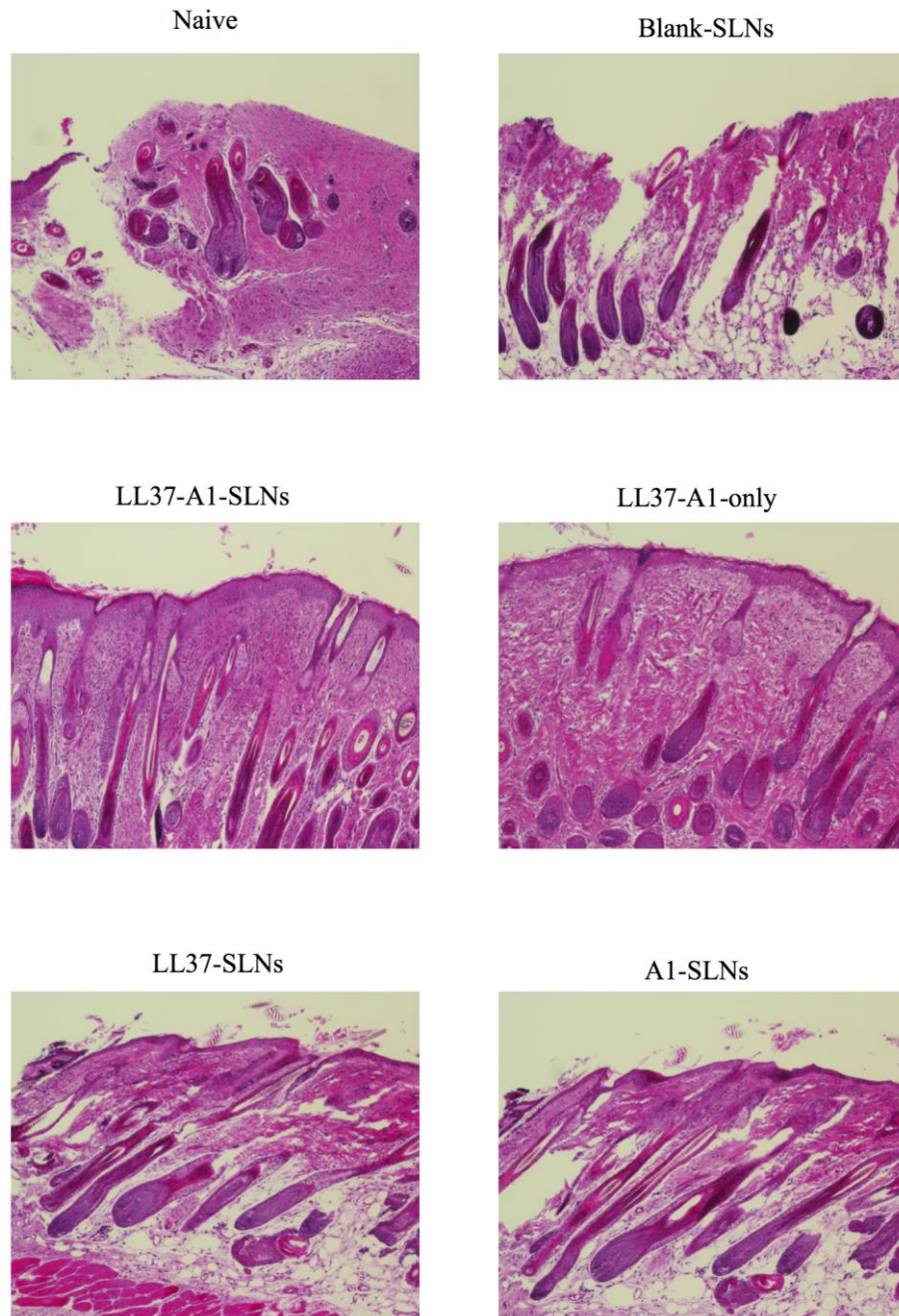
Figure 15. Combination SLNs increased wound re-epithelialization. Representative images of wound sections from day 13 post wounding of all six groups stained with hematoxylin and eosin (HE). Both LL37-A1-SLNs and LL37-A1-only treatment groups demonstrate well-organized epidermal and sub epidermal layers as well as better re-epithelialization and granulation tissue formation in comparison to untreated or individually treated groups. Values represent mean±S.D; n=2 (LL37-SLNs group); n=3 (all other treatment groups).
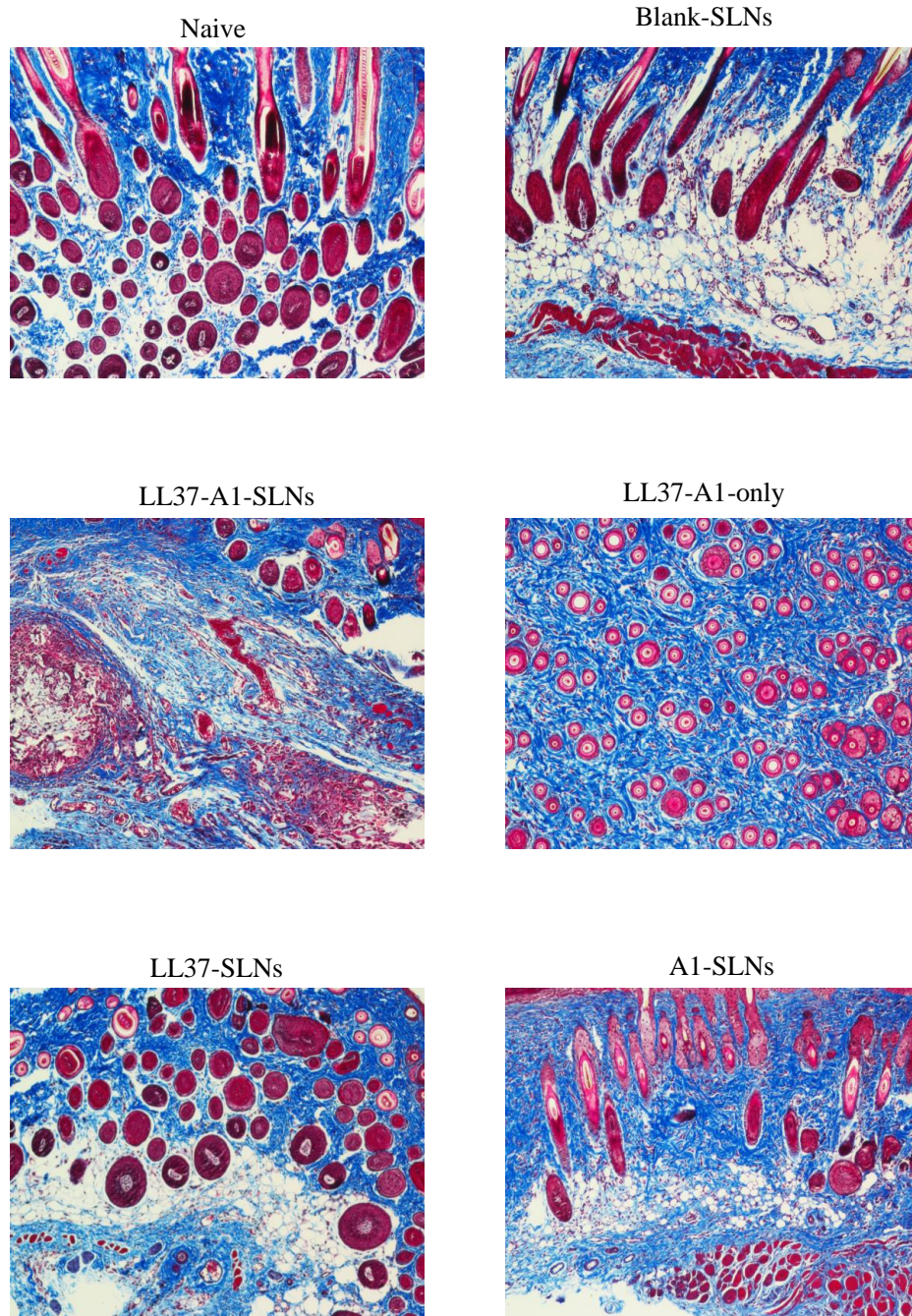
Figure 16. Combination SLNs increased collagen content of granulation tissue. Representative images of wound sections from day 13 post wounding of all six groups stained with Masson's trichrome (MT). Both LL37-A1-SLNs and LL37-A1-only treatment groups demonstrate denser and compact alignment of the deposited collagen in comparison to untreated or individually treated groups. Values represent mean±S.D; n=2 (LL37-SLNs group); n=3 (all other treatment groups).

A

Naive
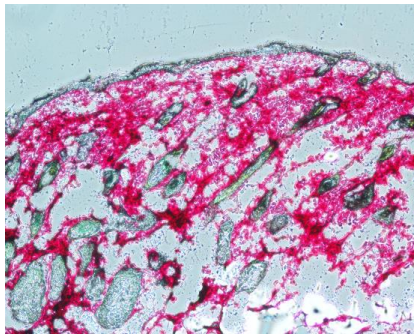
Blank-SLNs
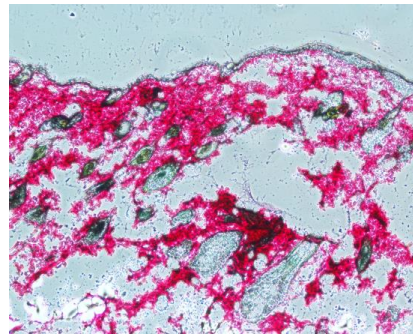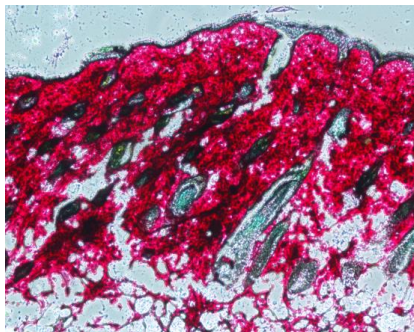
LL37-A1-SLNs

LL37-A1-only
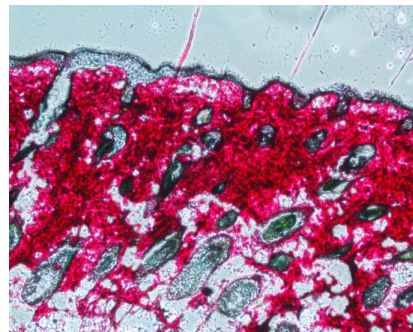
LL37-SLNs
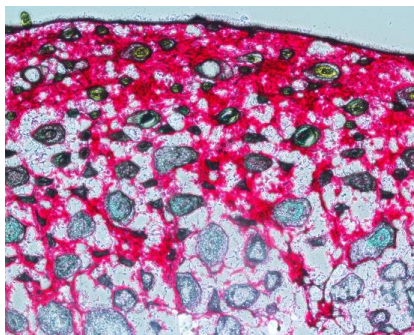
A1-SLNs
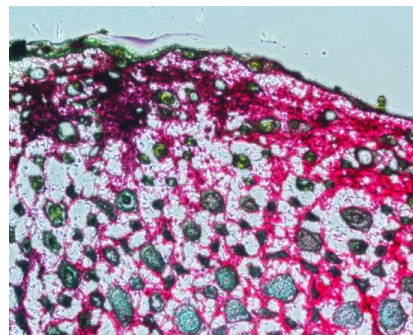
B
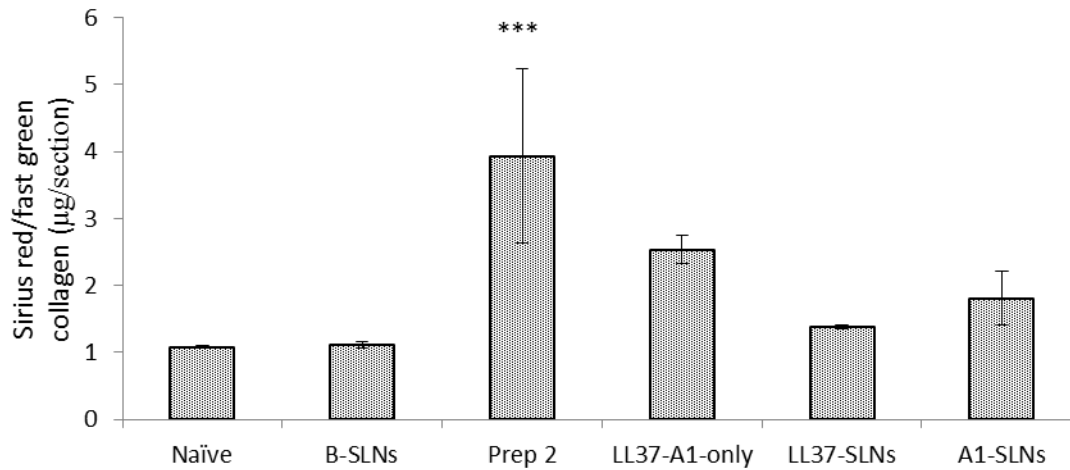
C
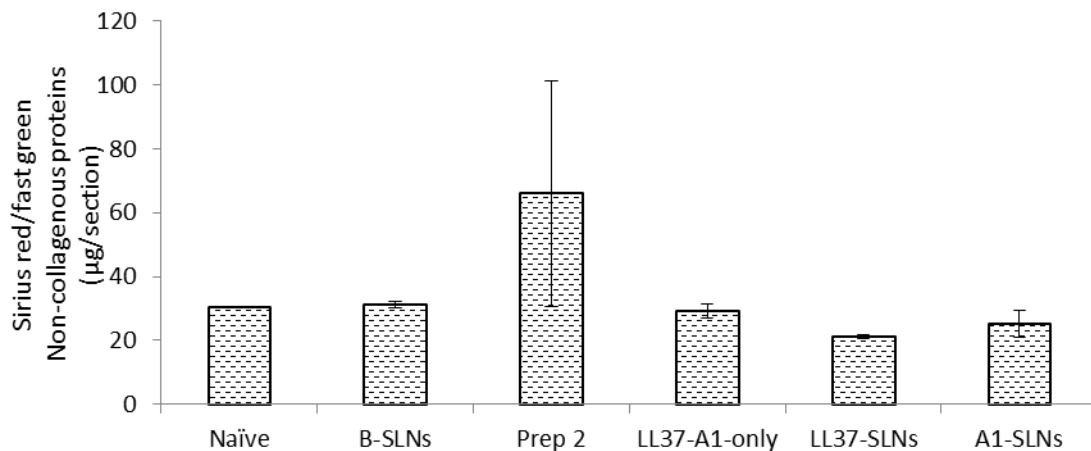
Figure 17. Combination SLNs demonstrated higher collagen and non-collagenous proteins deposition. Representative images of wound sections of all six groups stained with (A) Sirius Red/Fast Green are presented. Quantification of the (A) total collagen and (C) non-collagenous proteins amounts extracted from the wound sections from day 13 post wounding. Both LL37-A1-SLNs and LL37-A1-only treatment groups demonstrate higher amounts of total collagen and non-collagenous proteins in comparison to untreated or individually treated groups. Values represent mean±S.D; n=2 (LL37-SLNs group); n=3 (all other treatment groups). * *P<0.05*, ** *P<0.01*, and *** *P<0.001* vs. Naive.

3.8. **Combination effects of SLNs on angiogenesis process during wound healing *in vivo***

To determine the extent of angiogenesis during regeneration, the endothelial cell colonization in the wound sections were identified. The expression of CD31+ endothelial cells is prominent in both LL37-A1-SLNs and LL37-A1-only treated wounds, representing 75.58 ± 3.47 % and 71.97 ± 3.38 % of red pixels per surface area in comparison to untreated or individually treated groups were there is a significant decline in the frequency of CD31+ cells within the wound sections (Figure 5). Consistent with the previous observations, few vessels are observed in the wound section and the majority of CD31+ cells were individual elongated cells scattered throughout the tissue sections in case of both LL37-A1-SLNs and LL37-A1-only treated groups. These results indicate the extent of angiogenesis and vascularization during the regeneration process.

A

Naive
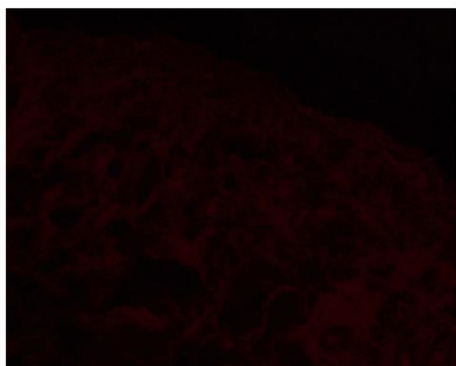
Blank-SLNs
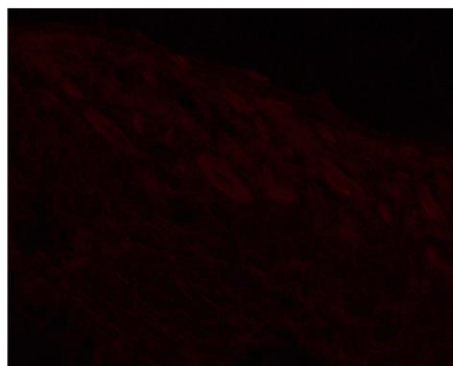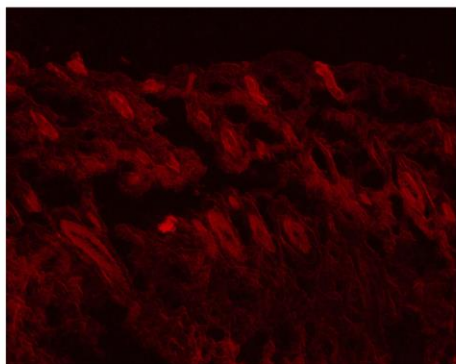
LL37-A1-SLNs

LL37-A1-only
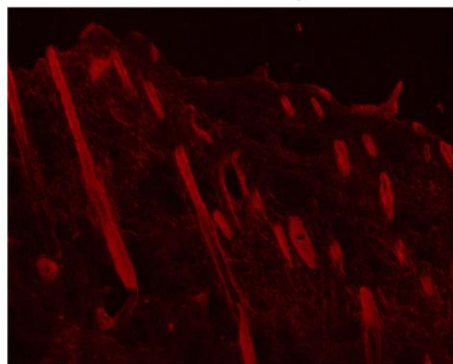
LL37-SLNs
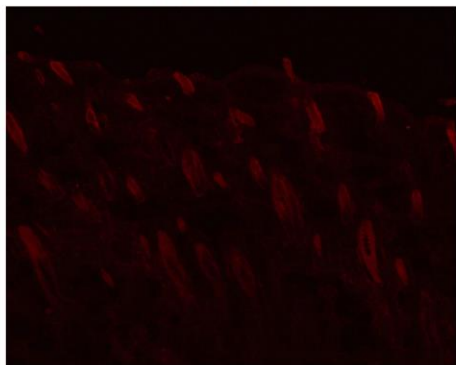
A1-SLNs
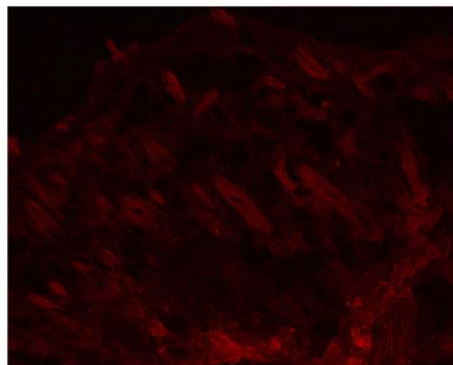
B
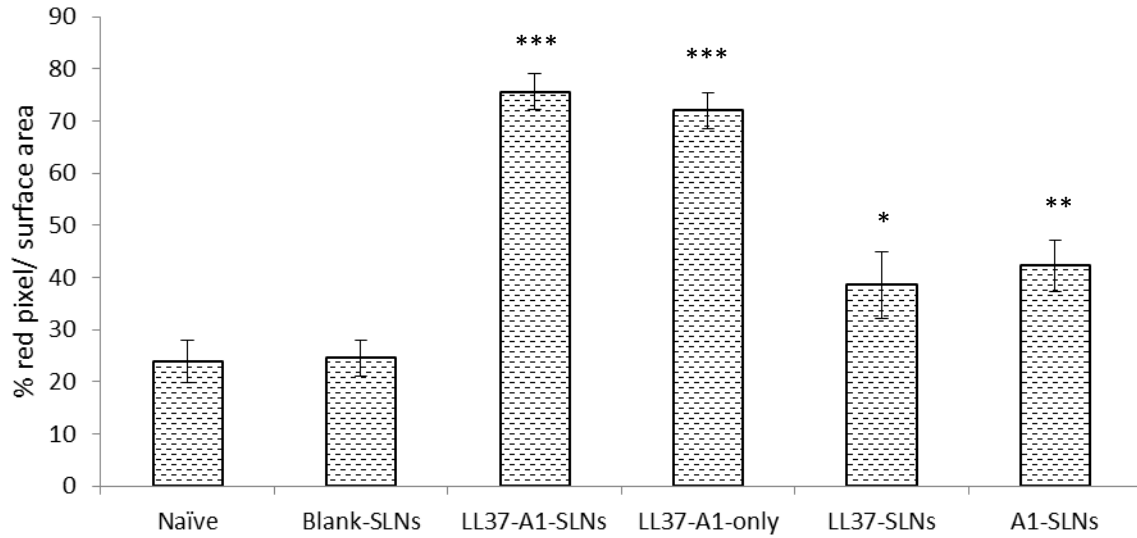
Figure 18. Combination SLNs demonstrated higher endothelial cell colonization. (A) Representative images of wound sections from day 13 post wounding of all six groups stained with an antibody directed against endothelial cell surface marker CD31+ antibody. (B) Quantification of red pixels representing the extent of CD31 marking. Both LL37-A1-SLNs and LL37-A1-only treatment groups demonstrate higher extent of angiogenesis in comparison to untreated or individually treated groups. Values represent mean±S.D; n=2 (LL37-SLNs group); n=3 (all other treatment groups). * *P<0.05*, ** *P<0.01*, and *** *P<0.001* vs. Naive.

CHAPTER 4: DISCUSSION

Wound healing is a complex and dynamic process of physiological responses involved in restoring tissue integrity after injury [7,16]. The ability of the body to repair tissue damage is an important survival tool for living organisms [13,16]. In view of the fact that impaired WH is associated with high morbidity and mortality rates in patients, an innovative nanoformulation for the delivery of combination peptides with both wound healing and antibacterial properties has been formulated and tested. It has been demonstrated that LL37-A1-SLNs could promote wound healing and possess antibacterial property in fixed combination concentration ratios in comparison to individual drug alone.

The w/o/w double emulsion method used to formulate SLNs offered protection to the peptides and is also one of the most appropriate methods to incorporate peptides into nanoparticles. Using our modified solvent diffusion-double emulsion method, our nanoparticles were smaller in size compared to SLNs prepared solely with just the solvent diffusion method [134,142]. The diffusion rate of the water miscible organic solvent to the aqueous phase of PVA was very rapid, indicating that the resulting turbulence from the emulsion droplet at the interface is due to the marangoni effect [143]. By using particles with a solid lipid matrix, drug leakage and coalescence related stability shortcomings, which are often observed with lipid dispersions such as emulsions and liposomes may be overcome.

It has been reported that chemically heterogeneous non-ionic lipids in combination with heterogeneous co-surfactants lead to the formation of spherical particles, slows down the inevitable separation of the SLNs, as well as reduces the particle size [144-146]. Here we used a combination of glyceryl monostearate as a non-ionic surfactant with α-L-phosphatidylcholine as a co-surfactant resulting in the formation of SLNs with small particle size. In the current study, after evaluating different loading concentrations of LL37 and A1 into a single nanoformulation (data not shown), After taking into consideration the

encapsulation efficiency (EE%), we formulated prep 1 (final loading of 8.48 µg for LL37 and 43.5 µg for A1 per mg of SLNs) and prep 2 (final loading of 16.32 µg for LL37 and 62.47 µg for A1 per mg of SLNs) in order to maintain the initial 24 h release rate within the synergistic combination concentration ratio range. However, in the case of prep 2, we did not choose double the final loaded concentration for A1 in comparison to prep 1 as we observed an increase in particle size and a significant reduction in EE%. While Prep 2 loaded with 62.47 µg of A1 per mg of SLNs we were not only able to maintain the EE% but 24 h release rate was also sufficient to maintain the concentrations of LL37 and A1 within the synergistic combination concentration ranges. Thus, after taking all the above parameters into consideration we selected prep 1 and prep 2 as our final SLN formulations.

It has been proposed that AWF containing 2% albumin closely represents the composition of an exudating wound [147]. Release studies performed in AWF demonstrated that LL37 and A1 released from LL37-A1-SLNs followed a biphasic pattern with over 10% of both peptides released within 24 h, followed by a slow and sustained release over the entire study period. The slow and controlled release of both LL37 and A1 from LL37-A1-SLNs suggests that LL37 and A1 were homogeneously dispersed in the lipid matrix and the release rate was determined by the diffusion of drugs from the rigid matrix structure. After 48 h, the release profile of A1 from both prep 1 and prep 2 appeared to reach a plateau. One of the reasons behind this behavior may be due to the maximum drug depletion quantity (MDDQ) phenomenon [126,148]. The initial release of the peptides from SLNs during the first 48 h may be directly related to the amount of the peptides that existed both inside and on the surface of the SLN, while it has been previously reported that over a period of time, SLNs with their condensed and highly ordered molecular conformation tends to retain a part of the loaded drug inside the lipid core due to the strong hydrophobic interaction between the lipid and the drug, resulting in a reduction in release over time. Previous studies on SLNs have also observed similar plateau in the release pattern [118,126,148,149]. The fact that our formulations also demonstrated low % release over the entire study period with the release

reaching a plateau level may be ascribed by the high homogenous entrapment of the peptides within the lipid matrix and less association of the peptides on the nanoparticle surface [126,148]. Weibull and Higuchi equation describes the release rate of the drug from spherical nanoparticles suggesting that the time required to release 50% of the drug is normally expected to be 10% of the time, which is required to dissolve the drug in the center of the nanoparticle pellet. Thus, the equation describes the release of a drug from an insoluble matrix as the square root of a time-dependent process. Thus, the obtained release data demonstrated that LL37-A1-SLNs followed the Weibull and Higuchi equation (Figure 6) [150,151]. One of the greatest obstacles associated with dermal and transdermal routes of drug administration are the penetration across the stratum corneum, which is the outermost, least permeable layer of the skin. For our *ex vivo* skin permeation experiment, the pinna skin of the inner side of the rabbit ear was used to determine LL37 and A1 permeation across the stratum corneum when released from LL37-A1-SLNs. In our experiment, the pinna skin was chosen firstly, since the relative electro-osmotic and electrorepulsive contributions are almost similar for rabbit ear skin and human skin [152]. The density of hair follicles on rabbit ear skin is approximately $80/cm^2$ which is comparable to human skin ($29\text{-}93/cm^2$) but differs greatly from rodent skin (rat $8000/cm^2$) [153]. Secondly, studies have demonstrated comparable permeability of several drugs across rabbit ear skin and human skin [152]. During injury, the wound site not only constitutes of broken skin but it may also contain certain debris of skin cells. Similarly, there may be certain areas around the wound site with intact skin layers and hence the *ex vivo* skin permeation study was performed on an intact layer of stratum corneum in order to determine the ability of SLNs to permeate into and across the least permeable intact layer of the skin. The current study showed a sustained permeation of LL37 and A1 across the skin when released from LL37-A1-SLNs over the entire study period in comparison to individual drug alone, where permeation appeared to have stopped after 48 h (Figure 7). This decrease in the permeation of peptides across the skin (in comparison LL37-A1-SLNs) may be due to the degradation of the peptides particularly since the permeation studies were performed at 37ºC. Hence, our SLN formulation appeared to have

protected the peptides from degradation during the entire study period as well as the SLNs demonstrate their ability in permeating across intact skin in case when the injured wound site not only has broken skin but also is surrounded by intact skin.

To avoid opportunistic infections, the human skin has developed antimicrobial agents such as LL37 in the epithelia [154]. These antimicrobial agents play a crucial role in innate immunity to protect the human body against invading microorganisms. Several studies have investigated the synergistic effects of LL37 with other antibacterial peptides against *S. aureus* and *E. coli* [154,155]. Since LL37-A1-SLNs are composed of 2 drugs, it was of great interest to delineate whether the anti-bacterial and wound healing effects of prep 1 and prep 2 *in vitro* was attributed to the synergistic action of LL37 and A1.

As shown in the present study, different doses of LL37 and A1 were tested against gram-positive *S. aureus* and gram-negative *E. coli* to determine the synergistic potential of these peptides (Table 4 and Figure 8). The therapeutic potencies of LL37 and A1 in prep 1 and prep 2 against *S. aureus* and *E. coli* were found to be synergistic or even additive with certain fixed combination concentrations to be antagonistic. The checkerboard assay is used generally to test the activity of combination drugs by determining the ∑FICs of all the combinations tested. ∑FICs of the combination concentration ratios, which were used in the formulation of the combination, SLNs were found to be synergistic in agreement with the Chou-Talalay results. While some combination ratios showed antagonism by Chou-Talalay method, none of the combinations demonstrated antagonism but rather showed indifference as per the ∑FICs using checkerboard assay (Table 5 and 6). This difference may generally be due to the limitations related with the design, performance, and interpretation of the checkerboard method [156]. It can be speculated that A1 did not affect *S. aureus* and *E. coli* directly but potentiated the anti-bacterial action of LL37 when used in a combination. Based on the synergistic antibacterial studies, A1 alone was not able to achieve the desired bacterial inhibition. However, in the presence of LL37, the effect of A1 was potentiated and led to significant inhibition of *S. aureus* and *E. coli* (Table 4 and Figure 9). The

cationic LL37 can bind electrostatically with the anionic surface of the bacteria (phospholipid and LPS on gram negative bacteria and teichoic acid on gram positive bacteria) resulting in disruption of the membrane by pore formation [157-159]. A1 enhances the antibacterial activity of LL37 primarily by protecting against endotoxin-induced lethality by tissue modulation. This indirect antibacterial activity of A1 aids LL37 in the suppression of bacterial proliferation during infections due to its ability to bind to the bacterial-essential furin, and by undergoing S-nitrosylation in the presence of nitric oxide [158,160-162].

After revealing the synergistic interaction between LL37 and A1, two combination concentration ratios of LL37-A1-SLNs with synergistic potency were selected and evaluated *in vitro* for WH activity. Like its antibacterial action, LL37-A1-SLNs impact on WH is multi-faceted. Although LL37 itself exhibited more potent anti-bacterial activity, its efficacy in promoting wound healing *in vitro* was not satisfactory. It can be speculated that in the presence of A1 the effect of LL37 was potentiated and led to significant wound healing in both BJ fibroblast cells and keratinocytes (primary cells present in the skin). A1 is strictly involved in the coagulation, inflammatory and complement pathways affecting both WH and angiogenesis [94,163,164]. Similarly, LL37 is involved in many aspects of innate immunity such as chemotaxis and angiogenesis. As mentioned earlier, upon binding to the FPRL-1 receptor, LL37 can induce cellular signaling and calcium mobilizing effects. Thus, it can be speculated that the wound healing potential of LL37-A1-SLNs is related to its impact on chemotaxis via multiple pathways by affecting internal cell targets that have positive effects on its immunomodulatory properties. This can involve the induction of cellular signaling pathways that leads to calcium influx as well as its ability to regulate angiogenesis and collagen deposition that are prerequisite for the activation and migration of BJ fibroblast cells and keratinocytes. It is evident that both prep 1 and prep 2 induced migration of BJ fibroblast cells and keratinocytes as seen by the increase in filopodia-like protrusions on the plasma membrane (Figure 11) [165,166].

In developing a topical antibacterial and WH therapy, it is important that the agent is biocompatible and non-cytotoxic. Studies have shown that GMS and PC are non-cytotoxic [133,146]. In our study, we have demonstrated that prep 1, prep 2 and blank SLNs are non-cytotoxic to BJ fibroblast cells and keratinocytes. Toxicity was only observed at high concentrations and was dose-dependent (Figure 10).

A variety of endotoxins are released by the outer membrane of gram-negative bacteria, namely LPS-protein complex, which plays an important role in the pathogenesis of hard to heal wounds [167]. The activation of BJ fibroblast cells and keratinocytes is initiated when LPS binds to LPS-binding protein (LBP) [168]. In our study, we first evaluated the adverse effects of LPS on the cell barrier function *in vitro* using a monolayer of BJ fibroblast cells and keratinocytes and attempted to determine whether prep 1 and prep 2 can protect the monolayer from the negative impacts of LPS. As expected, LPS induced a marked increase in the permeability of the cells which is reflected in the TEER measurements (Figure 12). Co-exposure of LPS treated cells to LL37 (5 µg/mL) and A1 only (20 µg/mL) resulted in no significant increase in TEER. In contrast, co-treatment with LL37-A1-SLNs (prep 1 and prep 2) resulted in significant increases in TEER, indicating the benefit of LL37-A1-SLNs in protecting the membrane integrity and barrier function of BJ fibroblast cells and keratinocytes against LPS insult. It can be speculated that the combination of LL37 and A1 is indeed neutralizing the activity of LPS by binding to the binding site of LBP and activating the NF-κB pathway resulting in an increase in TEER value [169-171].

It has been reported that LPS can significantly induce an inflammatory response in BJ fibroblast cells and keratinocytes at high concentrations [172]. Studies have shown that free radicals and reactive oxygen metabolites produced during LPS insult can amplify and/or trigger inflammation via upregulation in the expression of a number of genes, including NF-κβ, which in turn, amplifies the inflammatory response by upregulating the production of several proinflammatory cytokines and enzymes, such as IL-1β, IL-6, TNF-α and iNOS [173,174]. Exposure of BJ fibroblast cells and keratinocytes to LPS (10 µg/mL)

resulted in marked increase in production of IL-1β, IL-6, and TNF-α, cytokines, which are over expressed during the inflammatory phase of CWs [175-177]. In contrast, co-treatment of BJ fibroblast cells and keratinocytes with LPS and LL37-A1-SLNs (prep 1 and prep 2) significantly attenuated the production of these proinflammatory cytokines (Figure 13). The amount of collagen deposition is indicative of the activities of BJ fibroblast cells and keratinocytes in the newly formed granulation tissue, which is a prerequisite step during the proliferation and re-modeling phases of wound healing. Treatment of BJ fibroblast cells and keratinocytes with LPS significantly decreased collagen-I production. Interestingly, co-treatment with LL37-A1-SLNs (prep 1 and prep 2) significantly increased collagen-I production in comparison to LL37 only, A1 only, and control treatment groups which can possibly be due to the collagen modulating activity of LL37-A1-SLNs. As a result, our SLNs can reverse the negative impacts of LPS to promote WH by reducing the upregulated inflammatory condition and thus potentiating the orderly healing process (Figure 13).

We have consistently shown the lack of toxicity following topical application of our nanoformulation. This is reflected in cell cytotoxicity assay as well as histologically in the current study, in which the wounds treated with LL37-A1-SLNs demonstrated well-organized granulation tissue without evidence of increase in inflammation or necrosis. LL37-A1-SLNs, blank-SLNs, LL37-SLNs, A1-SLNs, and LL37-A1-only groups were tested *in vivo* to determine their wound healing ability. By performing *in vivo* experiments with all six groups (naïve, Blank-SLNs, LL37-A1-SLNs, LL37-A1-only, LL37-SLNs, and A1-SLNs) we attempted to present a comprehensive comparative validation of the potential combination SLNs to promote wound healing (Figure 14). Both LL37-A1-SLNs and LL37-A1-only groups demonstrated higher % wound closure in comparison to untreated or individual treated groups which became highly significant from day 9 and by day 13 both LL37-A1-SLNs and LL37-A1-only treatment groups induced nearly complete wound closure, thus supporting the hypothesis of combined effects of LL37 and A1 in agreement to the *in vitro* results.

In line with the *in vitro* studies, histological and tissue analysis demonstrated that both LL37-A1-SLNs and LL37-A1-only treated groups enhanced granulation tissue formation, with more denser and compact collagen deposition and organization as well as increased neovascularization in comparison to untreated or individual treated groups.

Histological examination of the wound tissue sections presented insights on the predominant stages involved during the healing process. HE staining revealed that the regenerated epidermal and subepidermal layers were well organized and arranged in case of both LL37-A1-SLNs and LL37-A1-only treatment groups in comparison to untreated or individual treated groups (Figure 15). Similarly, LL37-A1-SLNs and LL37-A1-only treated mice showing advanced granulation tissue formation, demonstrating a mature healed tissue in comparison to untreated or individual treated groups. It can be speculated that the combined effects of LL37 and A1 delivered to the wound site simultaneously fastened the re-epithelialization process leading to accelerated maturation of the epidermal layer which clearly visible in the histological sections on day 13 after treatment (Figure 15).

MT staining evaluated the extent of collagen deposition during the healing process (Figure 16). Migration of keratinocyte at the wound site is one of the main factors contributing to epidermal wound healing [19]. Similarly, the extent of collagen deposition at the wound site is indicative of the activity of fibroblast in the newly formed granulation tissue, playing an important role in the healing process [178].

Sirius Red/ Fast Green assay was performed in order to quantitatively measure the collagen content as well as the non-collagenous proteins in the wound tissue sections. Sirius red specifically binds to the helical structure of collagen (type I to V) whereas, fast green binds to the non-collagenous proteins. In line with the previous results of MT staining, Sirius red/fast green assay confirmed that both LL37-A1-SLNs and LL37-A1-only treated groups demonstrated greater collagen deposition and a much denser compact alignment in comparison to untreated or individual treated groups (Figure 17).

In order to determine the endothelial cells populating the micro vessels during angiogenesis, we performed immunostaining with anti- mouse CD31 antibody. This antibody was specific to the CD31+ marker present on the endothelial cells. Both LL37-A1-SLNs and LL37-A1-only treated groups showed higher CD31+ staining of endothelial cells in wound tissue sections in comparison to untreated or individual treated groups (Figure 18). Thus, it can be speculated that higher angiogenesis was demonstrated due to the combined effects of LL37 and A1.

Thus, the activity of LL37-A1-SLNs as a combination formulation accelerated WH and enhanced antibacterial activity. Hence, the discussed results justify the use of LL37 and A1 in combination for WH therapy. However, further investigation is required to understand the mechanisms involved in the synergistic antibacterial and healing process as well as to optimize the ratio of LL37 and A1 for rapid WH.

CHAPTER 5: CONCLUSION

We have successfully developed a solid lipid nanoparticle (SLN) formulation that can simultaneously deliver LL37 and A1 at specific ratios resulting in acceleration in wound healing by promoting wound closure in BJ fibroblast cells and keratinocytes as well as enhancing antibacterial activity against *S. aureus* and *E. coli* in comparison to LL37 or A1 alone. Co-treatment of BJ fibroblast cells and keratinocytes with the combination nanomedicine resulted in a significant increase in transepithelial electrical resistance, indicating the benefits of LL37 and A1 combination in protecting cell membrane integrity and barrier function of cells against LPS insult. Combination SLNs exhibited appreciable anti-inflammatory activity in terms of their ability to inhibit LPS-induced inflammatory mediators and cytokines in BJ fibroblast cells and keratinocytes as well as demonstrated significantly higher collagen-I deposition in comparison to LL37 or A1 alone. In conclusion, we have developed a combination nanomedicine that can accelerate the wound healing process, enhance antibacterial activity, and exhibit anti-inflammatory activity due to combination effects of LL37 and A1 released from SLNs.

ABBREVIATIONS

ADAMs – A disintegrin and metalloproteinases

AWF – Artificial wound fluid

AWs – Acute wounds

bFGF – Basic fibroblast growth factor

BMZ – Basement membrane zone

BSA – Bovine serum albumin

CFUs – Colony forming units

CI – Combination index

CWs – Chronic wounds

ECM – Extracellular matrix

EE% – Encapsulation efficiency %

ELISA – Enzyme-linked immunosorbent assay

EMEM – Eagle's minimum essential medium

FBS – Fetal bovine serum

FDA – Food drug and administration

FPRL-1 – Formyl peptide receptor-like 1

GMS – Glyceryl mono stearate

HPLC – High-performance liquid chromatography

IL – Interleukin

iNOS – Inducible nitric oxide synthase (iNOS)

LHRH – luteinizing hormone-releasing hormone

LPS – Lipopolysaccharide

MMPs – Matrix metalloproteinases

MRSA – Methicillin-resistant staphylococcus aureus

NC – Negative control

NE – Neutrophil elastase

NF-κB – Nuclear Factor kappa B

OD – Optical density

PC – Positive control

PDGF – Platelet-derived growth factor

PVA – Poly vinyl alcohol

SLNs – Solid lipid nanoparticles

TEER – Transepithelial electrical resistance

TEM – Transmission electron microscope

TIMPs – Tissue inhibitors of metalloproteinases

TNF – Tumor necrosis factor

VEGF – Vascular endothelial growth factor

w/o – Water in oil

w/o/w – Water in oil in water

WH – Wound healing

REFERENCES

1   Health-Cares. "Skin care" (analysis). (2007).
2   Proksch, E., Brandner, J. M. & Jensen, J. M. The skin: an indispensable barrier. *Exp. Dermatol.* **17**, 1063-1072 (2008).
3   Madison, K. C. Barrier function of the skin: "la raison d'etre" of the epidermis. *J. Invest. Dermatol.* **121**, 231-241, doi:10.1046/j.1523-1747.2003.12359.x (2003).
4   Stucker, M. *et al.* The cutaneous uptake of atmospheric oxygen contributes significantly to the oxygen supply of human dermis and epidermis. *J. Physiol.* **538**, 985-994 (2002).
5   McCarcken et. al. *New Atlas of Human Anatomy*. 1-240 (2000).
6   McGrath, J. A. e. a. *Rook's Textbook of Dermatology (7th ed.)*. 3.1-3.6 (Blackwell Publishing, 2004).
7   Haake AR, H. K. *The biology of skin*. (2001).
8   Wysocki, A. B. A review of the skin and its appendages. *Advances in wound care : the journal for prevention and healing* **8**, 53-54, 56-62, 64 passim (1995).
9   P. F. Millington, R. W. *Skin*. Vol. 9 (Cambridge University Press, 1983).
10   Breitkreutz, D., Mirancea, N. & Nischt, R. Basement membranes in skin: unique matrix structures with diverse functions? *Histochem. Cell Biol.* **132**, 1-10, doi:10.1007/s00418-009-0586-0 (2009).
11   Malvi. *The Ageing Skin*, <pharmaxchange.info> (March 3, 2011).
12   Iozzo, R. V. Basement membrane proteoglycans: from cellar to ceiling. *Nat. Rev. Mol. Cell Biol.* **6**, 646-656, doi:10.1038/nrm1702 (2005).
13   WM, S. Structure and function of the skin. *Principles and practice of dermatology* (1990).
14   Reinke, J. M. & Sorg, H. Wound repair and regeneration. *Eur. Surg. Res.* **49**, 35-43, doi:10.1159/000339613 (2012).
15   Stadelmann, W. K., Digenis, A. G. & Tobin, G. R. Physiology and healing dynamics of chronic cutaneous wounds. *Am. J. Surg.* **176**, 26S-38S (1998).
16   Nguyen. et. al. *Biomaterials for treating skin loss*. 25-57 (2009).
17   Velnar, T., Bailey, T. & Smrkolj, V. The wound healing process: an overview of the cellular and molecular mechanisms. *J. Int. Med. Res.* **37**, 1528-1542 (2009).
18   Ruth A. Bryant et.al. *Acute and Chronic Wounds, current management concepts*. 4 edn, 63-82 (2012).
19   Martin, P. Wound healing--aiming for perfect skin regeneration. *Science* **276**, 75-81 (1997).
20   Mast, B. A. & Schultz, G. S. Interactions of cytokines, growth factors, and proteases in acute and chronic wounds. *Wound Repair Regen.* **4**, 411-420, doi:10.1046/j.1524-475X.1996.40404.x (1996).
21   Cheresh, D. A. & Stupack, D. G. Regulation of angiogenesis: apoptotic cues from the ECM. *Oncogene* **27**, 6285-6298, doi:10.1038/onc.2008.304 (2008).
22   Gill, S. E. & Parks, W. C. Metalloproteinases and their inhibitors: regulators of wound healing. *Int. J. Biochem. Cell Biol.* **40**, 1334-1347, doi:10.1016/j.biocel.2007.10.024 (2008).
23   Macri, L. & Clark, R. A. Tissue engineering for cutaneous wounds: selecting the proper time and space for growth factors, cells and the extracellular matrix. *Skin Pharmacol. Physiol.* **22**, 83-93, doi:10.1159/000178867 (2009).
24   Pullar, C. E., Manabat-Hidalgo, C. G., Bolaji, R. S. & Isseroff, R. R. beta-Adrenergic receptor modulation of wound repair. *Pharmacol. Res.* **58**, 158-164, doi:10.1016/j.phrs.2008.07.012 (2008).
25   Werner, S. & Grose, R. Regulation of wound healing by growth factors and cytokines. *Physiol. Rev.* **83**, 835-870, doi:10.1152/physrev.00031.2002 (2003).
26   Sandeman, S. R., Allen, M. C., Liu, C., Faragher, R. G. & Lloyd, A. W. Human keratocyte migration into collagen gels declines with in vitro ageing. *Mech. Ageing Dev.* **119**, 149-157 (2000).

27   Midwood, K. S., Williams, L. V. & Schwarzbauer, J. E. Tissue repair and the dynamics of the extracellular matrix. *Int. J. Biochem. Cell Biol.* **36**, 1031-1037, doi:10.1016/j.biocel.2003.12.003 (2004).

28   Cooper, D. M., Yu, E. Z., Hennessey, P., Ko, F. & Robson, M. C. Determination of endogenous cytokines in chronic wounds. *Ann. Surg.* **219**, 688-691; discussion 691-682 (1994).

29   Stroncek, J. D. & Reichert, W. M. in *Indwelling Neural Implants: Strategies for Contending with the In Vivo Environment*   (ed W. M. Reichert) (2008).

30   Michael Mercandetti et. al. Wound healing and repair. *Medscape* (2013).

31   Eming, S. A., Krieg, T. & Davidson, J. M. Inflammation in wound repair: molecular and cellular mechanisms. *J. Invest. Dermatol.* **127**, 514-525, doi:10.1038/sj.jid.5700701 (2007).

32   Leibovich, S. J. & Ross, R. The role of the macrophage in wound repair. A study with hydrocortisone and antimacrophage serum. *Am. J. Pathol.* **78**, 71-100 (1975).

33   Tziotzios, C., Profyris, C. & Sterling, J. Cutaneous scarring: Pathophysiology, molecular mechanisms, and scar reduction therapeutics Part II. Strategies to reduce scar formation after dermatologic procedures. *J. Am. Acad. Dermatol.* **66**, 13-24; quiz 25-16, doi:10.1016/j.jaad.2011.08.035 (2012).

34   Profyris, C., Tziotzios, C. & Do Vale, I. Cutaneous scarring: Pathophysiology, molecular mechanisms, and scar reduction therapeutics Part I. The molecular basis of scar formation. *J. Am. Acad. Dermatol.* **66**, 1-10; quiz 11-12, doi:10.1016/j.jaad.2011.05.055 (2012).

35   Cross, K. J. & Mustoe, T. A. Growth factors in wound healing. *Surg. Clin. North Am.* **83**, 531-545, vi, doi:10.1016/S0039-6109(02)00202-5 (2003).

36   Koh, T. J. & DiPietro, L. A. Inflammation and wound healing: the role of the macrophage. *Expert Rev. Mol. Med.* **13**, e23, doi:10.1017/S1462399411001943 (2011).

37   Monaco, J. L. & Lawrence, W. T. Acute wound healing an overview. *Clin. Plast. Surg.* **30**, 1-12 (2003).

38   Goldman, R. Growth factors and chronic wound healing: past, present, and future. *Adv Skin Wound Care* **17**, 24-35 (2004).

39   Staiano-Coico, L., Higgins, P. J., Schwartz, S. B., Zimm, A. J. & Goncalves, J. Wound fluids: a reflection of the state of healing. *Ostomy Wound Manage.* **46**, 85S-93S; quiz 94S-95S (2000).

40   Braiman-Wiksman, L., Solomonik, I., Spira, R. & Tennenbaum, T. Novel insights into wound healing sequence of events. *Toxicol. Pathol.* **35**, 767-779, doi:10.1080/01926230701584189 (2007).

41   Myers, S. R., Leigh, I. M. & Navsaria, H. Epidermal repair results from activation of follicular and epidermal progenitor keratinocytes mediated by a growth factor cascade. *Wound Repair Regen.* **15**, 693-701, doi:10.1111/j.1524-475X.2007.00297.x (2007).

42   Sorg, H., Krueger, C. & Vollmar, B. Intravital insights in skin wound healing using the mouse dorsal skin fold chamber. *J. Anat.* **211**, 810-818, doi:10.1111/j.1469-7580.2007.00822.x (2007).

43   Pradhan, L., Nabzdyk, C., Andersen, N. D., LoGerfo, F. W. & Veves, A. Inflammation and neuropeptides: the connection in diabetic wound healing. *Expert Rev. Mol. Med.* **11**, e2, doi:10.1017/S1462399409000945 (2009).

44   Eckes, B., Nischt, R. & Krieg, T. Cell-matrix interactions in dermal repair and scarring. *Fibrogenesis Tissue Repair* **3**, 4, doi:10.1186/1755-1536-3-4 (2010).

45   Barker, T. H. The role of ECM proteins and protein fragments in guiding cell behavior in regenerative medicine. *Biomaterials* **32**, 4211-4214, doi:10.1016/j.biomaterials.2011.02.027 (2011).

46   Hinz, B. Formation and function of the myofibroblast during tissue repair. *J. Invest. Dermatol.* **127**, 526-537, doi:10.1038/sj.jid.5700613 (2007).

47   Gurtner, G. C. & Evans, G. R. Advances in head and neck reconstruction. *Plast. Reconstr. Surg.* **106**, 672-682; quiz 683 (2000).

48   Rahban, S. R. & Garner, W. L. Fibroproliferative scars. *Clin. Plast. Surg.* **30**, 77-89 (2003).

49   Wilgus, T. A. Regenerative healing in fetal skin: a review of the literature. *Ostomy Wound Manage.* **53**, 16-31; quiz 32-13 (2007).

50   Thom, S. R. Oxidative stress is fundamental to hyperbaric oxygen therapy. *J Appl Physiol (1985)* **106**, 988-995, doi:10.1152/japplphysiol.91004.2008 (2009).

51   Witte, M. B. & Barbul, A. General principles of wound healing. *Surg. Clin. North Am.* **77**, 509-528 (1997).

52   Gosain, A. & DiPietro, L. A. Aging and wound healing. *World J. Surg.* **28**, 321-326, doi:10.1007/s00268-003-7397-6 (2004).

53   Pittman, J. Effect of aging on wound healing: current concepts. *J. Wound Ostomy Continence Nurs.* **34**, 412-415; quiz 416-417, doi:10.1097/01.WON.0000281658.71072.e6 (2007).

54   Chandra N. et. al. Extracellular Wound Matrices: Novel Stabilization and Sterilization Method for Collagen-based Biologic Wound Dressings. *Wounds* **19**, 148-156 (2007).

55   Minke G. et. al. Extracellular Wound Matrix (OASIS®): Exploring the Contraindications. Results of Its Use in 32 Consecutive Outpatient Clinic. *Wounds* **10** (2007).

56   Bjarnsholt, T. *et al.* Why chronic wounds will not heal: a novel hypothesis. *Wound Repair Regen.* **16**, 2-10, doi:10.1111/j.1524-475X.2007.00283.x (2008).

57   Chen, S. M., Ward, S. I., Olutoye, O. O., Diegelmann, R. F. & Kelman Cohen, I. Ability of chronic wound fluids to degrade peptide growth factors is associated with increased levels of elastase activity and diminished levels of proteinase inhibitors. *Wound Repair Regen.* **5**, 23-32, doi:10.1046/j.1524-475X.1997.50108.x (1997).

58   Menke, N. B., Ward, K. R., Witten, T. M., Bonchev, D. G. & Diegelmann, R. F. Impaired wound healing. *Clin. Dermatol.* **25**, 19-25, doi:10.1016/j.clindermatol.2006.12.005 (2007).

59   Shalini V. Gohil, E. N. J., and Lakshmi S.Nair. in *Nanotechnology and regenerative engineering: The Scafold, Second Edition* (ed Lakshmi S. Lair Cato T. Laurencin) Ch. 12, 343-364.

60   Brissett, A. E. & Hom, D. B. The effects of tissue sealants, platelet gels, and growth factors on wound healing. *Curr. Opin. Otolaryngol. Head Neck Surg.* **11**, 245-250 (2003).

61   Jan J. Clark et.al. Wound Repair and Factors Influencing Healing. *Crit. Care Nurs. Q.* **25**, 1-12 (2002).

62   Moore, K. Cell biology of chronic wounds: the role of inflammation. *J. Wound Care* **8**, 345-348 (1999).

63   Li, J., Chen, J. & Kirsner, R. Pathophysiology of acute wound healing. *Clin. Dermatol.* **25**, 9-18, doi:10.1016/j.clindermatol.2006.09.007 (2007).

64   Diegelmann, R. F. Excessive neutrophils characterize chronic pressure ulcers. *Wound Repair Regen.* **11**, 490-495 (2003).

65   Palolahti, M., Lauharanta, J., Stephens, R. W., Kuusela, P. & Vaheri, A. Proteolytic activity in leg ulcer exudate. *Exp. Dermatol.* **2**, 29-37 (1993).

66   Piaggesi, A. *et al.* Semiquantitative analysis of the histopathological features of the neuropathic foot ulcer: effects of pressure relief. *Diabetes Care* **26**, 3123-3128 (2003).

67   Lobmann, R., Schultz, G. & Lehnert, H. Proteases and the diabetic foot syndrome: mechanisms and therapeutic implications. *Diabetes Care* **28**, 461-471 (2005).

68   Nwomeh, B. C., Liang, H. X., Diegelmann, R. F., Cohen, I. K. & Yager, D. R. Dynamics of the matrix metalloproteinases MMP-1 and MMP-8 in acute open human dermal wounds. *Wound Repair Regen.* **6**, 127-134 (1998).

69   Wysocki, A. B., Staiano-Coico, L. & Grinnell, F. Wound fluid from chronic leg ulcers contains elevated levels of metalloproteinases MMP-2 and MMP-9. *J. Invest. Dermatol.* **101**, 64-68 (1993).

70   Yager, D. R., Zhang, L. Y., Liang, H. X., Diegelmann, R. F. & Cohen, I. K. Wound fluids from human pressure ulcers contain elevated matrix metalloproteinase levels and activity compared to surgical wound fluids. *J. Invest. Dermatol.* **107**, 743-748 (1996).

71   Lobmann, R. *et al.* Expression of matrix-metalloproteinases and their inhibitors in the wounds of diabetic and non-diabetic patients. *Diabetologia* **45**, 1011-1016, doi:10.1007/s00125-002-0868-8 (2002).

72   Nwomeh, B. C., Yager, D. R. & Cohen, I. K. Physiology of the chronic wound. *Clin. Plast. Surg.* **25**, 341-356 (1998).

73   Bullen, E. C. *et al.* Tissue inhibitor of metalloproteinases-1 is decreased and activated gelatinases are increased in chronic wounds. *J. Invest. Dermatol.* **104**, 236-240 (1995).

74   Brem, H. *et al.* Molecular markers in patients with chronic wounds to guide surgical debridement. *Mol. Med.* **13**, 30-39, doi:10.2119/2006-00054.Brem (2007).

75   Landis, S. J. Chronic wound infection and antimicrobial use. *Adv Skin Wound Care* **21**, 531-540; quiz 541-532, doi:10.1097/01.ASW.0000323578.87700.a5 (2008).

76   Kirketerp-Moller, K. *et al.* Distribution, organization, and ecology of bacteria in chronic wounds. *J. Clin. Microbiol.* **46**, 2717-2722, doi:10.1128/JCM.00501-08 (2008).

77   Pupp, G. What you should know about bioflims and chronic wounds. *Podiatry today* **21** (2008).

78   Dowd, S. E. *et al.* Survey of bacterial diversity in chronic wounds using pyrosequencing, DGGE, and full ribosome shotgun sequencing. *BMC Microbiol.* **8**, 43, doi:10.1186/1471-2180-8-43 (2008).

79   Gjodsbol, K. *et al.* Multiple bacterial species reside in chronic wounds: a longitudinal study. *Int Wound J* **3**, 225-231, doi:10.1111/j.1742-481X.2006.00159.x (2006).

80   James, G. A. *et al.* Biofilms in chronic wounds. *Wound Repair Regen.* **16**, 37-44, doi:10.1111/j.1524-475X.2007.00321.x (2008).

81   Markova, A. & Mostow, E. N. US skin disease assessment: ulcer and wound care. *Dermatol. Clin.* **30**, 107-111, ix, doi:10.1016/j.det.2011.08.005 (2012).

82   Vermeulen, H., van Hattem, J. M., Storm-Versloot, M. N. & Ubbink, D. T. Topical silver for treating infected wounds. *Cochrane Database Syst Rev*, CD005486, doi:10.1002/14651858.CD005486.pub2 (2007).

83   Eltzschig, H. K. & Collard, C. D. Vascular ischaemia and reperfusion injury. *Br. Med. Bull.* **70**, 71-86, doi:10.1093/bmb/ldh025 (2004).

84   Phillips, E. & Young, T. Methicillin-resistant Staphylococcus aureus and wound management. *Br. J. Nurs.* **4**, 1345-1349, doi:10.12968/bjon.1995.4.22.1345 (1995).

85   Dunford, C. E. Methicillin resistant Staphylococcus aureus. *Nurs. Stand.* **11**, 58, 61-52 (1997).

86   Kauffman, C. A. *et al.* Attempts to eradicate methicillin-resistant Staphylococcus aureus from a long-term-care facility with the use of mupirocin ointment. *Am. J. Med.* **94**, 371-378 (1993).

87   Drosou A, e. a. Antiseptics on Wounds: An Area of Controversy. *Wounds* **15** (2003).

88   Bianchi, J. Cadexomer-iodine in the treatment of venous leg ulcers: what is the evidence? *J. Wound Care* **10**, 225-229, doi:10.12968/jowc.2001.10.6.26085 (2001).

89   Jones, V. & Milton, T. When and how to use iodine dressings. *Nurs. Times* **96**, 2-3 (2000).

90   Sundberg J, e. a. A Retrospective Review of the Use of Cadexomer Iodine in the Treatment of Chronic Wounds. *Wounds* **9**, 68-86 (1997).

91   Lansdown, A. B. Silver. I: Its antibacterial properties and mechanism of action. *J. Wound Care* **11**, 125-130, doi:10.12968/jowc.2002.11.4.26389 (2002).

92   Lipsky, B. A. & Hoey, C. Topical antimicrobial therapy for treating chronic wounds. *Clin. Infect. Dis.* **49**, 1541-1549, doi:10.1086/644732 (2009).

93   Carter, M. J., Tingley-Kelley, K. & Warriner, R. A., 3rd. Silver treatments and silver-impregnated dressings for the healing of leg wounds and ulcers: a systematic review and meta-analysis. *J. Am. Acad. Dermatol.* **63**, 668-679, doi:10.1016/j.jaad.2009.09.007 (2010).

94   Grinnell, F. & Zhu, M. Identification of neutrophil elastase as the proteinase in burn wound fluid responsible for degradation of fibronectin. *J. Invest. Dermatol.* **103**, 155-161 (1994).

95   Fitch, P. M., Roghanian, A., Howie, S. E. & Sallenave, J. M. Human neutrophil elastase inhibitors in innate and adaptive immunity. *Biochemical Society transactions* **34**, 279-282, doi:10.1042/BST20060279 (2006).

96   Grinnell, F. & Zhu, M. Fibronectin degradation in chronic wounds depends on the relative levels of elastase, alpha1-proteinase inhibitor, and alpha2-macroglobulin. *The Journal of investigative dermatology* **106**, 335-341 (1996).

97   Rao, C. N. *et al.* Alpha 1-antitrypsin is degraded and non-functional in chronic wounds but intact and functional in acute wounds: the inhibitor protects fibronectin from degradation by chronic wound fluid enzymes. *J. Invest. Dermatol.* **105**, 572-578 (1995).

98   Acampa, W. *et al.* Myocardial perfusion imaging after coronary revascularization: a clinical appraisal. *Eur. J. Nucl. Med. Mol. Imaging* **40**, 1275-1282, doi:10.1007/s00259-013-2417-8 (2013).

99   Frohm, M. *et al.* Biochemical and antibacterial analysis of human wound and blister fluid. *Eur. J. Biochem.* **237**, 86-92 (1996).

100   Frohm, M. *et al.* The expression of the gene coding for the antibacterial peptide LL-37 is induced in human keratinocytes during inflammatory disorders. *J. Biol. Chem.* **272**, 15258-15263 (1997).

101   Vandamme, D., Landuyt, B., Luyten, W. & Schoofs, L. A comprehensive summary of LL-37, the factotum human cathelicidin peptide. *Cell. Immunol.* **280**, 22-35, doi:10.1016/j.cellimm.2012.11.009 (2012).

102   Steinstraesser, L. *et al.* Host defense peptides in wound healing. *Mol. Med.* **14**, 528-537, doi:10.2119/2008-00002.Steinstraesser (2008).

103   Heilborn, J. D. *et al.* The cathelicidin anti-microbial peptide LL-37 is involved in re-epithelialization of human skin wounds and is lacking in chronic ulcer epithelium. *J. Invest. Dermatol.* **120**, 379-389, doi:10.1046/j.1523-1747.2003.12069.x (2003).

104   Shaykhiev, R. *et al.* Human endogenous antibiotic LL-37 stimulates airway epithelial cell proliferation and wound closure. *Am. J. Physiol. Lung Cell Mol. Physiol.* **289**, L842-848, doi:10.1152/ajplung.00286.2004 (2005).

105   Tokumaru, S. *et al.* Induction of keratinocyte migration via transactivation of the epidermal growth factor receptor by the antimicrobial peptide LL-37. *J. Immunol.* **175**, 4662-4668 (2005).

106   Anne M. van der Does, P. B., Birgitta Agerberth, Lennart Lindbom. Induction of the human cathelicidin LL-37 as a novel treatment against bacterial infections. *Journal of leukocyte biology* **92**, 735-742 (2012).

107   Park, S. C., Park, Y. & Hahm, K. S. The role of antimicrobial peptides in preventing multidrug-resistant bacterial infections and biofilm formation. *International journal of molecular sciences* **12**, 5971-5992, doi:10.3390/ijms12095971 (2011).

108   Haisma, E. M. *et al.* LL-37-derived peptides eradicate multidrug-resistant Staphylococcus aureus from thermally wounded human skin equivalents. *Antimicrobial agents and chemotherapy* **58**, 4411-4419, doi:10.1128/AAC.02554-14 (2014).

109   Huining He, W. D., Junbo Gong, Jingkang Wang, Victor C. Yang. Developing macromolecular therapeutics: the future drug-of-choice. *Frontiers of Chemical Engineering in China* **4**, 10-17 (march 2010).

110   Han, M., Kickhoefer, V. A., Nemerow, G. R. & Rome, L. H. Targeted vault nanoparticles engineered with an endosomolytic peptide deliver biomolecules to the cytoplasm. *ACS Nano* **5**, 6128-6137, doi:10.1021/nn2014613 (2011).

111   Tauzin, B. Biotechnology Medicines in Development. (Pharmaceutical Research and Manufacturers Association, Washington DC, 2006).

112   Hillery, A. M. *Drug Delivery and Targeting: For Pharmacists and Pharmaceutical Scientists*. 1-48 (2001).

113   Frokjaer, S. & Otzen, D. E. Protein drug stability: a formulation challenge. *Nat Rev Drug Discov* **4**, 298-306, doi:10.1038/nrd1695 (2005).

114   D. Crommelin, e. a. *The Science of Dosage Forms Design*. (2001).

115   Wang, W. Instability, stabilization, and formulation of liquid protein pharmaceuticals. *Int. J. Pharm.* **185**, 129-188 (1999).

116   Wang, W. Protein aggregation and its inhibition in biopharmaceutics. *Int. J. Pharm.* **289**, 1-30, doi:10.1016/j.ijpharm.2004.11.014 (2005).

117   Mehnert, W. & Mader, K. Solid lipid nanoparticles: production, characterization and applications. *Adv Drug Deliv Rev* **47**, 165-196 (2001).

118   Muller, R. H. & Keck, C. M. Challenges and solutions for the delivery of biotech drugs--a review of drug nanocrystal technology and lipid nanoparticles. *J. Biotechnol.* **113**, 151-170, doi:10.1016/j.jbiotec.2004.06.007 (2004).

119   Castelli, F., Puglia, C., Sarpietro, M. G., Rizza, L. & Bonina, F. Characterization of indomethacin-loaded lipid nanoparticles by differential scanning calorimetry. *Int. J. Pharm.* **304**, 231-238, doi:10.1016/j.ijpharm.2005.08.011 (2005).

120   Manjunath, K. & Venkateswarlu, V. Pharmacokinetics, tissue distribution and bioavailability of clozapine solid lipid nanoparticles after intravenous and intraduodenal administration. *J. Control. Release* **107**, 215-228, doi:10.1016/j.jconrel.2005.06.006 (2005).

121   Demirel, M., Yazan, Y., Muller, R. H., Kilic, F. & Bozan, B. Formulation and in vitro-in vivo evaluation of piribedil solid lipid micro- and nanoparticles. *J. Microencapsul.* **18**, 359-371, doi:10.1080/02652040010018119 (2001).

122   Goppert, T. M. & Muller, R. H. Adsorption kinetics of plasma proteins on solid lipid nanoparticles for drug targeting. *Int. J. Pharm.* **302**, 172-186, doi:10.1016/j.ijpharm.2005.06.025 (2005).

123   Li, H. *et al.* Enhancement of gastrointestinal absorption of quercetin by solid lipid nanoparticles. *J. Control. Release* **133**, 238-244, doi:10.1016/j.jconrel.2008.10.002 (2009).

124   Uner, M. & Yener, G. Importance of solid lipid nanoparticles (SLN) in various administration routes and future perspectives. *Int J Nanomedicine* **2**, 289-300 (2007).

125   Mukherjee, S., Ray, S. & Thakur, R. S. Solid lipid nanoparticles: a modern formulation approach in drug delivery system. *Indian J. Pharm. Sci.* **71**, 349-358, doi:10.4103/0250-474X.57282 (2009).

126   Muller, R. H., Mader, K. & Gohla, S. Solid lipid nanoparticles (SLN) for controlled drug delivery - a review of the state of the art. *Eur. J. Pharm. Biopharm.* **50**, 161-177 (2000).

127   Almeida, A. J. & Souto, E. Solid lipid nanoparticles as a drug delivery system for peptides and proteins. *Adv Drug Deliv Rev* **59**, 478-490, doi:10.1016/j.addr.2007.04.007 (2007).

128   Muller, R. H., Radtke, M. & Wissing, S. A. Solid lipid nanoparticles (SLN) and nanostructured lipid carriers (NLC) in cosmetic and dermatological preparations. *Adv Drug Deliv Rev* **54 Suppl 1**, S131-155 (2002).

129   Wissing, S. A. & Muller, R. H. Cosmetic applications for solid lipid nanoparticles (SLN). *Int. J. Pharm.* **254**, 65-68 (2003).

130   Souto, E. B. & Muller, R. H. SLN and NLC for topical delivery of ketoconazole. *J. Microencapsul.* **22**, 501-510, doi:10.1080/02652040500162436 (2005).

131   Mustoe, T. A., O'Shaughnessy, K. & Kloeters, O. Chronic wound pathogenesis and current treatment strategies: a unifying hypothesis. *Plast. Reconstr. Surg.* **117**, 35S-41S, doi:10.1097/01.prs.0000225431.63010.1b (2006).

132   Chen, Y., Yang, S. & Ho, E. A. Development of an Analytical Method for the Rapid Quantitation of Peptides Used in Microbicide Formulations. *Chromatographia* **77**, 1713-1720, doi:10.1007/s10337-014-2777-7 (2014).

133   Hu, F. Q., Yuan, H., Zhang, H. H. & Fang, M. Preparation of solid lipid nanoparticles with clobetasol propionate by a novel solvent diffusion method in aqueous system and physicochemical characterization. *Int. J. Pharm.* **239**, 121-128 (2002).

134   Hayakawa, T. *et al.* Concanavalin A-immobilized polystyrene nanospheres capture HIV-1 virions and gp120: potential approach towards prevention of viral transmission. *J. Med. Virol.* **56**, 327-331 (1998).

135   Lutz, J. B., Zehrer, C. L., Solfest, S. E. & Walters, S. A. A new in vivo test method to compare wound dressing fluid handling characteristics and wear time. *Ostomy Wound Manage.* **57**, 28-36 (2011).

136   Woodrow, K. A. *et al.* Intravaginal gene silencing using biodegradable polymer nanoparticles densely loaded with small-interfering RNA. *Nat Mater* **8**, 526-533, doi:10.1038/nmat2444 (2009).

137   Blanco, M. D., Bernardo, M. V., Teijon, C., Sastre, R. L. & Teijon, J. M. Transdermal application of bupivacaine-loaded poly(acrylamide(A)-co-monomethyl itaconate) hydrogels. *International journal of pharmaceutics* **255**, 99-107 (2003).

138   Horrevorts, A. M. *et al.* Chequerboard titrations: the influence of the composition of serial dilutions of antibiotics on the fractional inhibitory concentration index and fractional bactericidal concentration index. *J. Antimicrob. Chemother.* **19**, 119-125 (1987).

139   Wang, X., Ge, J., Tredget, E. E. & Wu, Y. The mouse excisional wound splinting model, including applications for stem cell transplantation. *Nat. Protoc.* **8**, 302-309, doi:10.1038/nprot.2013.002 (2013).

140   des Rieux, A. *et al.* 3D systems delivering VEGF to promote angiogenesis for tissue engineering. *Journal of controlled release : official journal of the Controlled Release Society* **150**, 272-278, doi:10.1016/j.jconrel.2010.11.028 (2011).

141   Chou, T. C. Drug combination studies and their synergy quantification using the Chou-Talalay method. *Cancer research* **70**, 440-446, doi:10.1158/0008-5472.CAN-09-1947 (2010).

142   Hu, F. Q., Hong, Y. & Yuan, H. Preparation and characterization of solid lipid nanoparticles containing peptide. *Int. J. Pharm.* **273**, 29-35, doi:10.1016/j.ijpharm.2003.12.016 (2004).

143   H. Fessi, F. P., J.Ph. Devissaguet, N. Ammoury, S. Benita. Nanocapsule formation by interfacial polymer deposition following solvent displacement. *International jounal of pharmaceutics* **55** (1989).

144   Schwarz, C. & Mehnert, W. Solid lipid nanoparticles (SLN) for controlled drug delivery. II. Drug incorporation and physicochemical characterization. *J. Microencapsul.* **16**, 205-213, doi:10.1080/026520499289185 (1999).

145   Cavalli, R., Caputo, O., Marengo, E., Pattarino, F., Gasco, M.R. The effect of the components of microemulsions on both size and crystalline structure of solid lipid nanoparticles (SLN) containing a series of model molecules. *Pharmazie* **53**, 392-396 (1998).

146   Trotta, M., Debernardi, F. & Caputo, O. Preparation of solid lipid nanoparticles by a solvent emulsification-diffusion technique. *Int. J. Pharm.* **257**, 153-160 (2003).

147   Falanga, V. Growth factors and chronic wounds: the need to understand the microenvironment. *The Journal of dermatology* **19**, 667-672 (1992).

148   Hossein Ali Ebrahimi, Y. J., Mehrdad Hamidi, Mohammad Barzegar Jalali. Repaglinide-loaded solid lipid nanoparticles: effect of using different surfactants/stabilizers on physicochemical properties of nanoparticles. *DARU Journal of Pharmaceutical Sciences* **23**, 46, doi:10.1186/s40199-015-0128-3 (2015).

149   Liu, J., Gong, T., Wang, C., Zhong, Z. & Zhang, Z. Solid lipid nanoparticles loaded with insulin by sodium cholate-phosphatidylcholine-based mixed micelles: preparation and characterization. *Int. J. Pharm.* **340**, 153-162, doi:10.1016/j.ijpharm.2007.03.009 (2007).

150   Chen, D. B., Yang, T. Z., Lu, W. L. & Zhang, Q. In vitro and in vivo study of two types of long-circulating solid lipid nanoparticles containing paclitaxel. *Chemical & pharmaceutical bulletin* **49**, 1444-1447 (2001).

151   Venkateswarlu, V. & Manjunath, K. Preparation, characterization and in vitro release kinetics of clozapine solid lipid nanoparticles. *Journal of controlled release : official journal of the Controlled Release Society* **95**, 627-638, doi:10.1016/j.jconrel.2004.01.005 (2004).

152   Nicoli, S. *et al.* Characterization of rabbit ear skin as a skin model for in vitro transdermal permeation experiments: histology, lipid composition and permeability. *Skin pharmacology and physiology* **21**, 218-226, doi:10.1159/000135638 (2008).

153   Nicoli, S., Cappellazzi, M., Colombo, P. & Santi, P. Characterization of the permselective properties of rabbit skin during transdermal iontophoresis. *Journal of pharmaceutical sciences* **92**, 1482-1488, doi:10.1002/jps.10405 (2003).

154   Chen, X. *et al.* Synergistic effect of antibacterial agents human beta-defensins, cathelicidin LL-37 and lysozyme against Staphylococcus aureus and Escherichia coli. *Journal of dermatological science* **40**, 123-132, doi:10.1016/j.jdermsci.2005.03.014 (2005).

155   Ong, P. Y. *et al.* Endogenous antimicrobial peptides and skin infections in atopic dermatitis. *The New England journal of medicine* **347**, 1151-1160, doi:10.1056/NEJMoa021481 (2002).

156   Hsieh, M. H., Yu, C. M., Yu, V. L. & Chow, J. W. Synergy assessed by checkerboard. A critical analysis. *Diagnostic microbiology and infectious disease* **16**, 343-349 (1993).

157   Durr, U. H., Sudheendra, U. S. & Ramamoorthy, A. LL-37, the only human member of the cathelicidin family of antimicrobial peptides. *Biochimica et biophysica acta* **1758**, 1408-1425, doi:10.1016/j.bbamem.2006.03.030 (2006).

158   De, Y. *et al.* LL-37, the neutrophil granule- and epithelial cell-derived cathelicidin, utilizes formyl peptide receptor-like 1 (FPRL1) as a receptor to chemoattract human peripheral blood neutrophils, monocytes, and T cells. *The Journal of experimental medicine* **192**, 1069-1074 (2000).

159   Ramos, R. *et al.* Wound healing activity of the human antimicrobial peptide LL37. *Peptides* **32**, 1469-1476, doi:10.1016/j.peptides.2011.06.005 (2011).

160   Porat, R., Clark, B. D., Wolff, S. M. & Dinarello, C. A. Enhancement of growth of virulent strains of Escherichia coli by interleukin-1. *Science* **254**, 430-432 (1991).

161   Forney, J. R., Yang, S. & Healey, M. C. Synergistic anticryptosporidial potential of the combination alpha-1-antitrypsin and paromomycin. *Antimicrobial agents and chemotherapy* **41**, 2006-2008 (1997).

162   Miyamoto, Y. *et al.* Novel functions of human alpha(1)-protease inhibitor after S-nitrosylation: inhibition of cysteine protease and antibacterial activity. *Biochemical and biophysical research communications* **267**, 918-923, doi:10.1006/bbrc.1999.2046 (2000).

163   Huntington, J. A., Read, R. J. & Carrell, R. W. Structure of a serpin-protease complex shows inhibition by deformation. *Nature* **407**, 923-926, doi:10.1038/35038119 (2000).

164   Lomas, D. A. New insights into the structural basis of alpha 1-antitrypsin deficiency. *QJM : monthly journal of the Association of Physicians* **89**, 807-812 (1996).

165   Carretero, M. *et al.* In vitro and in vivo wound healing-promoting activities of human cathelicidin LL-37. *The Journal of investigative dermatology* **128**, 223-236, doi:10.1038/sj.jid.5701043 (2008).

166   Congote, L. F., Temmel, N., Sadvakassova, G. & Dobocan, M. C. Comparison of the effects of serpin A1, a recombinant serpin A1-IGF chimera and serpin A1 C-terminal peptide on wound healing. *Peptides* **29**, 39-46, doi:10.1016/j.peptides.2007.10.011 (2008).

167   Golec, M. Cathelicidin LL-37: LPS-neutralizing, pleiotropic peptide. *Annals of agricultural and environmental medicine : AAEM* **14**, 1-4 (2007).

168   Rosenfeld, Y., Papo, N. & Shai, Y. Endotoxin (lipopolysaccharide) neutralization by innate immunity host-defense peptides. Peptide properties and plausible modes of action. *The Journal of biological chemistry* **281**, 1636-1643, doi:10.1074/jbc.M504327200 (2006).

169   Larrick, J. W. *et al.* Human CAP18: a novel antimicrobial lipopolysaccharide-binding protein. *Infection and immunity* **63**, 1291-1297 (1995).

170   Mookherjee, N. *et al.* Modulation of the TLR-mediated inflammatory response by the endogenous human host defense peptide LL-37. *Journal of immunology* **176**, 2455-2464 (2006).

171   Subramaniyam, D. *et al.* C-36 peptide, a degradation product of alpha1-antitrypsin, modulates human monocyte activation through LPS signaling pathways. *The international journal of biochemistry & cell biology* **38**, 563-575, doi:10.1016/j.biocel.2005.09.021 (2006).

172   Larsen, C. G., Anderson, A. O., Oppenheim, J. J. & Matsushima, K. Production of interleukin-8 by human dermal fibroblasts and keratinocytes in response to interleukin-1 or tumour necrosis factor. *Immunology* **68**, 31-36 (1989).

173   Grimble, R. F. Nutritional antioxidants and the modulation of inflammation: theory and practice. *New horizons* **2**, 175-185 (1994).

174   Conner, E. M. & Grisham, M. B. Inflammation, free radicals, and antioxidants. *Nutrition* **12**, 274-277 (1996).

175   Lynch, J. P., 3rd & Toews, G. B. Tumor necrosis factor-alpha. A multifaceted mediator of inflammation. *Chest* **96**, 457-459 (1989).

176   Ren, K. & Torres, R. Role of interleukin-1beta during pain and inflammation. *Brain research reviews* **60**, 57-64, doi:10.1016/j.brainresrev.2008.12.020 (2009).

177   Feghali, C. A. & Wright, T. M. Cytokines in acute and chronic inflammation. *Frontiers in bioscience : a journal and virtual library* **2**, d12-26 (1997).

178   Gallucci, R. M., Sloan, D. K., Heck, J. M., Murray, A. R. & O'Dell, S. J. Interleukin 6 indirectly induces keratinocyte migration. *The Journal of investigative dermatology* **122**, 764-772, doi:10.1111/j.0022-202X.2004.22323.x (2004).